DOKUZ EYLÜL UNIVERSITY

GRADUATE SCHOOL OF NATURAL AND APPLIED SCIENCES

SPATIAL AND TEMPORAL VARIATION OF AEROSOL OPTICAL DEPTH OVER TURKEY FROM MODIS SATELLITE DATA

by

Esra DUĞRAL

April, 2021

İZMİR

SPATIAL AND TEMPORAL VARIATION OF AEROSOL OPTICAL DEPTH OVER TURKEY FROM MODIS SATELLITE DATA

A Thesis Submitted to the
Graduate School of Natural and Applied Sciences of Dokuz Eylül University
In Partial Fulfillment of the Requirements for the Degree of Master of Science
in Environmental Engineering, Environmental Science Program

by
Esra DUĞRAL

April, 2021
İZMİR

M.Sc THESIS EXAMINATION RESULT FORM

We have read the thesis entitled **“SPATIAL AND TEMPORAL VARIATION OF AEROSOL OPTICAL DEPTH OVER TURKEY FROM MODIS SATELLITE DATA”** completed by **ESRA DUĞRAL** under supervision of **PROF.DR. TOLGA ELBİR** and we certify that in our opinion it is fully adequate, in scope and in quality, as a thesis for the degree of Master of Science.

Prof. Dr. Tolga ELBİR

Supervisor

Asst. Prof.Dr. Akın ALTEN

(Jury Member)

Prof.Dr. Abdurrahman BAYRAM

(Jury Member)

Prof. Dr. Özgür ÖZÇELİK

Director

Graduate School of Natural and Applied Sciences

ACKNOWLEDGMENT

This work was financially supported by the Scientific and Technological Research Council of Turkey (TUBITAK) 2210-C National Scholarship Programme for MSc Students. This study also supported by TUBITAK Project No: 119Y005. I would like to thank to TUBITAK for this financial support.

I would like to thank the Atmosphere Archive and Distribution System (LAADS) for providing the MODIS data, and the Principle Investigators for establishing and maintaining the AERONET sites.

I would like to thank my advisor Prof.Dr. Tolga ELBİR for his invaluable suggestions, guidance, sincere and support during research and preparing of the thesis. His encouragement and valuable advice often served to give me a sense of direction during my studies.

I also wish to thank to Gizem TUNA TUYGUN for all support and moral motivation during preparation of my thesis.

Finally, I am notably thankful to my family, İzzet ÖZDEMİR, Esma ÖZDEMİR and Erol DUĞRAL for the endless understanding and support during my educational life.

Esra DUĞRAL

SPATIAL AND TEMPORAL VARIATION OF AEROSOL OPTICAL DEPTH OVER TURKEY FROM MODIS SATELLITE DATA

ABSTRACT

The most recent release of Moderate Resolution Imaging Spectroradiometer (MODIS) Collection 6.1 (C6.1) aerosol optical depth (AOD) products were available with various improvements made to both the radiometric calibration and Dark Target (DT) and Deep Blue (DB) algorithms. However, the performances of the recent MODIS aerosol products have not been investigated over Turkey. This study provides an evaluation of C6.1 Terra and Aqua MODIS aerosol products with reference to the ground based AOD measurements by the Aerosol Robotic Network (AERONET) Version 3 Level 2.0 data at 10 sites in the period of 2002–2019. Considering that sparse AERONET sites are available in Turkey, 8 sites from neighboring countries were also used. The AOD retrievals were validated over different surface types defined by monthly NDVI (Normalized Difference Vegetation Index) values. Analysis was performed with direct comparisons between MODIS retrievals and AERONET measurements at regional to site scales. Meanwhile, the spatial and temporal variations were also discussed. The retrieval errors illustrated that the performance of datasets changed with surface types. Overall, the DB AOD products showed the best performance in partially vegetated urban areas. DT products matched more closely with the AERONET AODs than DB products over moderately or densely vegetated areas. DT and DB tended to overestimate and underestimate AOD, respectively. There were small differences between Terra and Aqua aerosol products. In general, Aqua AOD products were more reliable in describing the AOD over the region and recommended for selection in related aerosol studies at regional scale.

Keywords: MODIS, Collection 6.1, Aerosol optical depth, AERONET, validation, Turkey

MODIS UYDU VERİLERİNDEN ELDE EDİLEN AEROSOL OPTİK DERİNLİĞİNİN TÜRKİYE'DE ZAMANSAL VE MEKANSAL DEĞİŞİMİ

ÖZ

Koleksiyon 6.1 (C6.1) Moderate Resolution Imaging Spectroradiometer (MODIS) aerosol optik derinlik (AOD) güncel verileri, hem kalibrasyon hem de Dark Target (DT) ve Deep Blue (DB) algoritmalarında yapılan çeşitli iyileştirmelerle kullanıma sunulmuştur. Ancak güncel MODIS aerosol verilerinin performansları Türkiye'de incelenmemiştir. Bu çalışmada, Terra ve Aqua MODIS C6.1 AOD verisinin 2002–2019 yılları arasında 10 AERONET istasyonunda Versiyon 3 Seviye 2.0 yer bazlı AOD ölçümleriyle değerlendirilmesi yapılmıştır. Türkiye'de AERONET istasyonlarının az olduğu düşünülerek, komşu ülkelerden 8 istasyon da kullanılmıştır. AOD verileri, aylık NDVI (Normalized Difference Vegetation Index) değerleriyle tanımlanan farklı yüzey türleriyle doğrulanmıştır. Analizler, bölgesel ölçeklerde MODIS verileri ve AERONET ölçümleri arasında doğrudan karşılaştırmalar ile gerçekleştirilmiştir. Ayrıca, AOD verilerinin zamansal ve mekansal değişimleri incelenmiştir. Hata değerleri, veri setlerinin performansının yüzey türüne göre değiştiğini göstermiştir. Genel olarak, DB AOD ürünleri, kısmen bitki örtülü kentsel alanlarda en iyi performansı göstermiştir. DT ürünleri, AERONET AOD verileri ile orta veya yoğun bitki örtüsüne sahip alanlarda DB ürünlerine göre daha iyi eşleşmiştir. DT ve DB, sırasıyla AOD versini fazla ve az tahmin etme eğilimindedir. Terra ve Aqua aerosol ürünleri arasında küçük farklılıklar vardır. Genel olarak, Aqua AOD ürünleri bölge genelinde AOD verisini tanımlamada daha güvenilir ve bölgesel ölçekte ilgili aerosol çalışmalarında kullanım için daha uygundur.

Anahtar Kelimeler: MODIS, Koleksiyon 6.1, Aerosol optik derinliği, AERONET, doğrulama, Türkiye

CONTENTS

Page

LIST OF FIGURES

Page

LIST OF TABLES

Page

CHAPTER ONE
INTRODUCTION

1.1 Introduction

Aerosols are colloidal forms consisting of very little soil particles and/or liquid drops hanging onto the troposphere or stratosphere layers of the atmosphere. These particles can get lifted to the atmosphere naturally or as a result of some anthropogenic activities. Volcanoes, forest fires, dust-storms, sea salts, etc., are considered as natural sources, while the use of fossil fuels and industrial activities are anthropogenic sources. It is well-known that aerosols can affect the atmosphere because of some photo-chemical reactions caused by the sun and humidity (Chan & Chan, 2017). Therefore, aerosols are one of the main air pollutants in the studies focusing on air quality, weather, and human health (Bellouin, 2015; Zhou et al., 2015; Zhang et al., 2016; Banerjee et al., 2017; Horne & Dabdub, 2017). Aerosols do not only affect the local air quality around the sources, but they can also be transported to the long distances such as hundreds or thousands of kilometers in the atmosphere (Lee et al., 2013; Tsai et al., 2014; Zhang et al., 2014; Rupakheti et al., 2019; Shen et al., 2020; Filonchyk et al., 2020).

While aerosols could cause the absorption or scattering of sunlight directly, they could also indirectly affect the absorption and scattering of radiation through clouds by preventing the cloud formation at the bottom layers of atmosphere (NASA, 2021a). Therefore, aerosols are considered as the primary factor that affect the radiation balance around the world (NASA, 2021a). Aerosols can reduce visibility under some specific cases as dust-storms, forest fires, volcanisms, and foggy weathers (Kloog et al., 2015). Therefore, it is quite critical to determine the amount of aerosol particles, identify its physical and chemical properties, investigate its part causing the radiation change and analyze its effects on the weather, air quality, ecosystems, and human health (Kloog et al., 2015).

In order for obtaining information on the aerosols in the atmosphere, particulate matter (PM) measurements are usually performed at the ground level by using analyzers situated in the air quality monitoring stations. These PM measurements represent the air quality where the station is located, and they are usually insufficient for determining the air quality of a wider region. Consequently, for being able to monitor the air quality on a regional scale, a large number of air quality monitoring stations are required. However, establishing such an infrastructure is not always easy or affordable. Therefore, satellite based remote sensing techniques have been recently used in order to be able to monitor the air quality on larger areas (Bibi et al., 2015; Xu et al., 2015; You et al., 2016; Sever et al., 2017; Ahmad et al., 2019; Park et al., 2019; Yang et al., 2019; Jin et al., 2020).

Nowadays, data generation for determining air quality by using satellites and remote sensing techniques is a field that is still under development. Around the earth, there are many satellites that have been sent to the space and still serving in their orbits for the purposes of monitoring the aerosols and gases in the atmosphere (Bibi et al., 2015). These satellites can detect some pollutants directly or measure some physical parameters of the pollutants to facilitate the identification of the ones that cannot identified directly. For example, there are numerous succeeded studies for estimating ground-level particulate matter concentrations by identifying the change arising from the absorption or scattering of solar radiation (Wang et al., 2013; Lee et al., 2014; Hu et al., 2014; Van Donkelaar et al., 2015; Zhang et al., 2015; Lee et al., 2016; You et al., 2016; Park et al., 2019; Yang et al., 2019; Wei et al., 2020).

For detection of aerosols in the atmosphere via satellites, basic parameter that is monitored is Aerosol Optical Depth (AOD). AOD is briefly defined as the decrease of electromagnetic energy at a certain wavelength due to aerosols in the atmosphere (Douglas, 2015). With the help of this information, it is possible to determine the aerosol amount in a column that is having a unit base area and a height equal to atmosphere depth. Several satellite systems that have been developed to produce AOD data exist and in use over the world. Terra and Aqua satellites, that are equipped with a special instrument named Moderate Resolution Imaging Spectroradiometer

(MODIS) are the most preferred satellites in the literature, since they produce AOD data twice a day (Wang et al., 2013; Lee et al., 2014; Van Donkelaar et al., 2015; Zhang et al., 2015; Lee et al., 2016; You et al., 2016; Tian et al., 2018; Wei et al., 2019; Zheng et al., 2019; Wei et al., 2020).

While AOD is being detected by observing the earth's atmosphere from space with satellites, AOD observation on earth (at ground level) is being performed simultaneously. For this purpose, several sun photometers that are connected to the global Aerosol Robotic Network (AERONET) are used (NASA, 2020a). By using sun photometers, solar radiation at different wavelengths at ground level is measured and by processing the measured data at NASA (National Aeronautics and Space Administration) AERONET center. AOD at different wavelengths, particle size distribution and other optical properties (single scattering albedo) and refractive indices are derived. AOD data obtained from this network has been used for validating the aerosol data commonly obtained from the satellites (Guo et al., 2014; Loría-Salazar et al., 2016; Bilal et al., 2017; Bilal et al., 2018; Wei et al., 2019; Bright & Gueymardb, 2019; Huang et al., 2019; Zheng et al., 2019; Wei et al., 2020).

Owing to newly developed data processing algorithms used, aerosols are being identified more accurately with satellites (Mhawish et al., 2018). Remote sensing of aerosols has extensive applications in identifying aerosol columnar properties, especially in terms of optical depth, composition, morphology, and vertical distribution. This ultimately provides evidence in establishing the source-transport-receptor relations of aerosols over a synoptic scale (Kloog et al., 2015). Although there are numerous international studies in the literature examining the correlation between the aerosol amount in the atmosphere and the AOD data obtained from the satellites, number of similar studies are very limited in Turkey (Zeydan & Yildirim, 2012; Dundar et al., 2015; Zeydan & Wang, 2019; Aldabash et al., 2020; Shaheen et al., 2020). In most of these studies, AOD data belonging to old collection MODIS data was used. But, just in two recent studies (Aldabash et al., 2020; Shaheen et al., 2020), it was observed that, new collection MODIS data has been used. In these two studies, only the quality of MODIS Dark Target&Deep Blue combined product (DTB) was evaluated, their differences compared to other algorithms were not discussed. Besides, the two satellites were evaluated as merged, and the differences between Terra and Aqua were not emphasized. Zeydan & Yildirim (2012) and Zeydan & Wang (2019) mostly aimed to monitor particulate matter concentrations with the help of AOD and several meteorological parameters. On the other hand, Dundar et al. (2015) compared 10 km resolution AOD data obtained from Aqua satellite with meteorological parameters observed at ground level between 2002-2013 and examined the statistical relationship between dusty days and AOD data.

Within the scope of this study, the spatial and temporal variations of AOD data obtained from Terra and Aqua MODIS satellites having two different algorithms (DT and DB), two different spatial resolutions (3 km and 10 km) were determined for Turkey. AOD data obtained from the satellites have been validated with the AOD data monitored in the IMS-METU-ERDEMLI AERONET station. The other national AERONET station (TUBITAK_UZAY_Ankara) together with eight more stations situated in the neighboring countries were also included. This study span eighteen years period (2002-2019). Two different AOD products having 10 km and 3 km spatial resolutions were validated against AERONET AOD. NASA's (National Aeronautics and Space Administration) most updated data processing algorithms (Collection 6.1) released in 2018 were used and the expected errors and correlations were evaluated as a whole.

CHAPTER TWO
LITERATURE

2.1 Monitoring Atmospheric Aerosol with Satellites

Aerosol Optical Depth (AOD) in the atmosphere is a parameter that has been continuously monitored by both satellites from space and sun photometers at the ground. Briefly, AOD can be defined as a measure of the extinction of the solar beam by dust and haze. (Ghotbi et al., 2016). A value of 0.01 corresponds to an extremely clean atmosphere, and a value of 0.4 would correspond to a very hazy condition (NOAA, 2021). The maximum value 5 indicates that aerosols are so dense that people would have difficulty seeing the Sun, even at mid-day.

Over the last decades several satellite instruments like the Moderate Resolution Imaging Spectroradiometer (MODIS), the Multiangle Imaging Spectroradiometer (MISR), the Ozone Monitoring Instrument (OMI), the Sea-viewing Wide Field-of-view Sensor (SeaWiFS) and Visible/Infrared Imager Radiometer Suite (VIIRS) that are using different retrieval algorithms are utilized for characterizing physical and chemical properties of aerosols (Bibi et al., 2015). These satellites provide AOD products with various spatial and temporal resolutions (Bibi et al., 2015). There are also some new sensors that have recently entered to the service or planned to be available in near future. Among these GEOS-R, GEOS-16, HIMAWARI-8, TROPOMI (TROPOspheric Monitoring Instrument), TEMPO (Tropospheric Emissions: Monitoring of Pollution) and MAIA (Multi-Angle Imager for Aerosols) are the main ones (ARSET, 2018).

MODIS instrument is the most advantageous one among the ones in the service since it is located on two different satellites (Terra and Aqua) and accordingly passing over a certain point on the earth twice daily, generating more than one data at different hours (for example, 10:30 am and 13:30 pm for Turkey) on daily basis. Therefore, in many studies MODIS has been chosen as the main data source to determine the atmospheric aerosols in the literature (Wang et al., 2013; Lee et al., 2014; Van

Donkelaar et al., 2015; Zhang et al., 2015; Lee et al., 2016; You et al., 2016; Sever et al., 2017; Faharat et al., 2018; Almazroui et al., 2019; Rupakheti et al., 2019; Wei et al., 2019). Another reason for wide use of MODIS sensor is that the AOD data generated by this sensor has high compliance (correlation) with the data generated by the AERONET which makes measurements at ground level (Bibi et al., 2015).

MODIS was launched into earth orbit by NASA in 1999 on board the Terra (EOS AM) satellite, and in 2002 on board the Aqua (EOS PM) satellite. MODIS has 36 different spectral bands with wavelengths between 410 and 15000 nm, and 7 of them (470-2130 nm) are used completely for determining of aerosol optical properties (NASA, 2020b).

Two types of the independent MODIS AOD algorithms, namely Deep Blue (DB) and Dark Target (DT) generates data over the dark (e.g., vegetated region) and bright (e.g, desert, and metropolitan region) surfaces respectively. MODIS DB AOD algorithm tends to the issue on a superficial level brightness along these lines, however using the attributes of the darker surface in two blue channels 0.412 and 0.470 µm and absorption by dust in a red channel (e.g., 0.670 µm). MODIS DT land AOD algorithm utilizes the presence of a dark surface in two noticeable channels 0.47 and 0.66 µm and the proximate transparency of the air at a generally long wavelength 2.12 µm to get a true assessment of the atmosphere scattering. With DB algorithm, AOD data is generated only in 10 km-resolution (Remer et al., 2013). On the other hand, DT algorithm can produce AOD data with higher spatial resolution (3 km) and with better results over vegetated areas, as a result of recent algorithm development done by NASA (Gupta et al., 2018).

AOD data obtained from Terra and Aqua satellites is processed by NASA at four different levels. The MODIS Level-0 Production Data Set (PDS) is the raw package consisting of a 5-minute swath of data. It is utilized to generate calibrated and geolocated MODIS radiances, or Level-1 data. The Level-1B data contains calibrated radiances for all thirty-six MODIS bands and reflectance for the reflective Solar bands (Bands 1 through 19 and 26) (NASA, 2020c). The Level 2 items are coordinated along the satellite orbital track, individual retrieval labeled with its geolocation and orbital (or area) data is not gridded. A similar scene might be seen on ensuing days, yet those daily perspectives on the scene will be seen at various review geometries, not showing up in a similar area in the swath and, thusly, not representing a similar spatial resolution from day-to-day. Therefore, the calculation of spatio–temporal statistics at Level 2 is complicated. The Level 2 data incorporate diverse supporting boundaries, for example, cloud cover, quality flags, sun-satellite calculation, and other metadata. These extra boundaries can be utilized to screen the informational collections further to address certain applications or exploration questions. Along these lines, examining Level 2 information requires programming capabilities as well as huge information processing on extra boundaries and a good understanding of the retrieval algorithm. For mitigating the difficulty in interpreting and analyzing the data, the MODIS processing system offers a gridded product operationally. In a gridded product, the orbital data are aggregated to a uniform standardized array in which each cell in the array has the same angular dimensions with all the other cells. Furthermore, the array remains unchanged each consecutive day, so that spatio–temporal statistics are easily calculated, and raster-based software can be easily applied. The present MODIS aerosol gridded data is denoted as Level 3, and it is provided by the processing system only at a spatial resolution of 1 degree^2 (~110 × 110 km^2) with temporal averaging ranging from a day to eight days and to a month. The spatial resolution has a much coarser resolution than the native Level 2 product of nominal 10 km or 3 km (NASA, 2020c).

MODIS Adaptive Processing System (MODAPS) has formed an enhanced Collection 6.1 (C6.1) for Level-1, Level-2 and a higher one the Level-3 Atmosphere team products. Starting point of forming a new, enhanced collection (C6.1) is the need of handling number of problems for the Collection 6 (C6) Level-3 data. Because of the negative effects of these problems on MODIS Atmosphere Level-2 and Level-3 products, MODIS Atmosphere team decided to use the chance of reprocessing the data for applying some of the scientific enhancements on L2 and L3 products and they developed the data. Reprocessing of Collection 6.1 started on 28th of September in 2017 and completed on 7th of March in 2018 (NASA, 2021b).

The difference in C6.1 DT data obtained via development of enhanced surface reflection algorithms. The surface reflection algorithms are enhanced specifically where fractions of urban areas are more than 20% (Mattoo et al., 2017). Compared to DT, DB algorithm has been more affected from various changes such as reducing to make mistakes on heterogenous topographical surfaces and using the enhanced surface reflection values on highly elevated surfaces (Hsu et al., 2017).

2.2 Monitoring Atmospheric Aerosols from Ground Level with Sun Photometers

The AERONET (AErosol RObotic NETwork) is a cooperation formed by NASA and PHOTONS (PHOtométrie pour le Traitement Opérationnel de Normalisation Satellitaire) for the purposes of executing joint studies, aerosol researches and also controlling the quality of data generated by satellites with national public institutions, universities and institutes on a global scale**.** With the help of ground level solar photometers installed at more than a total of 1200 different stations of this network covering the whole world, AOD data is generated continuously (NASA, 2020a). The AOD data produced by AERONET is mostly used to validate the aerosol data obtained from the satellites (Guo et al., 2014; Loría-Salazar et al., 2016). By using a solar-powered CIMEL Electronique 318A spectral radiometer sun and sky radiances at various fixed wavelengths within the visible and near-infrared (VNIR) spectrum is being estimated. AERONET collaboration provides globally distributed monitoring of spectral aerosol optical depth (AOD), inversion products, and precipitable water in diverse aerosol regimes. The average of the total aerosol column is represented by these products within the atmosphere (NASA, 2020a). The sun photometer used in the IMS-METU-ERDEMLI station located in the Erdemli district of Mersin city is shown in Figure 2.1.

Figure 2.1 Sun photometer used at AERONET station in Erdemli district of Mersin (Kubilay & Koçak, 2009)

All sun photometer stations of the AERONET perform and record AOD measurements in every 15 minutes at the wavelengths of 340, 380, 440, 500, 675, 870, 940 and 1020 nm (NASA, 2020a). Among those, 940 nm is used for column water abundance determination whereas 500 nm is used to monitor aerosols in the atmosphere (NASA, 2020a). AERONET collaboration provides globally distributed monitoring of spectral AOD, inversion products, and precipitable water in diverse aerosol regimes. Version 3 AOD data is computed for three data quality levels: Level 1.0 (unfiltered), Level 1.5 (cloud effects eliminated and quality improved), and Level 2.0 (quality-assured). Inversions, precipitable water, and other AOD-dependent products are derived from these levels (NASA, 2020a).

In the global AERONET network, there are five national stations from Turkey. The IMS-METU-ERDEMLI station located in the southern region of Turkey is the only station that continuously monitors AOD. Other four Turkish stations (TUBITAK_UZAY_Ankara, Tuz_Golu, Tuz_Golu_2, Tuz_Golu_3) were used for various short-term scientific studies in the past. Among these, TUBITAK_UZAY station is the only station that generate data for a longest period between 2009 and 2012. The mobile station that was deployed at three different locations around Tuz

Lake, produced less amount of discontinuous AOD data between 2009 and 2017. Locations of national AERONET stations are shown in Figure 2.2.

Figure 2.2 The location of the AERONET stations in Turkey

2.3 Validation of Satellite Based AOD Data with Ground Based Data

The AERONET provides a continuous monitoring over time while the satellites (Terra and Aqua) generate data at higher spatial resolution in an instant. To determine the spatial and temporal differences of aerosol variations, the AERONET observations and the MODIS retrievals need to be collocated both spatially and temporally (NASA, 2020d). Since the data obtained from MODIS is cellular (raster), it is not possible to compare it with the data from AERONET.

A standard methodology by Ichoku et al. (2002) for spatio-temporal matching of AERONET AOD measurements and MODIS retrievals is suggested. AERONET measurements within ±30 min period of the MODIS overpass is averaged and compared against MODIS retrievals averaged within a 50-km diameter circular region centered over the AERONET sites. It means that using a 5 x 5 pixels sampling window centered on the latitude and longitude of the AERONET site, the average value of the MODIS AOD image is taken for comparison. There are many studies using this approach in the literature (Ichoku et al., 2002; Remer et al., 2013; Tao et al., 2015; Tian et al., 2018; Wei et al., 2019; Wang et al., 2019; Jin et al., 2020). The approach for temporal and spatial matching of AERONET and MODIS AOD data is shown in Figure 2.3.

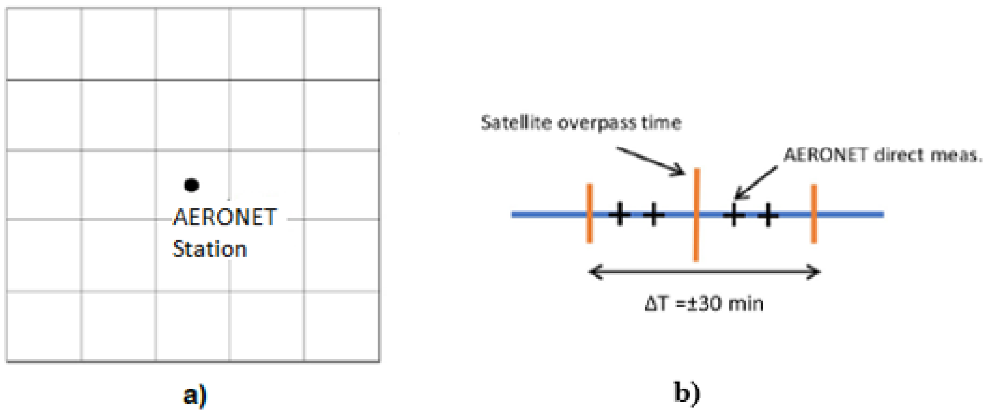

Figure 2.3 The approach applied in spatial (a) and temporal (b) matching of MODIS and AERONET AOD data

Although matching of MODIS and AERONET AOD data gives an idea about the success of algorithms on a global or regional scale, there is not any regular guide indicating which AOD products are proper for which regions (Bright & Gueymard, 2019). However, it was known that there are factors affecting the regional quality of the data such as topography, land cover and normalized difference vegetation index (Wei et al., 2019). Therefore, performance of AOD products may differ at different regions.

2.4 A Review of AOD Studies in the Literature

Satellite based AOD data are commonly used in different studies for determining atmospheric aerosols and their properties. AOD data are used successfully to identify the spatial and temporal changes and trend analysis of aerosols (Floutsi et al., 2016; Georgoulias et al., 2016; Glantz et al., 2019; Filonchyk et al., 2020; Shen et al., 2020), to determine the characterization of aerosols (De Meij & Lelieveld, 2011; Nabat et al., 2013; Shaheen et al., 2020; Tutsak & Koçak, 2020), and to determine the particulate matter concentrations having high level of spatial and temporal resolution by using meteorological parameters and different statistical and chemical models at the ground level regionally and globally (Benas et al., 2013; Seo et al., 2015; You et al., 2015; Ghotbi et al., 2016; Kamarul Zaman et al., 2017; Chen et al., 2018; Shtein et al., 2018; Ahmad et al., 2019; Park et al., 2019; Stafoggia et al., 2019; Jin et al., 2020; Wei et al., 2020; Jiang et al., 2021). Several studies investigating the statistical relationships of PM, AOD and meteorological parameters (Kong et al., 2016; Yang et al., 2019; Jin et al., 2020), and case studies such as dust transport and forest fires (Rea et al., 2015; Taheri Shahraiyni et al., 2015; Chouza et al., 2016; Jing et al., 2017; Zhang et al., 2018) are also available in the literature.

A great number of studies in the literature have attempted to validate the satellite based AOD with AERONET AOD. Besides the studies that are performed at the hundreds of stations on a global scale (Gupta et al., 2018; Bright & Gueymardb, 2019; Wei et al., 2019; Wei et al., 2020), there are other studies focusing on the regions covering one or more than one country (Nichol & Bilal, 2016; Bilal et al., 2018a; Almazroui et al., 2019; Che et al., 2019; Huang et al., 2019; Aldabash et al., 2020; Liv et al., 2020) or in a multiple stations on an urban scale (Butt et al., 2017; Tian et al., 2018; Bilal et al., 2018b; Zhang et al., 2019). Some of these studies revealed the effect of developments in the data generation algorithms used in satellite instruments measuring AOD data and demonstrated the improved data quality in different geographical regions in the world (Georgoulias et al., 2016; Bilal et al., 2018b; Huang et al., 2019; Wei et al., 2019; Rupakheti et al., 2019).

AOD data obtained from Terra and Aqua satellites were validated on a global scale by Gupta et al. (2018). Within the scope of this study, MODIS data for the period of 2000-2015 were validated with AERONET data. The stations were categorized as regions or continents such as South America, Middle America, Africa, East Asia, Europe- Mediterranean Sea etc. and compared to each other. However, where some results were provided for the "Euro-Mediterranean" region including Turkey, this study did not provide any result specific to Turkey or any other individual country.

There are many studies in the literature that examined the AOD data obtained from the MODIS instrument. Remer et al. (2013) and Levy et al. (2013) reported that the 3 km spatial resolution data produced with the MODIS Collection 6 dataset determined the aerosol properties more accurately than the 10 km resolution dataset on the coastal regions, islands, and oceans. Therefore, the dataset with 3 km resolution is more preferable than the dataset in 10 km resolution for the regions and urban areas having high albedo. Similarly, in another study carried out by Ghotbi et al. (2016), better results were obtained from 3 km dataset instead of 10 km data in Tehran, Iran. However, He et al. (2017), identified AOD data quality in 3 km and 10 km resolution by using eighteen different AERONET stations across the China and the results indicated that 3 km resolution dataset gave worse results than 10 km resolution dataset at the southern parts of the country.

Global validation of C6.1 AOD data from Terra and Aqua satellites were performed by Wei et al. (2019) and DT, DB and DTB algorithms were used in these studies. Within the scope of this study, MODIS data for the period of 2003-2017 and data obtained from 431 AERONET stations in different regions were validated. It was found that MODIS AOD data from C6.1 were globally well-matched with AERONET AOD measurements, and DTB algorithm showed the best performance in most of the regions. On the other hand, the DT product generated AOD data with high level of accuracy compared to other regions in Europe and North America. In general, DTB algorithm identified aerosol changes with high accuracy and the algorithm was recommended to be used in aerosol studies performed on a global scale. In the study carried out by Li et al. (2009), the dataset with 10 km spatial resolution for the period of 2003-2006 was obtained from only Aqua satellite. These datasets were validated in 13 AERONET stations located in China. In this study, data from C5, an old MODIS product, were used and discussed. It was reported that bias value on this region was higher than the results in the validation studies performed globally. These results also showed that validation studies on satellites and sensors must be performed on a regional scale.

Collections of C6 and C6.1 Terra AOD were compared using all three algorithms DT, DB and DTB in China (Bilal et al., 2019). Results of the study showed that AOD data in C6.1 collection gave better results than C6 since the surface reflectance ratios were improved in this collection. In addition, monthly Normalized Difference Vegetation Index (NDVI) data were validated with MODIS AOD for different land types. Types were categorized as lands with no vegetation (NDVI<0.2), lands covered partially with vegetation (0.2≤NDVI≤0.3), lands covered moderately with vegetation (0.3<NDVI<0.5) and lands covered densely with vegetation (NDVI≥0.5). C6 DT and C6.1 DT were validated by Huan et al. (2019) in the regions with different enhanced vegetation indexes in China. While improvements in northern and middle parts of China with the C6.1 collection data were observed, same results could not be achieved on the western side of the country. It has also been revealed that data quality varies with seasonal changes. Improvements achieved with new algorithms differ according to the vegetation index and urban area. In another validation study carried out by Che et al. (2019), the accuracy of C6.1 MODIS DT AOD data was examined under different land usage conditions. With the new collection data (C6.1) significant improvements were obtained in urban areas, whereas there was a decrease in the number of matching data of coastal region, however this has not resulted in significant changes on the correlations. In another study carried out by Wang et al. (2019), DT and DB AOD data with 10 km resolution were compared using MODIS AOD data from C6.1 and C6 collections between 2001-2016. They were validated in 20 AERONET stations in China. In this validation study, effect of aerosol properties, vegetation index, land cover and topographical data were also examined. C6.1 MODIS AOD data gave better results. On the other hand, the DB algorithm found out to be more successful than the DT algorithm. It has been observed that, because of various land cover classes, different surface reflections vary vastly across regions, and DB AOD data giving better performance in urban areas than the DT data.

Anderson et al. (2013) emphasized that especially regional analyses must be performed in order to be able to evaluate the uncertainty of AOD data thoroughly. Wei et al. (2019) reported that the success of PM prediction models would not be high if region-specific AOD products were not selected. In fact, it has been emphasized that even between Terra and Aqua satellites, significant data quality differences occur due to small differences between sampling times, and it is very important to demonstrate this situation (Wei et al., 2019).

There are almost no similar studies in Turkey to validate MODIS AOD data with AERONET AOD data. Scopes of the studies in which MODIS AOD data is used are different. They mainly focus on analyzing the dust transportation from the Sahara Desert to Turkey on some episode days (Kabatas et al., 2014; Agacayak et al., 2015). In addition, there are also some studies (Zeydan & Yıldırım, 2012; Zeydan & Wang, 2019) examining the correlation between the PM levels measured at ground level with MODIS AOD data in an urban scale. Dundar et al. (2015) compared raw Aqua AOD data with 10 km resolution with several meteorological parameters that was observed at ground level during 2002-2013 period and examined the statistical relation between the AOD data and the number of dusty days. In all these studies, MODIS data from old collection (C6) were used. There are two recent studies using data from the new collection (C6.1) and examining a wider geographic region in which Turkey is also included (Aldabash et al., 2020; Shaheen et al., 2020). They used only the combined DT&DB algorithm in their studies and made regional evaluations. In both studies, other algorithms were not examined separately, and the individual performances of Terra and Aqua satellites were not evaluated.

This study aims to determine spatial and temporal variations of AOD data in Turkey by using up-to-date MODIS data collection (C6.1) from Terra and Aqua satellites for two different algorithms (Dark Target-DT and Deep Blue-DB) and two different spatial resolutions (3 km and 10 km). The AOD data generated by two satellites were validated with simultaneous AOD data generated by the sun photometers located at 10 AERONET stations located in Turkey and its surroundings. Spatial variations of different AOD products were also investigated in the study area by examining the relationship between AOD data and several surface parameters such as land use and normalized difference vegetation index (NDVI). Also, the temporal variations were also examined in different time periods as annual, seasonal, and monthly. This study is the first known study conducted in Turkey in this context.

CHAPTER THREE
MATERIALS AND METHOD

3.1 Datasets

3.1.1 MODIS and AERONET AOD

MODIS was launched in earth orbit by NASA in 1999 installed on board the Terra (EOS AM) satellite, and in 2002 on board of the Aqua (EOS PM) satellite. In this study, for examining two satellites simultaneously, daily AOD data were obtained for eighteen years period (2002-2019) from both Terra and Aqua satellites. AOD data was generated with two different algorithms (DT and DB) of the MODIS instrument. All data investigated were from NASA latest collection (C6.1) Level 2 (L2) data. They were generated separately by 3 km and 10 km resolution. AOD data were downloaded from NASA website (http://ladsweb.nascom.nasa.gov/) as a HDF (Hierarchical Data Format) file and archived. HDF files are multi-objective files, and they restore the data from 53 different parameters in a special format (SDS- Scientific Data Set) with their cellular structure in a matrix form. To evaluate the performance, a total of collocated 211628 MODIS aerosol retrievals (105701 for 3 km AOD product and 105927 for 10 km product) were downloaded between 2002-2019 period. AOD data in 550 nm wavelength (AOD_{550}) were extracted from the hdf files by MATLAB scripts. AOD_{550} data were obtained in two different datasets based on the DT (Optical_Depth_Land_and_Ocean) and DB (Deep_Blue_Aerosol_Optical_Depth_550_Land_Best_Estimate) parameters. In this study, the DT retrievals were obtained from the SDS "Optical_Depth_Land_And_Ocean" including the recommended high-quality flag (QF = 3) AOD retrievals over land. Quality flag 2 and 3 (QF=2-3) for DB algorithm were used together (Bilal et al., 2018).

MODIS AOD data were validated with concurrent AERONET AOD data. The validation process was carried out primarily for the AERONET stations in Turkey. The IMS-METU-ERDEMLI station located in the campus of Institute of Marine Sciences of Middle East Technical University (METU) in Erdemli district of Mersin.

This site is located on the coastline of southern part of Turkey (36.57°N and 34.26°E, Figure 2.2). Apart from this, although it seems that Turkey has 4 more national stations (TUBITAK_UZAY_Ankara, Tuz_Golu, Tuz_Golu_2, Tuz_Golu_3) connected to the AERONET network, they have been used for a short time for research purposes in the past years and are not currently in service. Therefore, it was not possible to carry out long-term validation studies of MODIS AOD data with the AERONET data obtained from these stations. Due to the inadequacy of the number of stations in Turkey, eight AERONET stations located in the countries border on to Turkey were included in the study. Four stations from Greece, one from Bulgaria, one from Romania, one from Southern Cyprus and one from Ukraine were included. Even though it served discontinuously the AOD data from TUBITAK_UZAY_Ankara station was also used in this study since it provided data for various years (all months in 2010 and 2011, one month in 2009, four months in 2012 and one month in 2017). This site was located in central Anatolia part of Turkey (Ankara) and the instrument was mounted on the roof of TUBITAK UZAY's building (39.89°N and 32.78°E, Figure 2.2). Therefore, two stations in Turkey and eight stations in its neighboring countries were investigated together. Locations of these ten stations used in the study are given in Figure 3.1, while their geographical coordinates and observation periods are given in Table 3.1.

In this study, AERONET level 2 version 3 (L2/V3) AOD data (cloud-screened and quality-assured) were used. Data was downloaded from the AERONET website (https://aeronet.gsfc.nasa.gov/cgi-bin/webtool_aod_v3) and archived in Microsoft-Excel files.

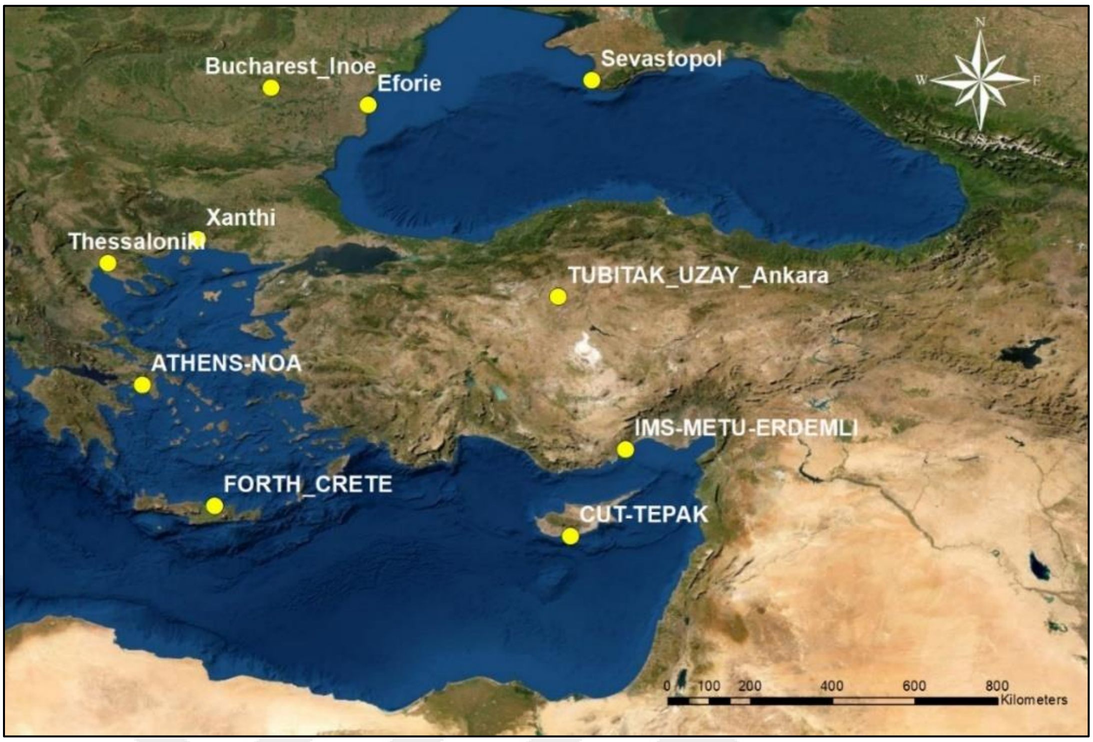

Figure 3.1 Study area including ten AERONET sites

Table 3.1 AERONET sites in the study area.

Station	Country	Latitude (N°)	Longitude (E°)	Period
IMS-METU-ERDEMLI	Turkey	36.565	34.255	2004 - 2019
TUBITAK_UZAY_Ankara	Turkey	39.891	32.778	2009 - 2017*
ATHENS-NOA	Greece	37.972	23.718	2008 - 2018
FORTH_CRETE	Greece	35.332	25.282	2003 - 2017
Thessaloniki	Greece	40.630	22.960	2005 - 2019
Xanthi	Greece	41.146	24.918	2008 - 2015
Bucharest_Inoe	Romania	44.450	26.525	2007 - 2016
CUT-TEPAK	Cyprus	34.674	33.042	2010 - 2019
Eforie	Romania	44.075	28.632	2009 - 2018
Sevastopol	Ukraine	44.615	33.517	2006 - 2014

**All months in 2010 and 2011, one month in 2009, four months in 2012 and one month in 2017*

AOD data obtained from MODIS instrument and AERONET are not directly comparable. While MODIS AOD data are produced in 550 nm wavelength, AERONET AOD data are measured in eight different wavelengths (340, 380, 440, 500, 675, 870, 940 and 1020 nm) and this does not include 550 nm. Therefore, the Angstrom Exponent ($AE_{440-675}$) was used to interpolate the AOD values at 550 nm using the available AOD measurements at the nearest wavelengths (Wei et al., 2019). This procedure was performed by Equation 3.1 as given below:

$$AOD_{550} = AOD_{500} \times \left(\frac{550}{500}\right)^{-\alpha} \quad (3.1)$$

where,

AOD_{550}: Aerosol optical depth at 550 nm

AOD_{500}: Aerosol optical depth at 500 nm

α: Angstrom Exponent ($AE_{440-675}$)

3.1.2 Normalized Difference Vegetation Index (NDVI)

NDVI data is used to identify the spatial variation of AOD data as suggested in the literature (Huang et al., 2019; Wei et al., 2019; Filonchyk et al., 2020). In this study, the analysis method suggested by Jin et al. (2020) was used. This method requires the use of the average NDVI values at 5 x 5 pixels sampling window centered on the latitude and longitude of the AERONET stations for analysis. It means that these regions represent 15 km x 15 km areas for MODIS AOD data in 3 km resolution, and 50 km x 50 km areas in 10 km resolution.

Monthly NDVI values with 1 km spatial resolution from Terra and Aqua satellites (MOD13A1-MYD13A1) were provided in the study. The value range of the NDVI is -1 to 1. Negative values of NDVI (values approaching -1) correspond to water. Values close to zero (-0.1 to 0.1) generally correspond to barren areas of rock, sand, or snow. Low, positive values represent shrub and grassland (approximately 0.2 to 0.4), while high values indicate temperate and tropical rainforests (values approaching 1). Long term mean NDVI data in the study area were given in Figure 3.2. Categorization method used by Tian et al. (2018) was preferred in this study. According to this method, the areas where NDVI value is lower than 0.2 mean no vegetation, the areas having the NDVI values of 0.2-0.3 are partially vegetated surface ($NDVI_P$), the areas where NDVI value changes between 0.3-0.5 are moderately vegetated surface ($NDVI_M$) and the areas with the values higher than 0.5 are densely vegetated surface ($NDVI_D$). The NDVI values at the AERONET stations were summarized in Table 3.2.

Table 3.2 indicates that NDVI is low in three stations and moderate in the other four stations. Two stations, one of them located in Greece, another located in Romania, were covered by densely vegetated surfaces. When the area was 50x50 km^2, 70% of the stations were categorized as lands covered moderately vegetated surfaces. As the area expands, change is seen in NDVI category of two AERONET stations (ATHENS-NOA VE CUT-TEPAK) that are known to be located in the urban area, and consequently they were evaluated as lands covered moderately vegetated surfaces. In this study, seasonal variations were also analyzed since the NDVI may vary seasonally.

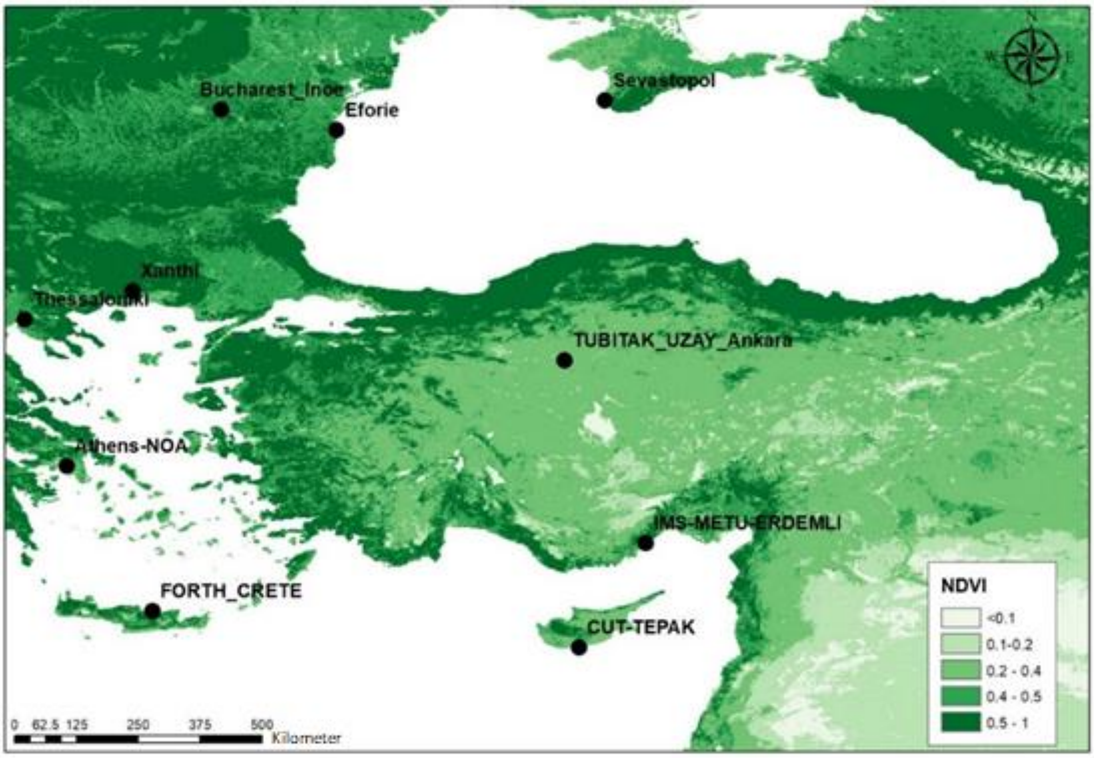

Figure 3.2 Multiannual mean NDVI values in the study area

Since NDVI data varies seasonally, the seasonal variation of NDVI and its effect on the AOD validation studies were also investigated for the study area. Figure 3.3 shows that the high NDVI values were observed in the region especially in summer and spring seasons. NDVI values in inner and eastern parts of Turkey were mainly low in winter and autumn.

Seasonal NDVI values in the study area were given in Figure 3.4. The mean NDVI values generally increase as the area expands. The seasonal variations of NDVI values were similar at ten different AERONET stations. The NDVI values at all stations are typically high in spring and summer, and slightly lower in winter and autumn seasons. The NDVI values at the stations located in the islands such as Cyprus and Crete reach high values in winter. In the ATHENS-NOA station, it was observed that the mean NDVI value increased much more than the other stations while the area is expanded. This shows that the vegetation density of the area where the station is located is less than its surrounding areas.

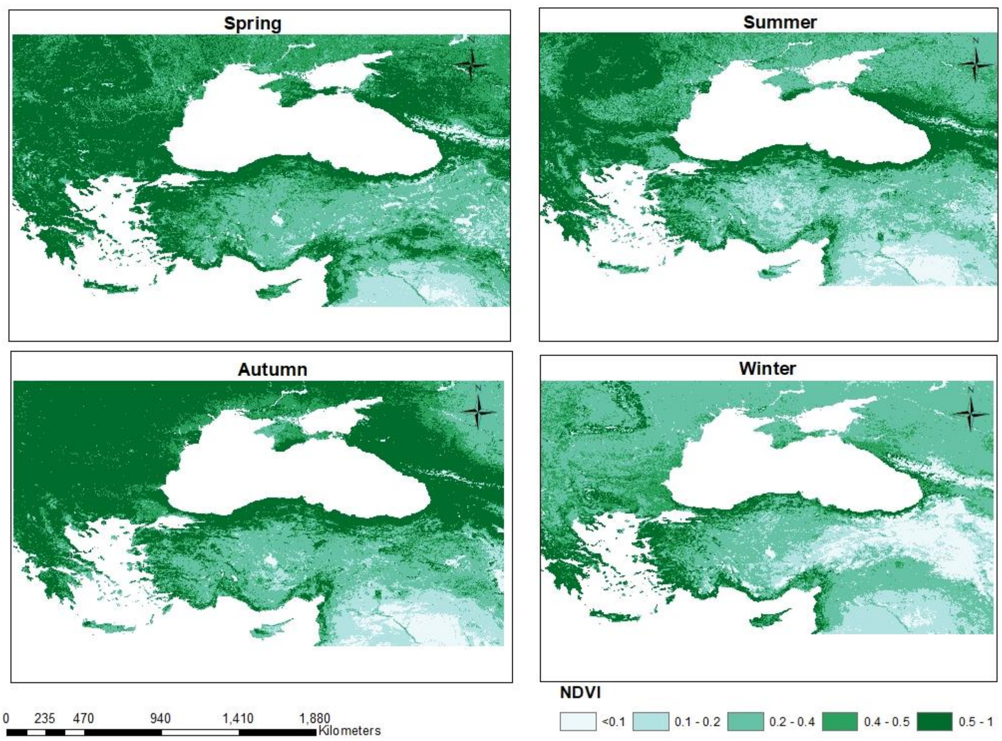

Figure 3.3 Multiannual seasonal mean NDVI

Table 3.2 NDVI values at the AERONET stations

Stations	**Mean NDVI (15 x 15 km^2)**	**Vegetation Cover Type**	**Mean NDVI (50 x 50 km^2)**	**Vegetation Cover Type**
ATHENS-NOA	0.22	partially vegetated surface	0.37	moderately vegetated surface
Bucharest_Inoe	0.50	densely vegetated surfaces	0.50	densely vegetated surfaces
CUT-TEPAK	0.26	partially vegetated surface	0.36	moderately vegetated surface
Eforie	0.36	moderately vegetated surface	0.43	moderately vegetated surface
FORTH_CRETE	0.39	moderately vegetated surface	0.45	moderately vegetated surface
IMS-METU-ERDEMLI	0.41	moderately vegetated surface	0.47	moderately vegetated surface
Sevatopol	0.35	moderately vegetated surface	0.47	moderately vegetated surface
Thessaloniki	0.36	moderately vegetated surface	0.44	moderately vegetated surface
TUBITAK_UZAY _Ankara	0.28	partially vegetated surface	0.26	partially vegetated surface
Xanthi	0.50	densely vegetated surfaces	0.53	densely vegetated surfaces

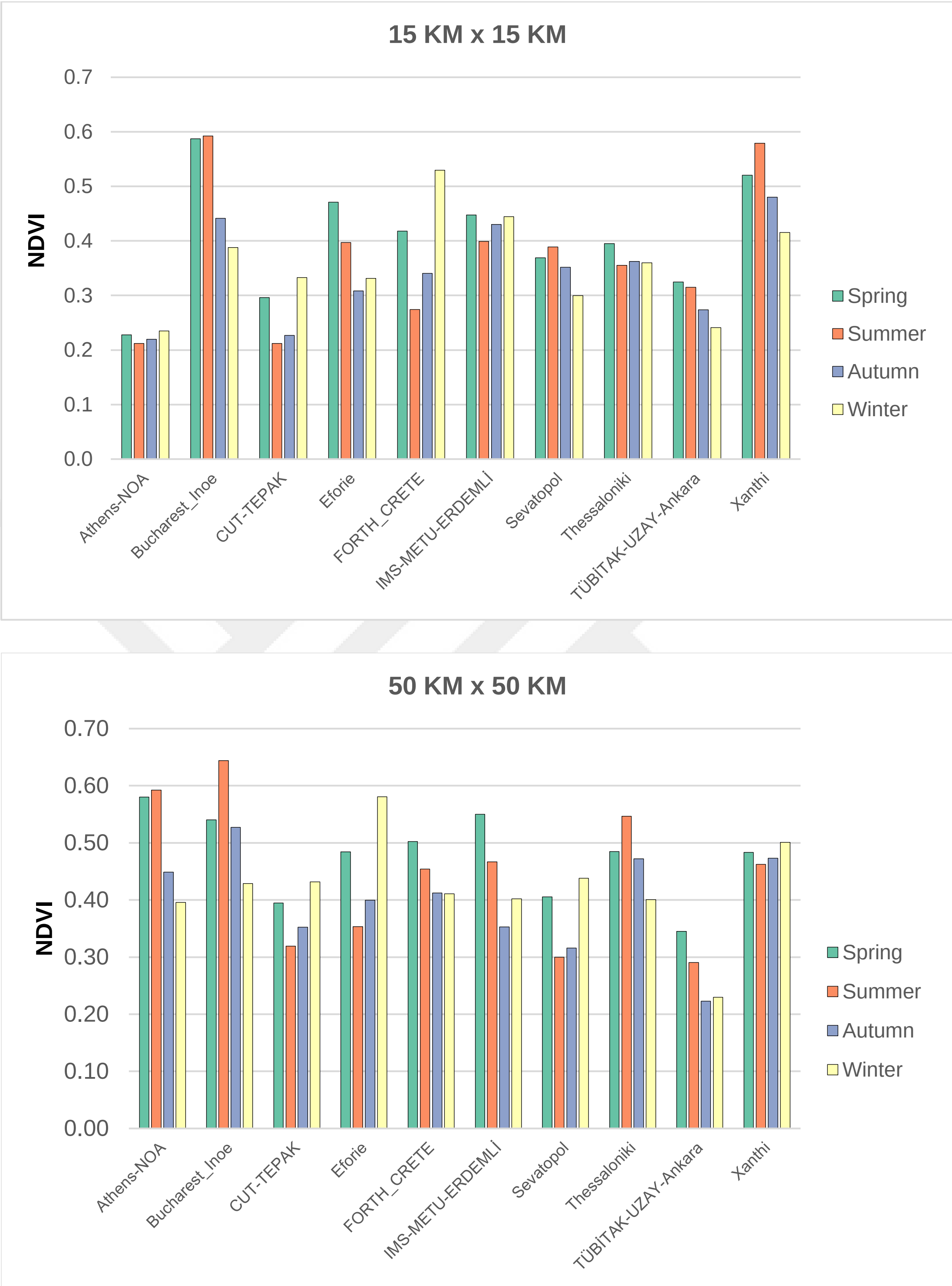

Figure 3.4 Variations of seasonal NDVI values in the study area

All datasets and their sources used in this study were summarized in Table 3.3.

Table 3.3 Summary of all datasets used in the study

Data	**Scientific Data Set**	**Level**	**Collection**	**Dataset**	**Spatial and temporal resolution**
MODIS	AOD_{550}	Level 2	C6.1	MOD/MYD04 DT	Daily, 10 km
	AOD_{550}	Level 2	C6.1	MOD/MYD04 DB	Daily, 10 km
	AOD_{550}	Level 2	C6.1	MOD/MYD04 DT	Daily, 3 km
	NDVI	Level 2	C6	MOD/MYD13A1	Monthly, 1 km
AERONET	AOD_{500}	Level 2	Version 3	AERONET	15 minute, point

3.2 Validation of MODIS AOD Data Using AERONET Observations

MODIS AOD data is required to remain within the standard expected error (EE) ratios for being usable in a region. Therefore, in this study, all the expected errors were calculated for all datasets obtained from MODIS. Accordingly, the expected error is defined as ±0.05 + 15% x $AOD_{AERONET}$ for DT algorithm with Level 3 quality and 10 km spatial resolution (Levy et al., 2013). In order for AOD data obtained through this algorithm to be usable the expected error is required to remain above 66% (Gupta et al., 2018). The expected error is ±0.05 + 20% x $AOD_{AERONET}$ for the DT algorithm with 3 km resolution (Gupta et al., 2018). The expected error is defined as ±0.03 + 20% x $AOD_{AERONET}$ for DB products (Wei et al., 2019).

Validation process was carried out for the same period and same geographical location. Therefore, the method suggested by Ichoku et al. (2002) and detailed in Section 2.3 were used for matching the data from MODIS and AERONET whose data structure are different from each other. This matchup and validation processes were carried out on the station-base using MATLAB and R programming languages.

Statistical indicators including the correlation coefficient (R), the Relative Mean Bias (RMB), the Root Mean Square Error (RMSE) were used to quantify the accuracy of MODIS data against AERONET ground measurements. Expected errors were calculated in terms of the part (ratio) remained within the expected error values (= EE), below (< EE) and above (> EE). As the performances of AOD products differ seasonally, all statistical evaluations were also calculated on the basis of seasons. The statistical equations used in the study were given below:

$$RMSE = \sqrt{\frac{1}{n}\sum_{i=1}^{n}(AOD_{MODIS} - AOD_{AERONET})^2} \tag{3.2}$$

$$RMB = \overline{AOD_{MODIS}} \Big/ \overline{AOD_{AERONET}} \tag{3.3}$$

$$EE_{DT-3KM} = \pm 0.05 \pm 0.20 AOD_{AERONET} \tag{3.4}$$

$$EE_{DT-10KM} = \pm 0.05 \pm 0.15 AOD_{AERONET} \tag{3.5}$$

$$EE_{DB-10KM} = \pm 0.03 \pm 0.20 AOD_{AERONET} \tag{3.6}$$

CHAPTER FOUR
RESULTS

4.1 Evaluation of the AOD Products from MODIS and AERONET

4.1.1 Retrieval Statistics of AERONET AOD in Turkey

In this study, the AERONET measurements were available for January 2004-December 2019 period from IMS-METU-ERDEMLI site and for December 2009-April 2012 period from TUBITAK_UZAY_Ankara site. Table 4.1 gives the summary of statistical indicators for data from these two stations.

Table 4.1 Statistical summary of AOD_{500} from two AERONET sites in Turkey

AOD_{500}	IMS-METU-ERDEMLI	TUBITAK_UZAY_Ankara
N	92376	13203
Available N	92343	13198
Mean	0.248	0.200
SD	0.147	0.097
Median	0.217	0.188
Min	0.017	0.035
Max	1.870	1.060

N: Total number of data, SD: Standard deviation, Min: Minimum value, Max; Maximum value

The total available number of AOD_{500} data the period of 2004-2019 was 92343 at the IMS-METU-ERDEMLI site, while this number was 13198 at the TUBITAK_UZAY_Ankara site. The annual variation of number of available AOD_{500} data at the coastal and urban sites are shown in Figure 4.1. In the IMS-METU-ERDEMLI site, most data were obtained in 2008 and 2009, while the least data was obtained in 2012 and 2019. In the other years of concern, number of available data was generally ranging from 4000 to 8000. The highest number of data was observed in 2010 and 2011 at the TUBITAK_UZAY_Ankara site. It was found that annual number of data at the site in these years were close to the number of data obtained in the IMS-METU-ERDEMLI site. These results indicated that the annual numbers of data are consistent with the literature (Meij & Lelieveld, 2011; Mallet et al., 2013; Nabat et al., 2013; Ningombam et al., 2019; Logothetis et al., 2020; Xu et al., 2020).

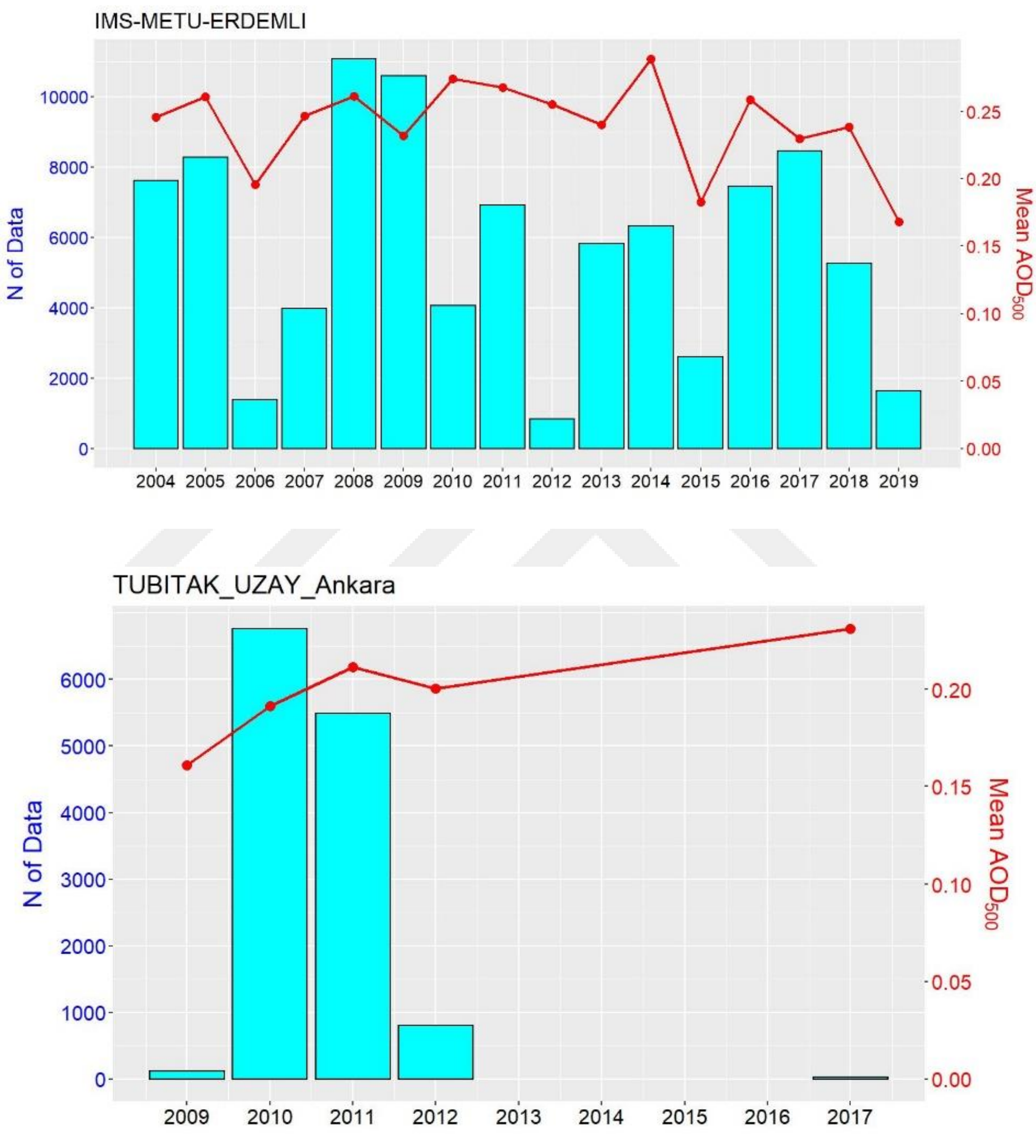

Figure 4.1 Annual variation of data numbers and mean AOD_{500} values at two sites in Turkey

The annual mean AOD_{500} values ranged from 0.17 to 0.29 at the IMS-METU-ERDEMLI site, while the annual mean AOD_{500} value ranged from 0.16 to 0.23 at the TUBITAK_UZAY_Ankara site (Table A1.6). Similar annual mean AOD_{500} values (except for 2006, 2015 and 2019) were obtained at the IMS-METU-ERDEMLI site. No significant change was observed for the mean AOD_{500} values between 2010 and 2011 at the TUBITAK_UZAY_Ankara site. The mean AODs were low in 2009 due to short service period in winter, while the number of measurements were high in 2017 because of short service period in the summer. In general, it was observed that higher AOD_{500} values were obtained in the rural sites compared to the urban sites.

Figure 4.2 shows the monthly variations of AOD_{500}. The number of AOD_{500} data was the highest in summer at both sites. The highest AOD_{500} data was obtained in July, August, and June, while these months were followed by the months of spring and autumn seasons, such as April, May, September and October. Lowest values were observed in the winter months (mainly January and December). This is mostly due to meteorological factors such as cloud cover and precipitation that are common in the atmosphere during winter. The influence of dust transported from North Africa and Middle East deserts during spring and summer was available in the IMS-METU-ERDEMLI site. It was known that this situation causes high AOD_{500} values (0.34 in August, 0.32 in July, 0.29 in June) at the station (Kubilay et al., 2000; Kubilay et al., 2005). The highest AOD values were obtained in summer (0.27 in August, 0.25 in July) and winter season (0.22 in February, 0.21 in December) at the TUBITAK_UZAY_Ankara site. It was found that AOD increased in winter at the TUBITAK_UZAY_Ankara site attributed to coal burning in residential areas.

Since AERONET AODs at 550 nm are not present, AOD was interpolated from 500 nm into 550 nm based on the Angstrom exponent at 440–675 nm ($AE_{440\text{-}675}$) (Wei et al., 2019). The mean AOD_{500} and $AE_{440\text{-}675}$ values at the two AERONET stations for the period of 2004-2019, and the AOD_{550} values calculated according to Equation 3.1 were statistically summarized in Table 4.2. After the interpolation, the AOD_{550} values generally decreased compared to the AOD_{500} values. The annual mean AOD_{550} value ranged from 0.15 to 0.26 at the IMS-METU-ERDEMLI site, while the annual mean AOD_{550} value ranged from 0.14 to 0.21 at the TUBITAK_UZAY_Ankara site. The annual, seasonal, and monthly variations of the AOD_{550} data were exactly the same as the AOD_{500} data.

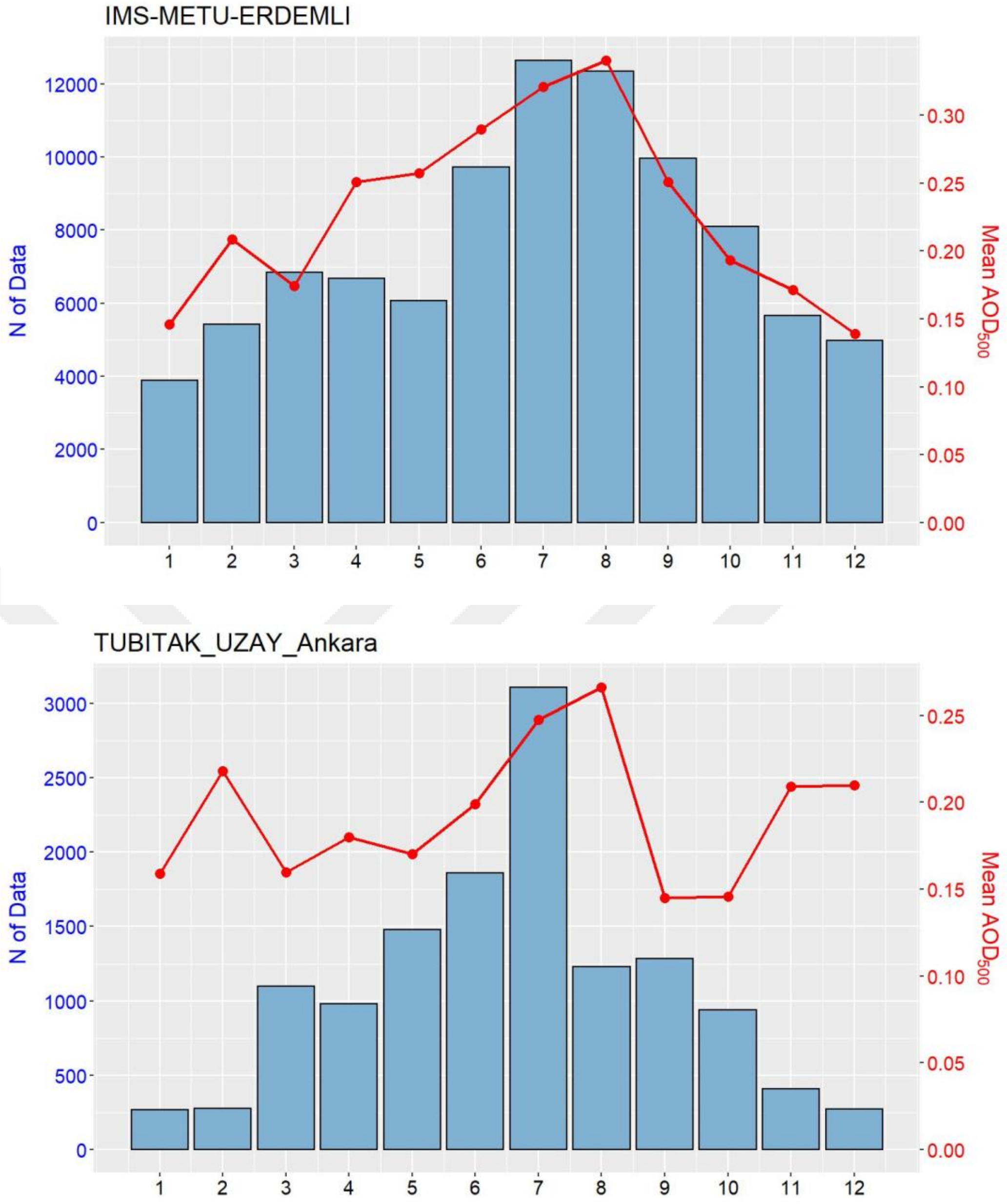

Figure 4.2 Seasonal and monthly variations of AOD_{500} over two sites in Turkey

Table 4.2. Statistical summary of AOD_{500}, $AE_{440-675}$ and interpolated AOD_{550} in two sites in Turkey

	IMS-METU-ERDEMLI			**TUBITAK_UZAY_Ankara**		
	AOD_{500}	**$AE_{440-675}$**	**AOD_{550}**	**AOD_{500}**	**$AE_{440-675}$**	**AOD_{550}**
Mean	0.248	1.350	0.220	0.200	1.460	0.175
SD	0.147	0.349	0.134	0.097	0.346	0.086
Median	0.217	1.420	0.191	0.188	1.540	0.163
Min	0.017	-0.104	0.014	0.035	0.051	0.029
Max	1.870	2.830	1.850	1.060	2.300	1.030

4.1.2 Retrieval Statistics of Terra and Aqua MODIS AOD for Turkey

AOD data at 550 nm wavelength obtained by MODIS instrument of Terra and Aqua satellites was provided for the period of 2002-2019. In this study, the performances of the MODIS Terra and Aqua AOD retrievals were compared on a local scale against two AERONET sites located at urban (TUBITAK_UZAY_Ankara) and rural (IMS-METU-ERDEMLI) areas. Product and site-based analysis was carried out by comparing the urban and rural observations with the MODIS retrievals. Performance of the C6.1 Terra and Aqua-MODIS DT and DB AOD_{550} retrievals at 3 km and 10 km spatial resolutions were investigated. Numbers of AOD_{550} data obtained in rural and urban areas between 2002 and 2019 were given in Figure 4.3.

It was observed that the number of data varies according to the regions, satellites, and algorithms. The DT retrievals had more data in rural areas for both satellites. The number of data was approximately 2.5-3 times higher than the number of the DB algorithm data. Previous studies have shown that the DT algorithm produced more data than the DB algorithm in rural areas with high vegetation density (Sayer et al., 2014; Bilal et al., 2019; Wei et al., 2019). However, the DB algorithm was successful in urban areas. In the studies carried out in Beijing, China which is the one of the largest urban centers in the world, the DB algorithm was preferred due to the density of many urban stations in China and the low vegetation index of the studied land (Tian et al., 2018). The DB algorithm gave the similar result in Turkey.

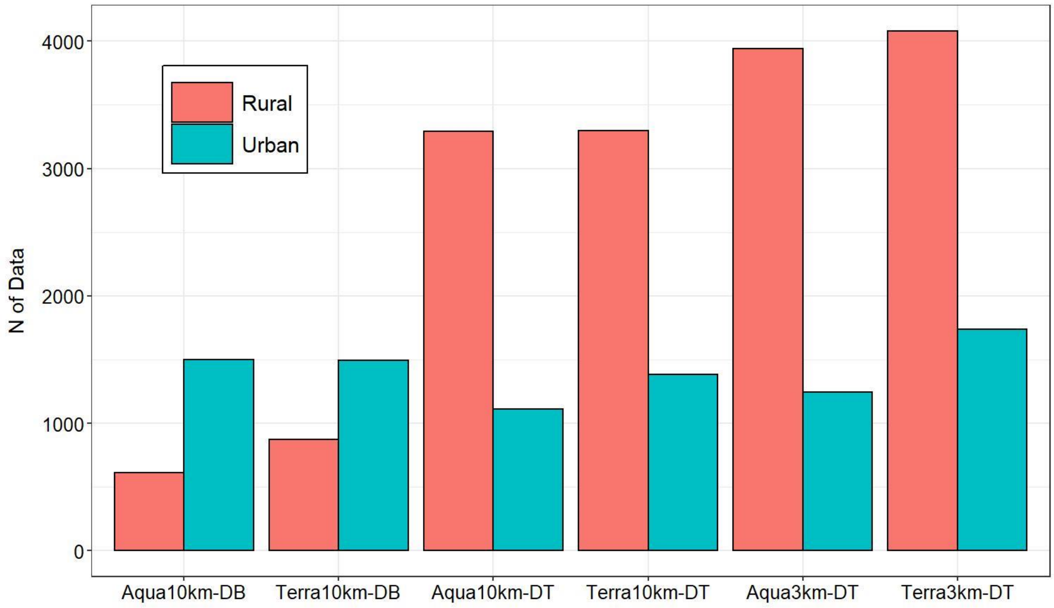

Figure 4.3 The number of AOD_{550} data for Terra and Aqua-MODIS over urban and rural sites

Spatial resolution in the AOD data obtained from satellites was found to be another important factor determining the numbers of data. For both satellites, it was found that products with 3 km resolution had more data than the ones with 10 km resolution. Therefore, in this study, the DT 3 km products were the algorithm-product match that provided the most AOD_{550} data. On the other hand, the DB 10 km products provided the lowest data for the the area. Annual and monthly changes of number of available data according to satellites, algorithms, and spatial resolutions are given in Figure 4.4 and Figure 4.5. The results showed that for both regions there was no significant difference between the numbers of data on yearly basis, but it does differ on the basis of months. The number for the DT was the largest for the months of summer season such as June, July, and August, while for the winter season namely December, January, and February had the smallest numbers of data. The number of data obtained in autumn was higher than in spring especially for products with 3 km product. The temporal differences in numbers of data depended on the varying vegetation index of the regions and atmospheric factors such as precipitation and cloud cover (Bilal et al., 2017; Che et al., 2019). In the previous studies conducted in different regions, fewer number of data was observed due to high precipitation, cloud cover, and low NDVI value. On the other hand, the high numbers of data were reached when cloud cover is low and vegetation is dense in the atmosphere (Bilal et al., 2017; Tian et al., 2018; Che et al., 2019; Wei et al., 2019). These results of the literature are compatible with the results of this study.

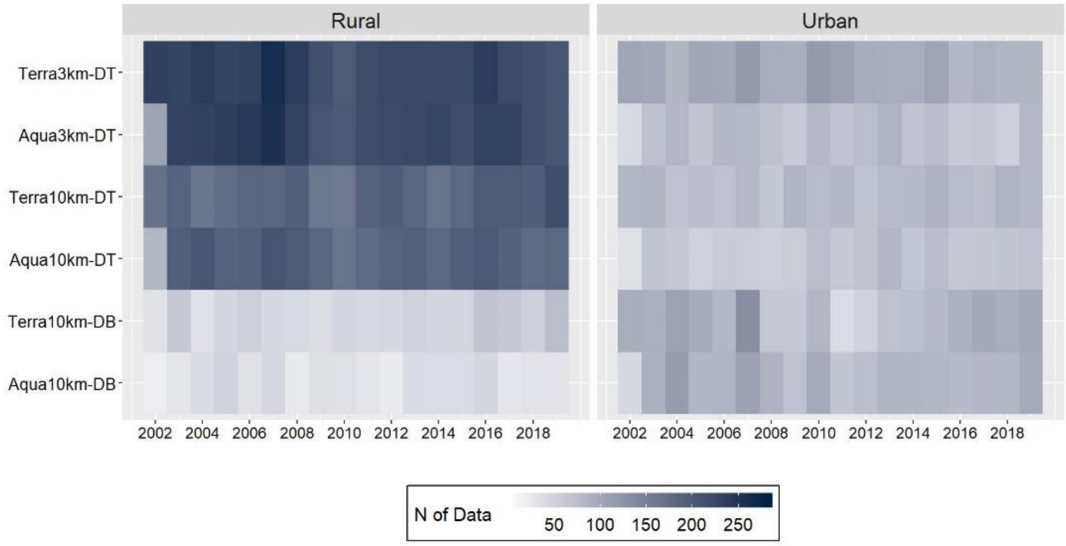

Figure 4.4 Annual variation of AOD_{550} data numbers over the urban and rural sites

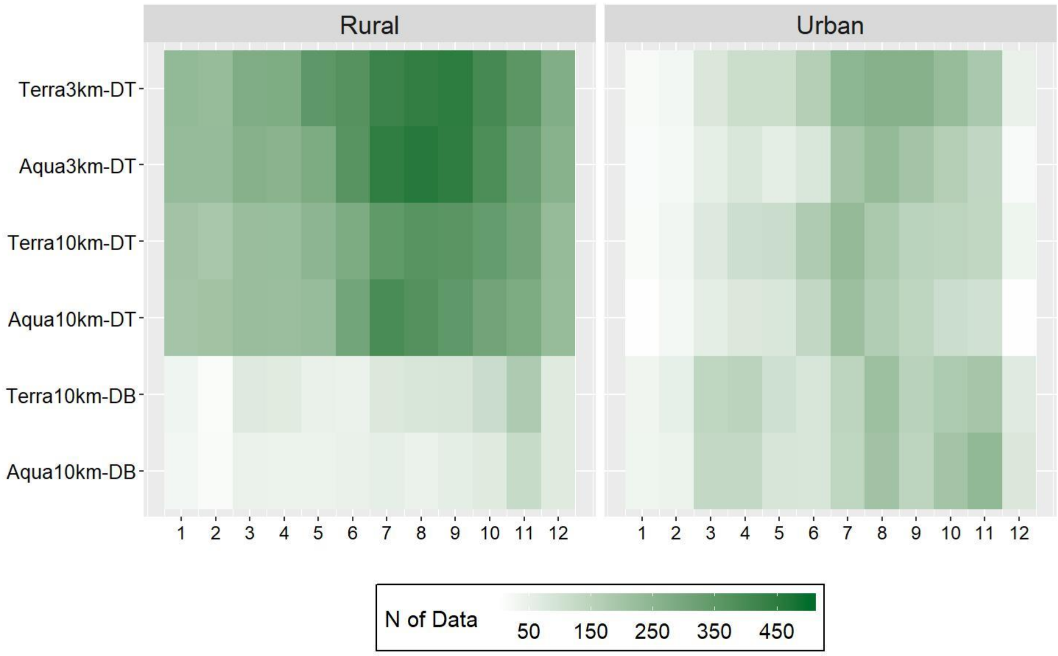

Figure 4.5 Monthly variation of AOD_{550} data numbers over the urban and rural sites

Terra and Aqua satellites cannot always generate a usable AOD data at a location on the earth. Atmospheric clouds, precipitation and humidity are key factors that influence the number of retrievals for both satellites. It is known that this situation occurs more frequently especially during winter months. Within the scope of this study, the lost (unavailable) data rates of satellites by years, seasons, and months were calculated in two separate locations representing urban and rural areas. Data losses were similar on the basis of years and algorithms. While the least data loss was obtained with DT algorithm in rural areas, there were also considerable data loss with the products obtained with DB algorithm in the same region. In the study, data loss rates for DT products were ranging 33-48% on annual basis in the rural site. Same rates were reached very high values as 71-87% in the urban area. The data loss value for the products using DB algorithm reached the highest values and increased to 78-93% especially in the rural area. These rates were ranging 56-87% in the urban area. In summary, DT algorithm was found to be more successful in rural areas. On the other hand, the performance of the DB algorithm in the urban area was found to be better.

The long-term mean AOD_{550} obtained in both regions for the period of 2002-2019 are shown in Figure 4.6. The higher AOD values were obtained from the DT algorithm compared to the DB algorithm. The long-term mean AOD_{550} values were 0.2 and 0.3 over both sites while the mean AOD_{550} values for the DB algorithm stayed between 0.09 and 0.17. Higher AOD_{550} values were obtained in urban areas with both DT and DB algorithms. When Terra and Aqua satellites were compared, it was found that slightly higher AOD_{550} values were obtained from the Terra satellite for both regions when compared to the Aqua satellite. Additionally, as it was stated in the literature of previous studies, DT 3 km products were observed to generate higher values than the DT products of 10 km (Zheng et al., 2019; Wei et al., 2020). Again, from the literature of previous studies, it is known that the 3 km product has a high tendency to give overestimate, especially in urban areas (Gupta et al., 2018; Wei et al., 2020). The annual variation of product based mean AOD_{550} values for both satellites were given in Figure 4.7. It was found that the AOD_{550} data obtained from the Terra satellite were greater than the Aqua satellite in all years.

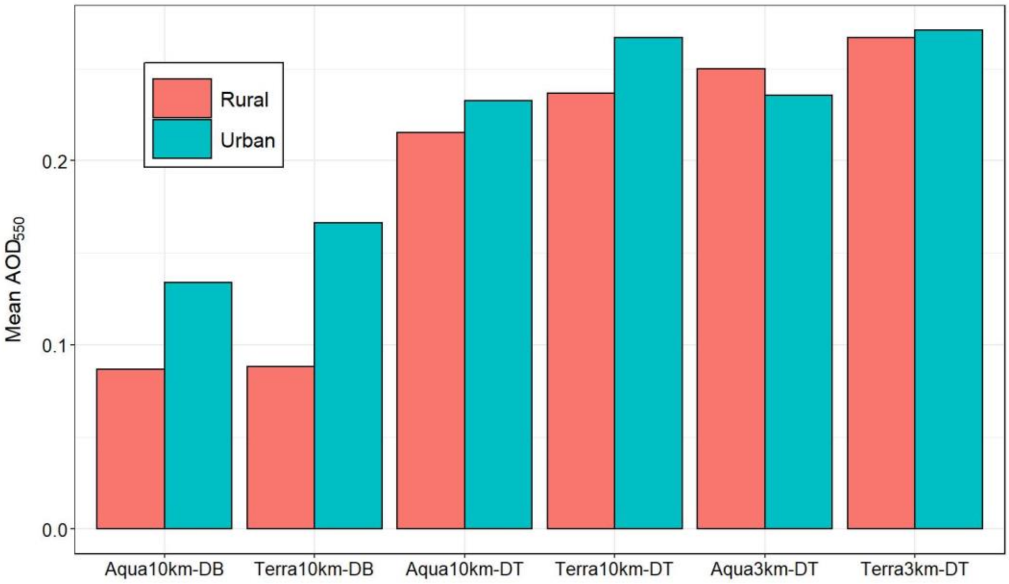

Figure 4.6 Multiannual mean Terra and Aqua-MODIS C6.1 AOD_{550} retrievals over rural and urban sites

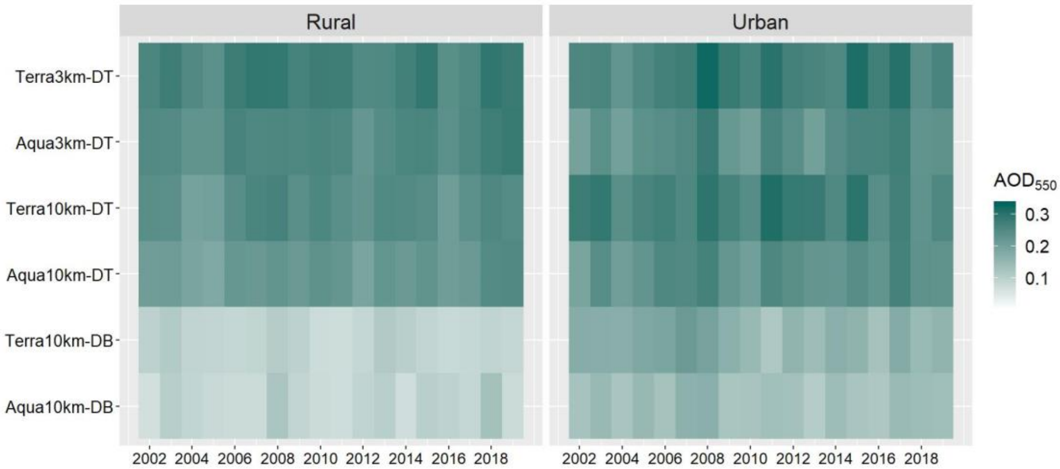

Figure 4.7 Annual mean Terra and Aqua-MODIS AOD_{550} retrievals over the rural and urban sites in Turkey

For both regions, the highest mean AOD_{550} was observed in summer while the lowest mean AOD_{550} was observed in winter (Figure 4.8). Relatively less cloud coverage under the prevailing meteorological conditions is the cause of observing the highest mean AOD_{550} in summer, while observing the lowest mean AOD_{550} in winter is due to precipitation (Tutsak & Kocak, 2020). High AOD_{550} values were more common in the urban area during the months of summer season, when compared to other seasons. It was observed that the rural area had higher mean AOD_{550} values than the urban area due to the dust transportation in the spring and summer months. Some studies from literature supported these results (Kubilay et al., 2003; Tutsak & Kocak, 2019; Tutsak & Kocak, 2020).

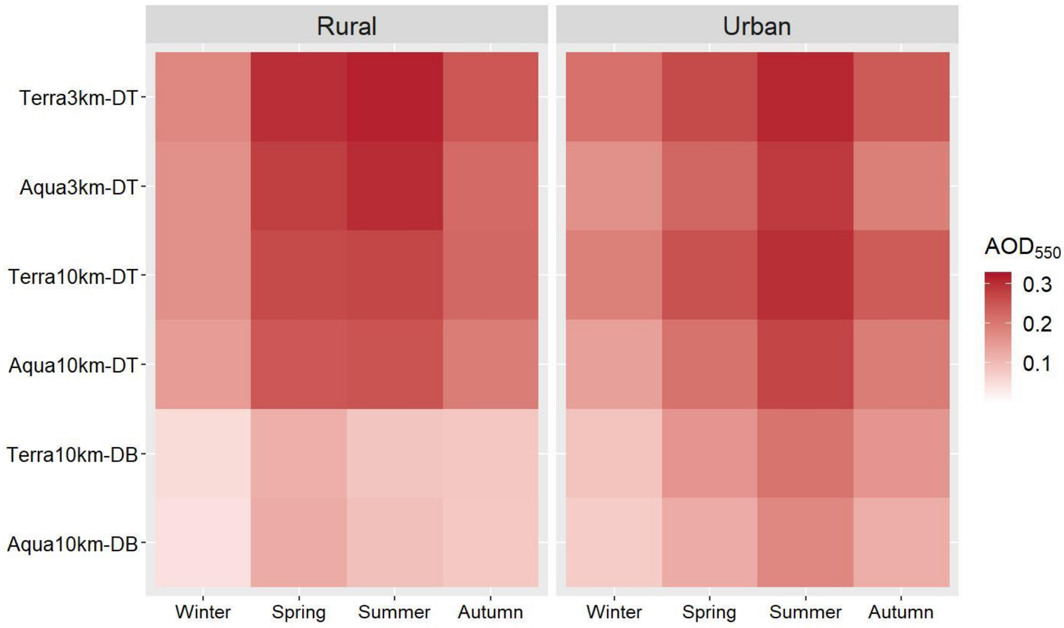

Figure 4.8 Seasonal mean Terra and Aqua-MODIS AOD550 retrievals over the rural and urban sites in Turkey

The long-term monthly mean AOD_{550} values were given in Figure 4.9. The high AOD_{550} values were observed in April and May in the rural area. AOD_{550} values were also high in the summer months such as June, July, and August due to the dust transportation and high temperature in the area (Ozdemir et al., 2020; Tutsak & Koçak, 2020). After December, a gradual increase in AOD_{550} values was observed due to the decrease of precipitation in the region (Tutsak & Koçak, 2020). Similar to the behaviour of DT algorithm, high AOD_{550} values were obtained in March, April, and August with the DB algorithm. In the urban area, July, August, and September had stand out with high values.

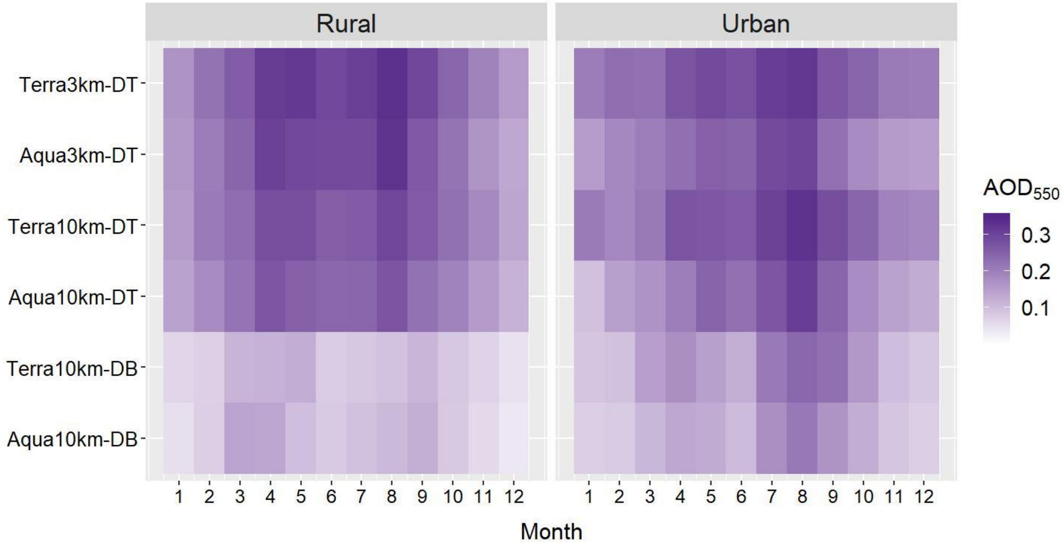

Figure 4.9 Multiannual monthly mean Terra and Aqua-MODIS AOD_{550} retrievals over the rural and urban sites in Turkey

4.1.3 Collocation of AERONET and MODIS AOD over the Study Area

Ten AERONET sites in the eastern Mediterranean and the Black Sea were selected in this study. Two of them are in Turkey and the remaining sites are in the neighboring countries having different NDVI values. The annual variation of number of usable AOD_{550} data and mean values at ten sites were given in Figure 4.10. It was observed that most of the sites had discrete measurements between 2004-2019, just like the TUBITAK_UZAY_Ankara site in Turkey. On the other hand, it was found that the stations of Thessaloniki and Athens-NOA in Greece, Eforie in Romania and FORTH_CRETE in Crete Island were continuously operated like the IMS-METU-ERDEMLI site in Turkey. Since there are only few months of available data in some years, while the annual mean AOD_{550} values at the stations were close to each other, it was observed that very high or low mean AOD values were obtained in some stations. It was found that monthly changes at all sites were similar and the highest number of data was reached in July and August. These months were followed by May and June. The least number of data were observed in December and January. Unlike other sites, the stations in the Mediterranean region such as ATHENS-NOA, CUT-TEPAK, FORTH_CRETE and Xanthi were known to be affected by dust transport.

These sites had high AOD values in spring as in summer (Ozdemir et al., 2020). The monthly data numbers and mean AOD_{550} values of the sites were given in Figure 4.11.

The variations of annual, seasonal, and monthly AOD_{550} data obtained from MODIS were given in Figures 4.12 and 4.13. Among the stations, Athens, Thessaloniki, and Sevastopol are in urban area, like TUBITAK_UZAY_Ankara site in Turkey. The other five sites are in coastal rural sites as the IMS-METU-ERDEMLI site in Turkey. According to the results obtained, the most similar station to the rural area (IMS-METU-ERDEMLI) in Turkey has been the rural area in Cyprus (CUT-TEPAK) where the Technology University was located. The highest number of data was obtained in these two regions with the DT algorithm. On the other hand, the regions where the least was data obtained with DB algorithm were also these two stations. While more data was in rural areas with the DT algorithm, it was observed that DB algorithm was successful in generating data in urban areas. For all the regions, the number of data obtained from the Terra satellite was higher than the Aqua satellite. DT data with a spatial resolution of 3 km was obtained as the algorithm-product match with the highest data number. The ATHENS-NOA station located in a high-altitude area close to Athens city center, had the minimum number of data with 3 km spatial resolution DT algorithm. Since most sites studied were in rural areas and the vegetation index of these regions was high, the number of data obtained by the DB algorithm was quite low. Despite the regions in Athens and Cyprus Limassol (CUT-TEPAK) had very similar vegetation indexes, it was observed that the algorithms did not give similar results for these regions. The stations in Bucharest and Thessaloniki had similar numbers of data with all algorithms. The results showed that AOD values did not change on the basis of algorithms in both regions studied in Romania.

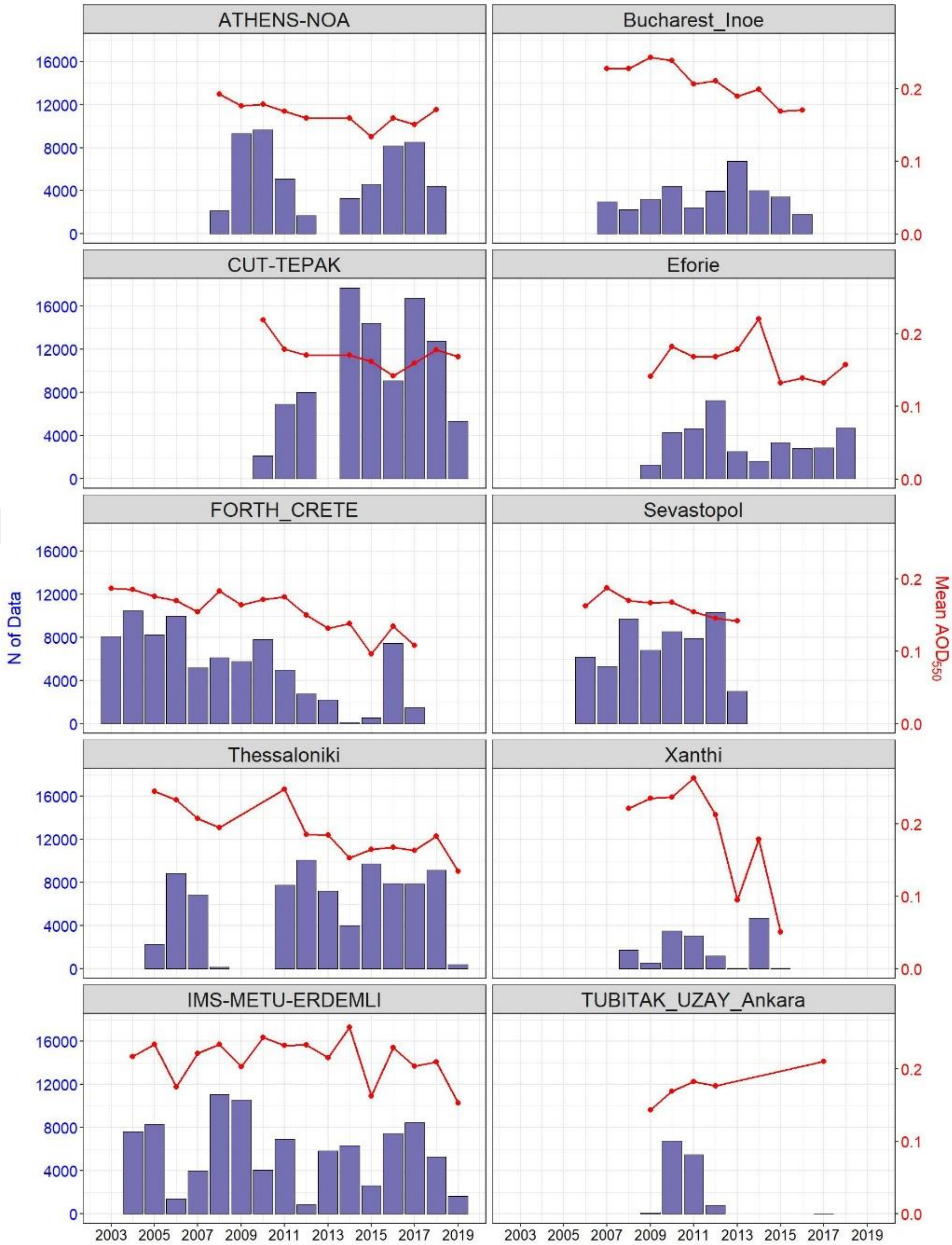

Figure 4.10 Annual mean AOD_{550} values and available data numbers in the ten AERONET sites

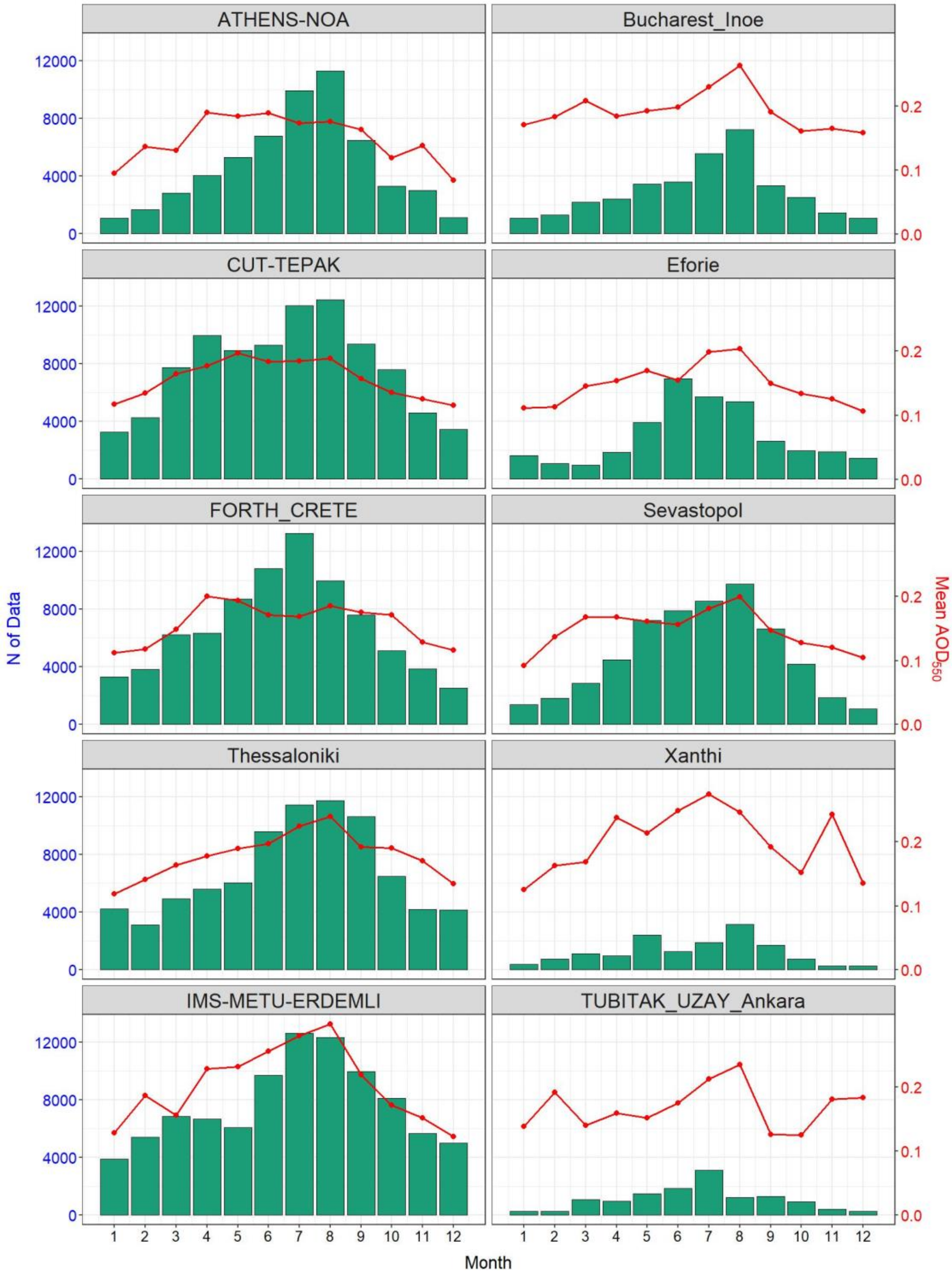

Figure 4.11 Multiannual monthly mean AOD_{550} values and available data numbers in the ten AERONET sites

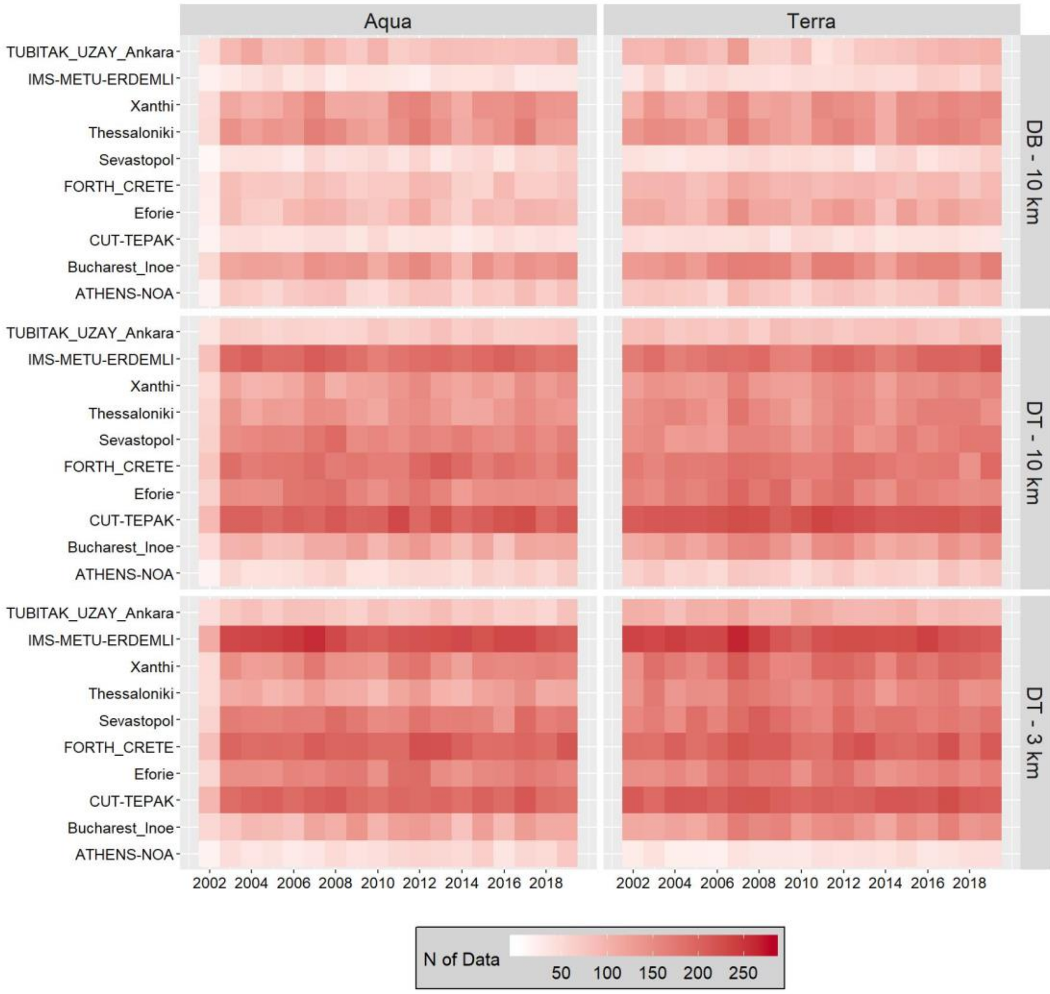

Figure 4.12 Annual numbers of Terra and Aqua MODIS C6.1 AOD retrievals in the ten AERONET sites

The annual variation of algorithm based AOD data obtained from MODIS was given in Figure 4.14. It was observed that the mean AOD values by years were very close to each other in all regions (except Athens) and the values generally vary between 0.1 to 0.3. Figure 4.15 shows the monthly variation of MODIS AOD data. Large AOD values were observed especially in March-April for both satellites, while in September and October the high AOD values were obtained from Terra satellite. The high AOD values were observed in July and August like AERONET data, and the low values were observed in winter months such as December and January. The AOD values were slightly higher in February compared to other months of winter. This situation was confirmed by MODIS data at these points that were known to be affected by dust transports from desert. For example, the higher values were observed with DB algorithm in Crete for the months of spring season, like April. The lower AOD values in the Bucharest site were obtained in December and January when compared with other regions. In the region, the high AOD values were observed in summer while the low values were observed in winter. In the regions as Athens, Thessaloniki, Limassol, and Crete Island which are known to be dusty, high values were observed in the spring season with the DT 10 km. While similar trends were observed in the same regions with 3 km data, except for winter, very large AOD values were observed for Athens when compared to other regions.

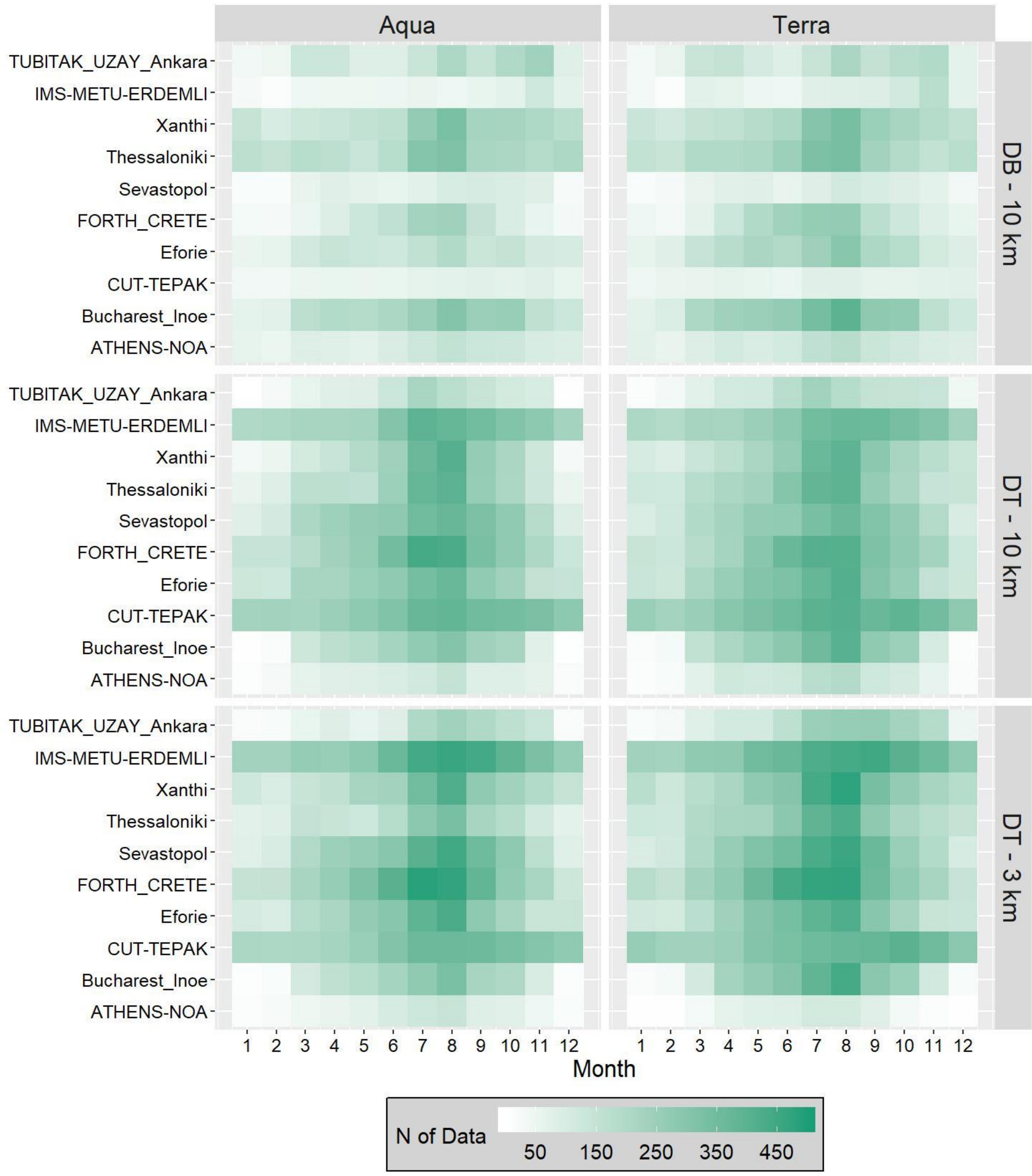

Figure 4.13 Monthly numbers of Terra and Aqua MODIS C6.1 AOD retrievals in the ten AERONET sites

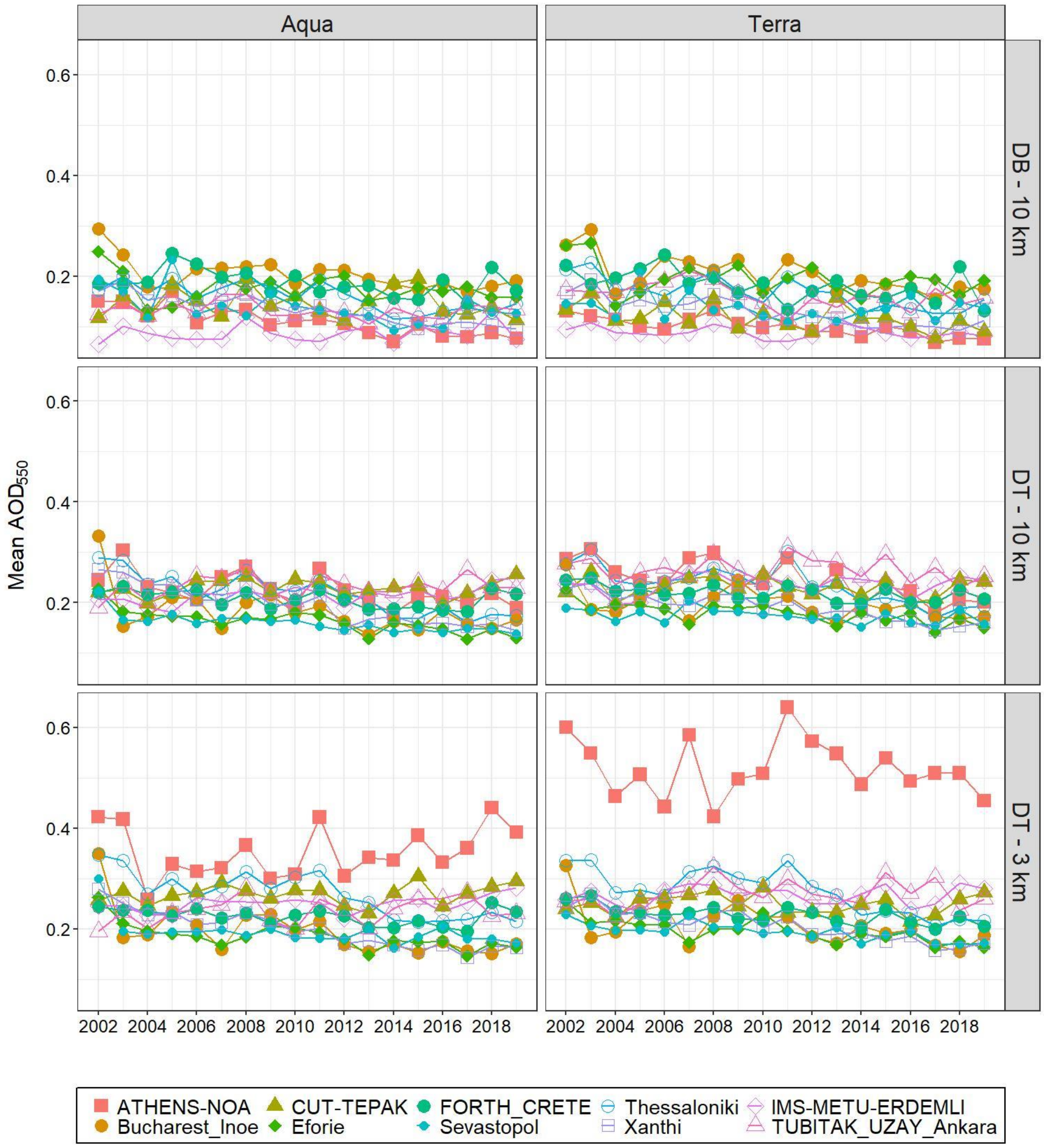

Figure 4.14 Annual variations of MODIS AOD_{550} values in the ten AERONET sites

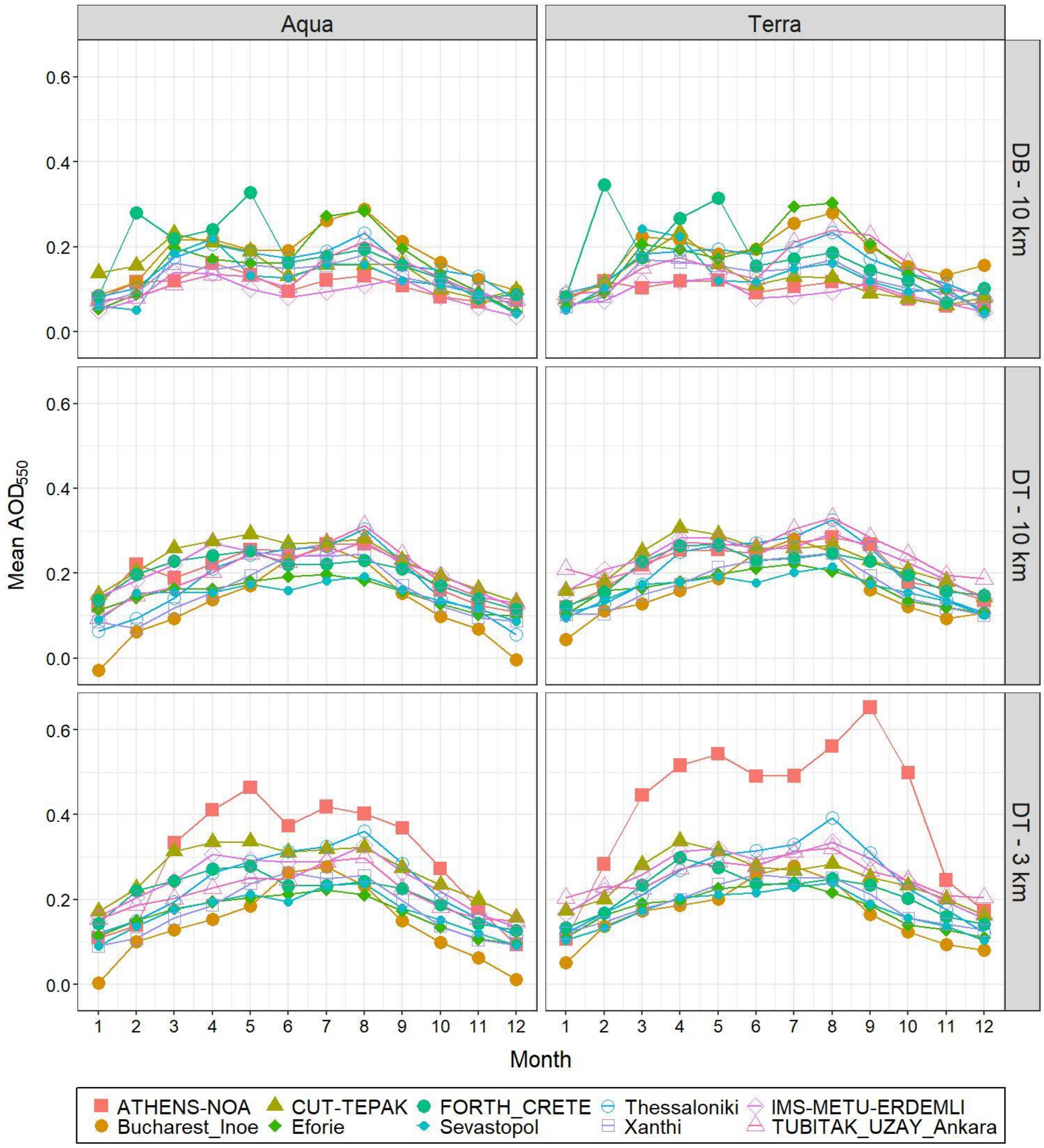

Figure 4.15 Multiannual monthly variations of MODIS AOD_{550} values in the ten AERONET sites

4.2 Validation of MODIS AOD Retrievals with AERONET

4.2.1. Assessment of Accuracy

Table 4.3 showed the overall accuracy of Terra and Aqua MODIS C6.1 DT and DB retrievals against the AERONET AOD observations over the coastal and urban sites in Turkey. The validations were done for the period of 2002–2019. Product-based validation results differed by regions. The difference in the number of data between the two regions was mainly due to the difference in the operating periods of the stations (Table 3.1). Considerably high differences between numbers of data between DT and DB algorithms were observed in the rural area. In rural region the highest number of data was obtained with the Terra satellite and DT-3km product (Table 4.3). When the correlation coefficients (R) examined, it was observed that greater values are obtained in the rural area for all products. In accordance with this, it was observed that the DB products for the rural area and the DT products for the urban area had higher RMSE values.

Table 4.3 Overall retrieval accuracy between AOD products in two sites

Station	Product	R	n	RMSE	RMB	mean MODIS AOD	mean AERONET AOD
Rural	Terra3km-DT	0.89	1789	0.08	1.18	0.25	0.21
	Terra10km-DT	0.86	1390	0.07	1.05	0.22	0.21
	Terra10km-DB	0.69	386	0.11	0.47	0.08	0.16
	Aqua3km-DT	0.92	1849	0.07	1.16	0.24	0.21
	Aqua10km-DT	0.90	1493	0.06	0.99	0.20	0.21
	Aqua10km-DB	0.77	304	0.10	0.48	0.07	0.15
Urban	Terra3km-DT	0.77	145	0.13	1.54	0.30	0.19
	Terra10km-DT	0.66	109	0.13	1.54	0.29	0.19
	Terra10km-DB	0.59	80	0.08	0.85	0.15	0.18
	Aqua3km-DT	0.69	81	0.11	1.48	0.24	0.16
	Aqua10km-DT	0.78	80	0.10	1.46	0.24	0.16
	Aqua10km-DB	0.62	88	0.08	0.95	0.14	0.15

n: Number of data

The RMB value is a parameter used to support evaluations of expected error. The RMB values showed that the DB algorithm tends to underestimate in rural areas (0.47-

0.48). At the same time, long-term mean MODIS AOD obtained with DB products were smaller than mean AERONET AOD. The RMB values of DB-10km products obtained near to value 1.0 in the urban area and DB algorithms represents the region with better performance when compared to the DT algorithms. The DT AODs found to be tended to overestimate at the urban site. The accuracy of the DT algorithm was directly correlated with the land cover class and the quality of surface reflectance values. The lower NDVI values contribute higher on surface reflectance and that decrease the quality of retrievals over urban areas (Che et al., 2019; Huang et al., 2019). When the mean MODIS and AERONET AOD data were investigated, it was observed that the 3 km resolution data had higher AOD values than the 10 km data. Previous studies have shown that 3 km dataset were higher AOD values than the 10 km dataset, especially for the urban area (Zheng et al., 2019). In the rural area, the RMB values of near to 1 obtained with DT-10 km products. It was observed that for a multi annual period, mean MODIS and AERONET AODs were closer to each other with DT-10km products than the other products in the rural area.

Within the scope of the study, in addition to other statistical parameters, expected error (EE) values were also calculated to evaluate the accuracy of the MODIS AOD retrievals. Algorithm and region-based EE distribution (within, below and above the EE) were calculated. The number of the retrievals falling within the expected error must be more than 67% (Gupta et al., 2016). The EE values for both regions were given in Figure 4.16. Figure 4.16 shows that there were regional differences in the validation results. Within the expected error (=EE) was greater than 82% at the rural site while less than 50% at the urban site for the DT algorithm (Figure 4.16). AOD data obtained in rural areas with the DB algorithm remained below the expected error (< EE) with 62% for Terra and Aqua satellites. These results are consistent with the RMSE and RMB values for the urban area. The DB 10 km product was the only convenient product for the urban area. No significant difference was observed in Terra and Aqua satellites regarding the expected errors. Figure 4.16 shows that the AOD data obtained from the Terra10km-DB product tended to underestimate (<EE = 22.5%), while Aqua10km-DB product tended to overestimate (>EE = 18.2%). Similar statistics were reported in the previous studies (Tian et al., 2018; Rupakheti et al., 2019; Wei et al., 2019a).

Figure 4.17 shows scatter plots of the AODs obtained from MODIS against the AODs obtained from the AERONET at the rural site (IMS-METU-ERDEMLI). The scatter plots showed that there was no significant difference between the DT products in the rural site, but the 3 km product showed better performance than the 10 km product. Slightly high AOD values were obtained with the Aqua satellite. Correlation coefficients and other statistical parameters showed that the Aqua AOD products indicated relatively better performance with the AERONET AOD than the Terra products. The differences between these two satellites in the same region were also reported in some other studies (Kharol et al., 2011; Wei et al., 2019). Figure 4.18 shows scatter plots of the AODs obtained from MODIS against the AODs obtained from the AERONET at the urban site (TUBITAK_UZAY_Ankara). The Aqua-MODIS AOD data showed better performance. It was also observed that the DT algorithm produced higher AOD values. It was determined that the AOD values obtained from the DB products in rural area were much lower than the AERONET AOD values.

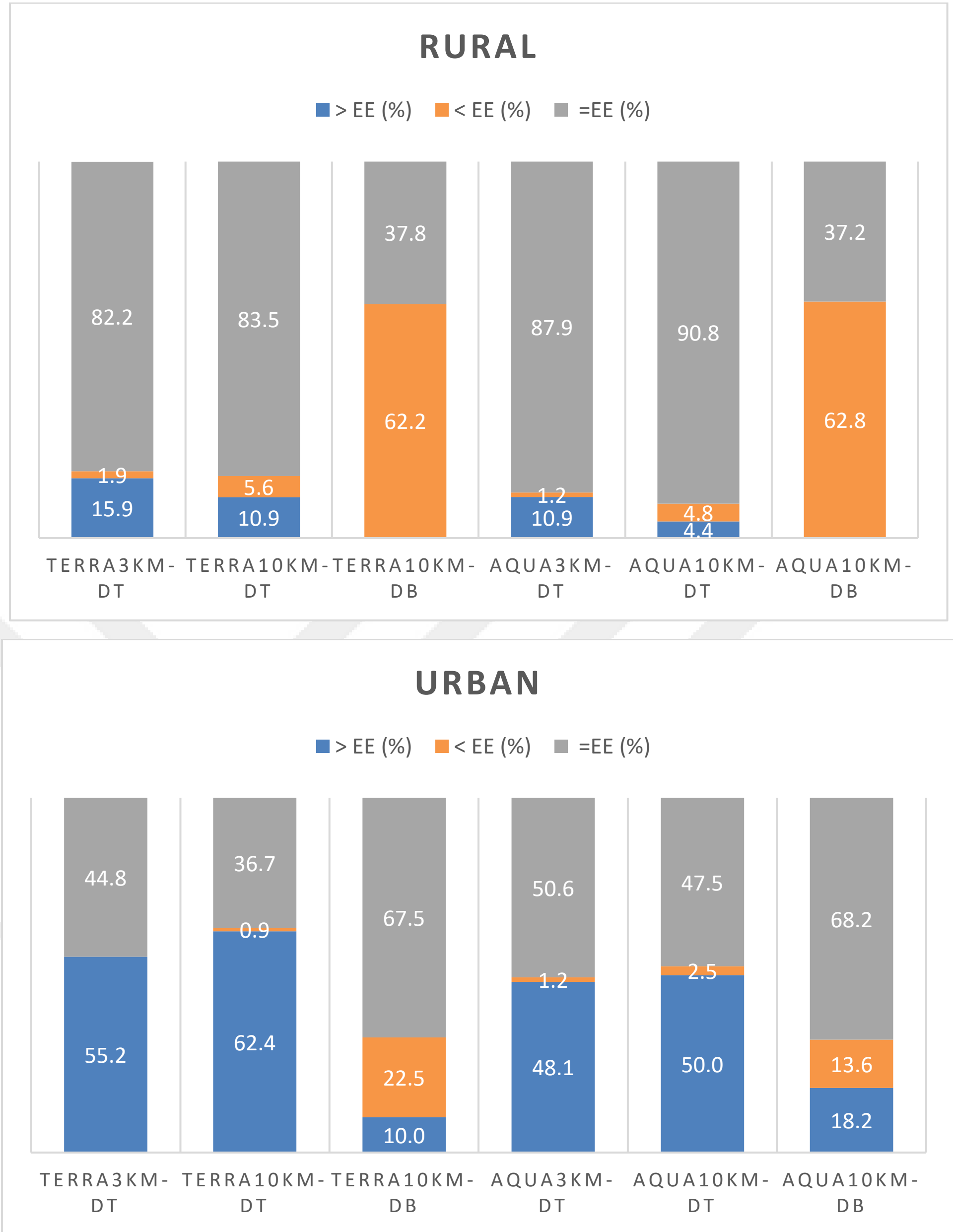

Figure 4.16 The distribution of the expected errors of collocated AODs over the urban and rural sites

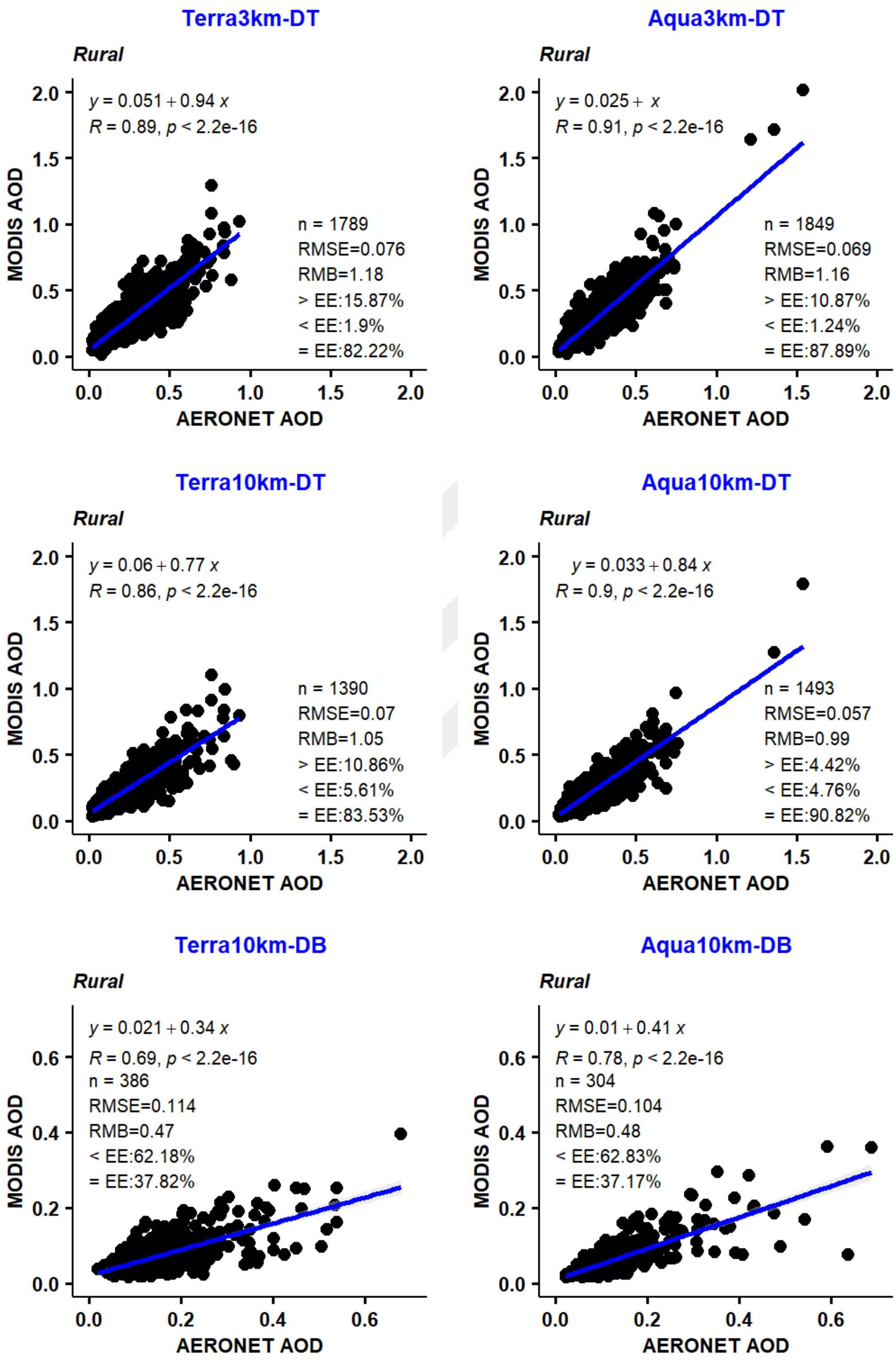

Figure 4.17 Scatter plots of Terra and Aqua MODIS AOD against AERONET AOD over the rural site

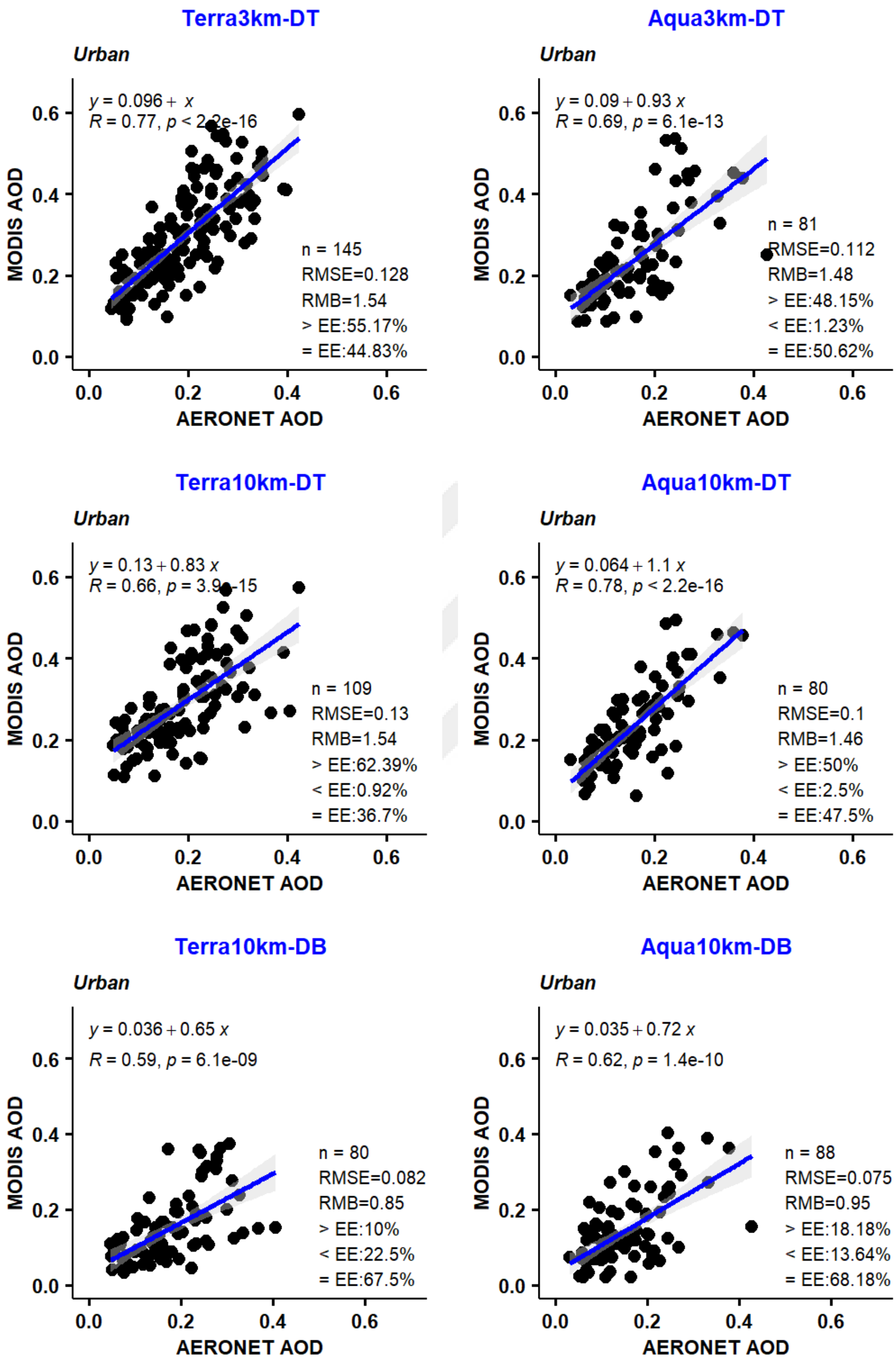

Figure 4.18 Scatter plots of Terra and Aqua MODIS AOD against AERONET AOD over the urban site

Figures 4.19 and 4.20 show the seasonal validation performance of Terra and Aqua MODIS C6.1 DT, and DB AOD retrievals against AERONET AOD measurements across two regions. The highest number of data was obtained in summer with the DT algorithm and in autumn with the DB algorithm. At the rural site, high accuracies were found for all seasons ($p<0.05$). The correlation coefficient (R) did not vary greatly depending on the seasons and the R value ranged from 0.82 to 0.95 for DT algorithm and 0.62 to 0.89 for DB algorithm. High RMSE values were found in spring at the rural site due to the high AOD values. With the DB products, high RMSE values were observed in summer. The RMB values showed that the DT-3km products tended to overestimate in all seasons. The RMB values closer to 1 were obtained in the summer season compared to other seasons. The minimum RMB values for DT-10km product were calculated for both satellites in summer. The Aqua10km-DT product had the best performance among the other DT products. Statistical results indicated that the Aqua10km-DT had higher R values and lower RMSE and close to 1 of RMB. It was observed that the data for DB products tended to underestimate in all seasons. The best seasonal performance was obtained in the spring season with high R and slightly lower RMB values. The validation results showed that the DT-10km product was more convenient than other products in the rural site. Especially, the Aqua satellite showed a more stable performance seasonally compared to the Terra satellite. According to the results, the DB algorithm is not very convenient for use in the region.

Due to insufficient data, the winter season was not included in the seasonal validation studies for the urban station. The highest number of data was obtained in summer with the DT algorithm and in spring with the DB algorithm. Consistent with the number of data, the highest correlation coefficients were also seen for the DT products in summer. Despite of that, the highest RMSE and RMB values were found in summer. Similar to the results of this study, Xia et al. (2013) reported that AODs were predicted more successfully in summer. With the DT algorithms, the RMB values were obtained much more higher values (>1.55) in the months of summer season. Therefore, the DT algorithm tended to overestimate in the urban area. Although higher correlation was found, it was observed that the algorithm was not convenient for aerosol studies in the region.

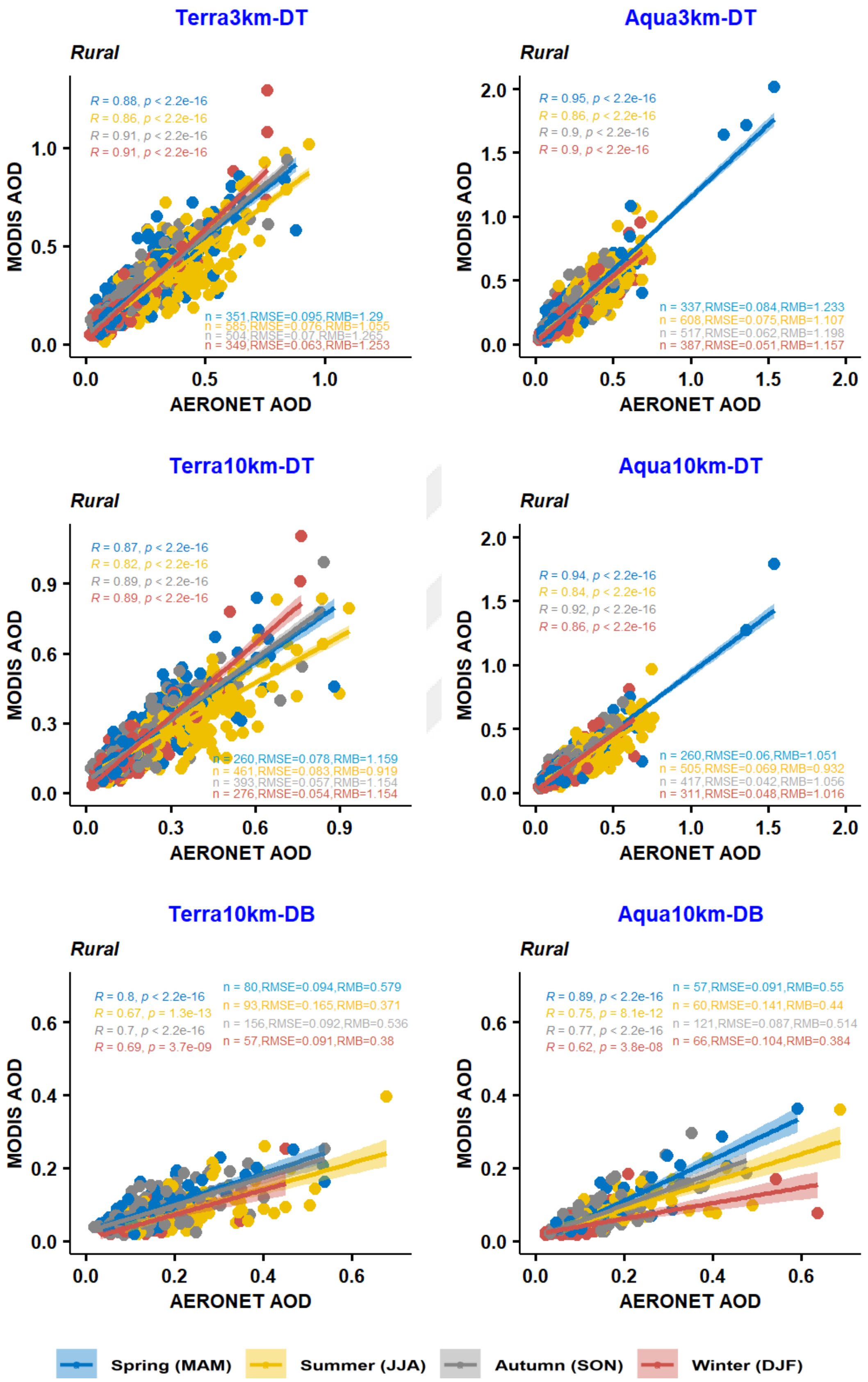

Figure 4.19 Seasonal scatter plots of Terra and Aqua MODIS AOD against AERONET AOD over the rural site

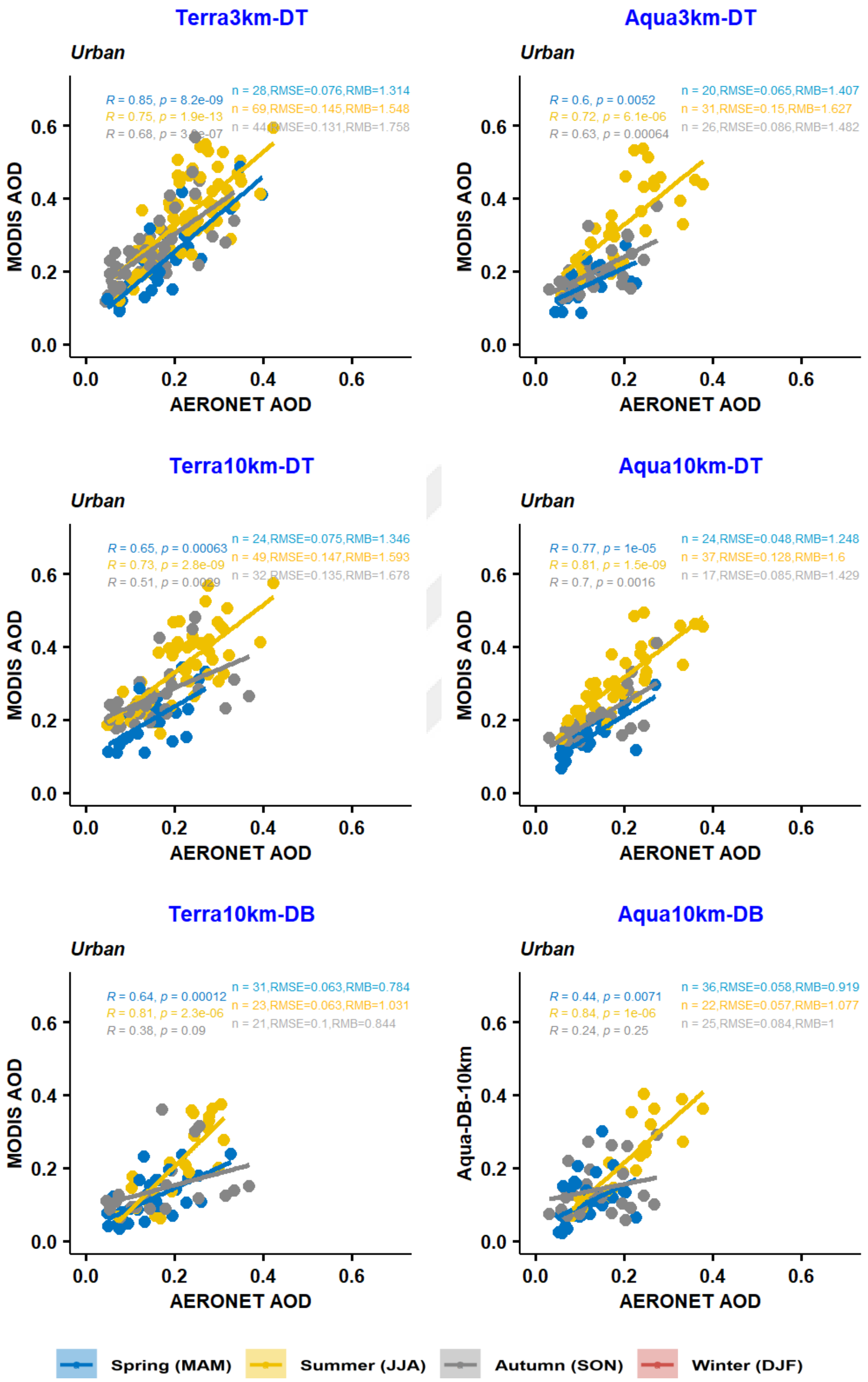

Figure 4.20 Seasonal scatter plots of Terra and Aqua MODIS AOD against AERONET AOD over the urban site

For both satellites, considerably low correlations with the DB algorithm were found in autumn. At the same time, in addition, the higher RMSE values were obtained when compared to other seasons. However, since the RMB values obtained especially from the Aqua satellite was close to 1, it was found that the DB data could represent the region. Terra satellite tended to underestimate during the autumn and spring seasons.

For examining the seasonal variations, the percentages of EE (=EE, < EE and > EE) in both regions were given in Table 4.4 for the Aqua satellite. The high percentages of retrievals within EE (=EE) were found for Aqua in all seasons (>81%). Percentages of data below EE (< EE) were very low (<9%) in the DT products. The highest percentages of retrievals above EE were found in spring. DB products did not meet EE criterias in any season. Especially in the summer season, it was observed that percentage of data below EE was 85%, so the data quality was quite poor. For the urban area, it was determined that the DT algorithm was only convenient in spring for the urban site and percentages of data above EE were considerably higher than in other seasons. The highest values for percentage of retrievals within EE obtained from DB were reached in summer and spring (80.6% and 86.4% respectively). Therefore, it was found that the AOD product was convenient for regional use.

The distribution of EE percentages (=EE, < EE and > EE) in both regions were given in Table 4.5 for the Terra satellite. For DT Products, the percentages of data within EE (=EE) achieved in rural areas in all seasons remain within the limits. The Terra DT product showed the worst performance in spring. The high percentages of data above EE were found in spring and autumn (28% and 18% respectively) in rural areas. Higher AODs observed in the months of spring season over the rural site could be because of dust transportation (Tuna Tuygun et al., 2020). Similar results to the Aqua satellite were achieved in the urban area as well as in the rural area. The =EE obtained from the Terra satellite was lower for both regions compared to the Aqua satellite. These results indicated that the Aqua satellite had high quality of retrievals than the Terra satellite for Turkey.

Table 4.4 Seasonal variations of the expected errors for Aqua retrievals over the urban and rural sites

Product	**Station**	**Season**	**= EE (%)**	**< EE (%)**	**> EE (%)**
Aqua3km-DT	Rural	spring (MAM)	81.01	0.59	18.40
		summer (JJA)	88.82	1.97	9.21
		autumn (SON)	88.39	0.77	10.83
		winter (DJF)	91.73	1.29	6.98
	Urban	spring (MAM)	75.00	-	25.00
		summer (JJA)	32.26	-	67.74
		autumn (SON)	50.00	-	50.00
		winter (DJF)	75.00	25.00	-
Aqua10km-DT	Rural	spring (MAM)	88.85	3.85	7.31
		summer (JJA)	88.32	9.11	2.57
		autumn (SON)	93.53	1.20	5.28
		winter (DJF)	92.93	3.22	3.86
	Urban	spring (MAM)	83.33	4.17	12.50
		summer (JJA)	27.03	-	72.97
		autumn (SON)	41.18	-	58.82
		winter (DJF)	50.00	50.00	-
Aqua10km-DB	Rural	spring (MAM)	43.86	56.14	-
		summer (JJA)	15.00	85.00	-
		autumn (SON)	46.28	53.72	-
		winter (DJF)	34.85	65.15	-
	Urban	spring (MAM)	80.56	2.78	16.67
		summer (JJA)	86.36	-	13.64
		autumn (SON)	48.00	24.00	28.00

=EE,>EE and <EE represent the percentages (%) of retrievals falling within, above, and below the EE, respectively. MAM: March-April-May, JJA: June-July-August, SON: September-October-November, DJF: December-January-February

Table 4.5 Seasonal variations of the expected errors for Terra retrievals over the urban and rural sites

Product	Station	Season	= EE (%)	< EE (%)	> EE (%)
Terra3km-DT	Rural	spring (MAM)	70.37	1.42	28.21
		summer (JJA)	89.23	4.44	6.32
		autumn (SON)	81.15	0.60	18.25
		winter (DJF)	83.95	-	16.05
	Urban	spring (MAM)	78.57	-	21.43
		summer (JJA)	39.13	-	60.87
		autumn (SON)	27.27	-	72.73
Terra10km-DT	Rural	spring (MAM)	75.77	3.46	20.77
		summer (JJA)	83.08	11.93	4.99
		autumn (SON)	87.53	2.04	10.43
		winter (DJF)	85.87	2.17	11.96
	Urban	spring (MAM)	70.83	-	29.17
		summer (JJA)	24.49	-	75.51
		autumn (SON)	25.00	-	75.00
Terra10km-DB	Rural	spring (MAM)	55.00	45.00	-
		summer (JJA)	11.83	88.17	-
		autumn (SON)	46.79	53.21	-
		winter (DJF)	31.58	68.42	-
	Urban	spring (MAM)	74.19	19.35	6.45
		summer (JJA)	73.91	13.04	13.04
		autumn (SON)	61.90	23.81	14.29

=EE,>EE and <EE represent the percentages (%) of retrievals falling within, above, and below the EE, respectively. MAM: March-April-May, JJA: June-July-August, SON: September-October-November, DJF: December-January-February

4.2.2 Validation of AOD Retrievals under Different NDVI Values

Within the scope of the study, the AERONET stations were categorized into three different NDVI categories; partially vegetated surface ($NDVI_P$), moderately vegetated surface ($NDVI_M$) and densely vegetated surface ($NDVI_D$).

The mean NDVI values of the stations vary according to the MODIS AOD products (3 km or 10 km). Jin et al. (2020) suggested the use of a 5 x 5 pixels sampling window centered on the latitude and longitude of the AERONET site when calculating the average NDVI value. It means that these regions represent 15 km x 15 km areas for MODIS AOD data in 3 km resolution, and 50 km x 50 km areas in 10 km resolution. The mean NDVI values of the stations according to these areas were given in Table 3.2 in Chapter 3.1.2. Due to the differing NDVI surfaces, the results of the validation studies of MODIS AOD data with AERONET AOD data at the ten AERONET stations were analyzed for three products (DT-3km, DT-10km and DB-10km).

AOD validation results for the DT-3km product at ten sites categorized according to NDVI classification were given in Table 4.6. The results indicated that the expected errors of all three sites belonging to the $NDVI_P$ were lower than the expected target (<67%). These three sites tended to overestimate over the partially vegetated surface. This was supported by high RMB (> 1) value and high expected error.

In Table 4.6, five sites of $NDVI_M$ surfaces were provided the percentage of collocations falling within the EE. It was observed that the Thessaloniki site had the lowest performance due to its location in urban area when compared to other stations. It is also known that this station is affected by dust transport at certain times of the year (Logothetis et al., 2020). The FORTH_CRETE site provided the expected target similar to the Thessaloniki site and low EE ratio and high RMB value were observed at this station compared to other stations. In addition, the difference between the MODIS and AERONET AOD values at both stations was higher than the other stations. The FORTH_CRETE site was also significantly affected by dust aerosols like the Thessaloniki site (Logothetis et al., 2020). As a result, the $NDVI_M$ surfaces had better AOD quality than $NDVI_P$.

In Table 4.6, two sites belonging to the $NDVI_D$ were higher than expected target (< 67%). Compared to other regions, percentage of retrievals below EE were higher especially in data obtained from Aqua satellite. The RMSE values were similar with the $NDVI_M$ surfaces, while the RMB values were very close to 1, especially in the data obtained from the Terra satellite.

The validation results according to NDVI categories were given in Figure 4.21. It was seen that MODIS AOD data was larger than AERONET data for $NDVI_P$ in terms of high RMSE and RMB value. It was determined that the Terra and Aqua satellites were not very different in terms of statistical indicators, but the percentages of within EE was higher in Terra than Aqua for $NDVI_D$. It was observed that, DT-3km product could be used with higher accuracy over $NDVI_M$ and $NDVI_D$ surfaces. The most important difference between the two NDVI surfaces was that the $NDVI_M$ tended to overestimate, while the $NDVI_D$ tended to underestimate.

Seasonal validation results according to NDVI are given in Figure 4.22. The highest numbers of data for all types of surfaces were obtained with DT-3km products in summer and autumn seasons. The lowest number of data was obtained in the winter season. Statistical results indicated that the correlation coefficients were high in all seasons. Lower correlation coefficients were observed especially in summer and autumn seasons compared to spring and winter for $NDVI_P$ surfaces (0.60-0.69). $NDVI_P$ and $NDVI_M$ surfaces tended to overestimate due to the high RMB value. The low RMB and RMSE values were obtained from these two surfaces in winter when compared to other seasons. Satellite-based AOD data tended to be smaller than ground-based data in autumn and winter over $NDVI_D$ surface. Scatter plots and low RMB value (~0.60) supported this trend.

Table 4.6 Validation results for MODIS DT-3km AOD retrievals over the different vegetated surfaces

NDVI	AERONET Station	Satellite	n	RMSE	RMB	Mean AOD		= EE	<EE	>EE
						MODIS	AERONET			
Partially vegetated surface ($NDVI_P$)	ATHENS-NOA	Aqua	196	0.283	2.02	0.37	0.18	40.31	0.51	59.18
		Terra	180	0.428	2.42	0.53	0.22	32.22	-	67.78
	CUT-TEPAK	Aqua	810	0.126	1.53	0.27	0.18	54.2	0.12	45.68
		Terra	900	0.101	1.50	0.24	0.16	60.22	0.11	39.67
	TUBITAK_UZAY_Ankara	Aqua	81	0.112	1.48	0.24	0.16	50.62	1.23	48.15
		Terra	145	0.128	1.54	0.3	0.19	44.83	-	55.17
Moderately vegetated surface ($NDVI_M$)	Eforie	Aqua	636	0.059	1.10	0.17	0.16	84.91	3.77	11.32
		Terra	604	0.063	1.16	0.19	0.16	86.09	1.82	12.09
	FORTH_CRETE	Aqua	1388	0.070	1.33	0.22	0.16	76.51	0.14	23.34
		Terra	1408	0.083	1.41	0.22	0.16	69.82	0.14	30.04
	IMS-METU- ERDEMLI	Aqua	1849	0.069	1.16	0.24	0.21	87.89	1.24	10.87
		Terra	1789	0.076	1.18	0.25	0.21	82.22	1.90	15.87
	Sevastopol	Aqua	958	0.049	1.16	0.18	0.16	92.8	0.31	6.89
		Terra	993	0.054	1.21	0.19	0.16	89.12	0.30	10.57
	Thessaloniki	Aqua	887	0.098	1.32	0.25	0.19	71.03	0.90	28.07
Densely vegetated surface ($NDVI_D$)		Terra	1170	0.106	1.34	0.26	0.19	67.09	1.03	31.88
	Xanthi	Aqua	281	0.069	0.88	0.19	0.22	84.7	12.1	3.20
		Terra	353	0.057	1.02	0.21	0.21	90.08	1.70	8.22
	Bucharest_Inoe	Aqua	434	0.092	0.83	0.17	0.21	67.05	25.35	7.60
		Terra	567	0.082	0.96	0.20	0.21	76.01	13.76	10.23

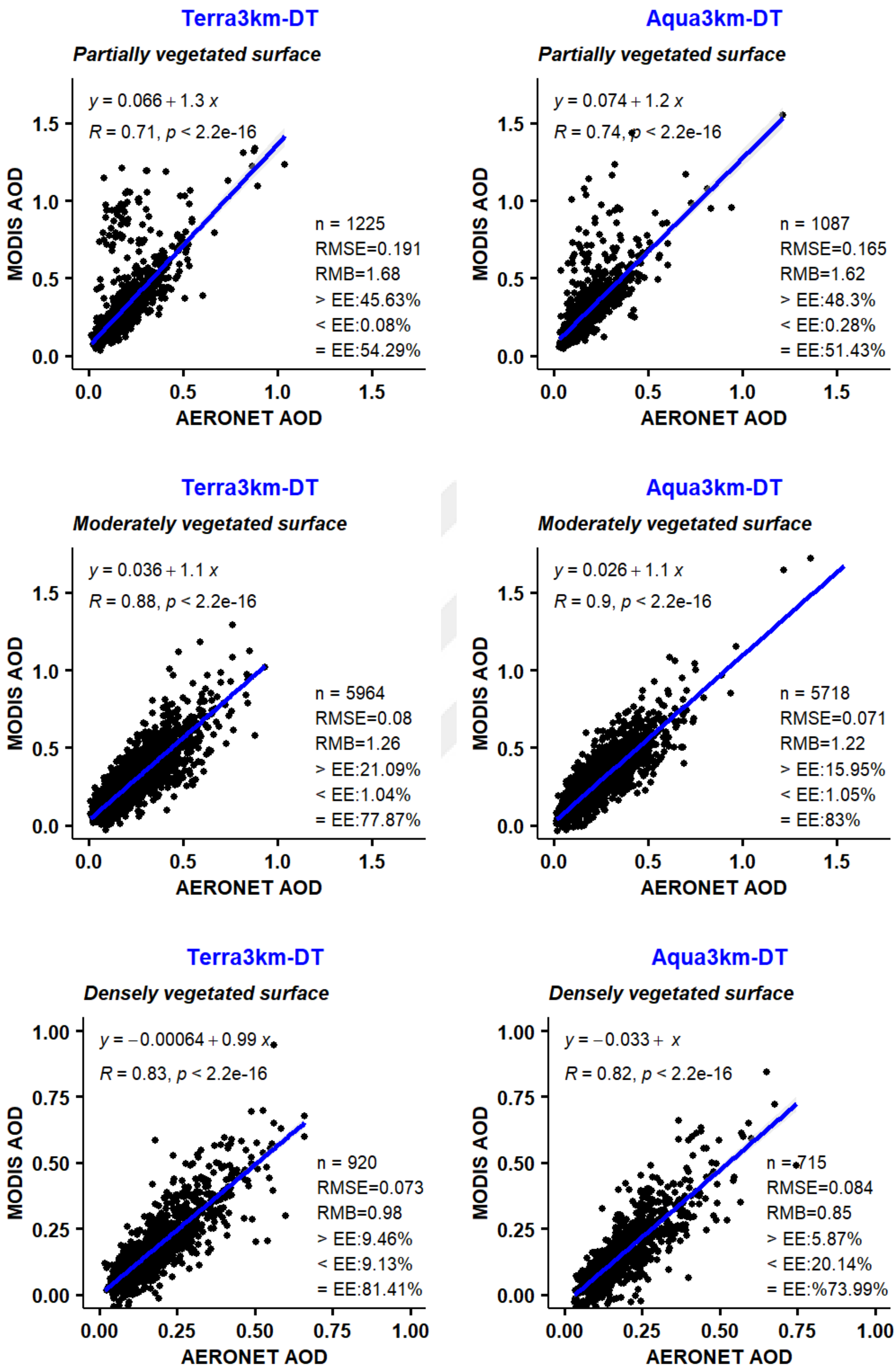

Figure 4.21 Validation of the MODIS DT-3km AOD retrievals against AERONET AOD in terms of NDVI categories

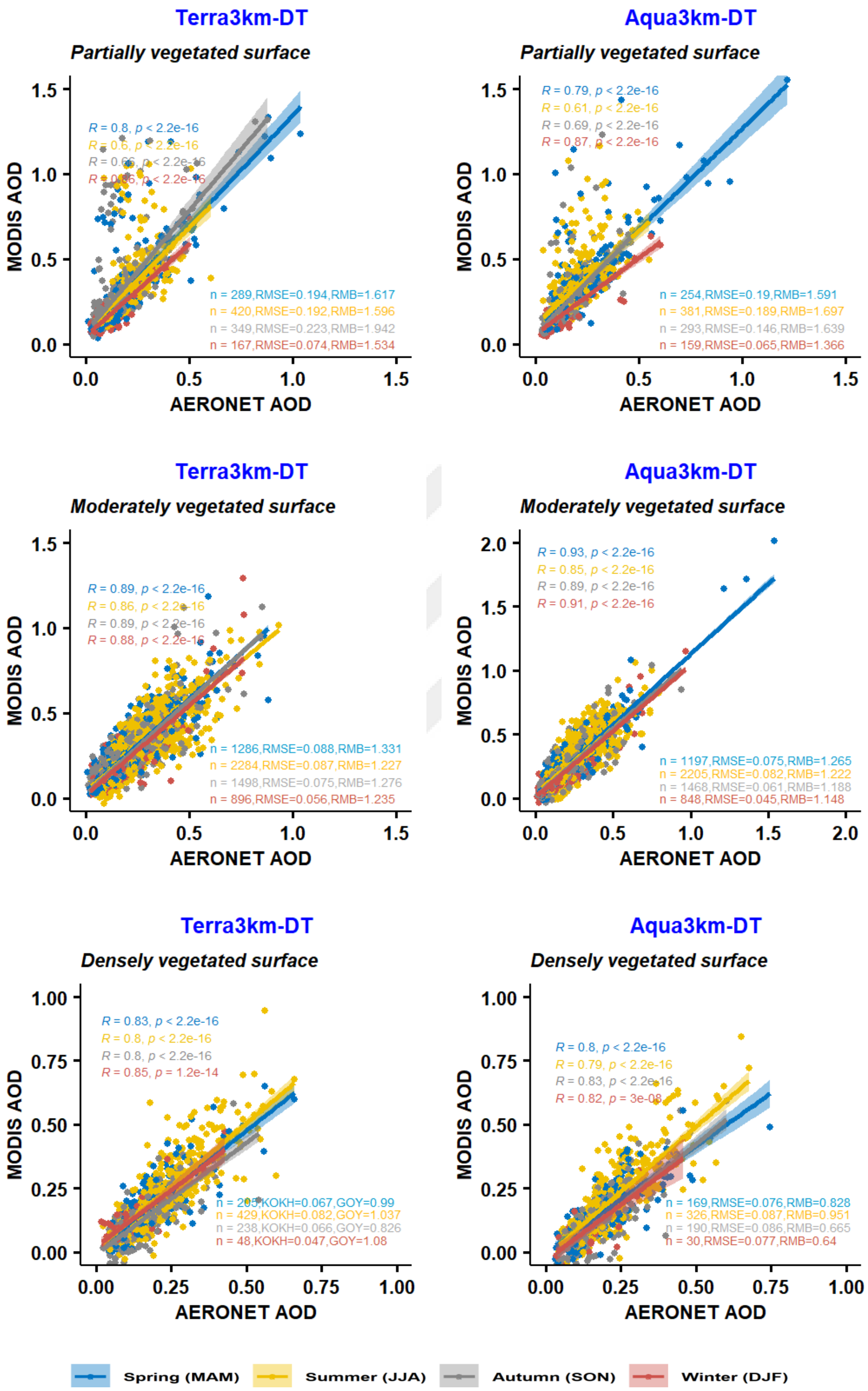

Figure 4.22 Seasonal validation of the MODIS DT-3km retrievals against AERONET in terms of NDVI categories

For 10 km products, some of the sites that fall previously in the $NDVI_P$ surface were tended to be included in the $NDVI_M$ surfaces due to the expanded area in the NDVI classification. The only urban site in Ankara, Turkey was in the category of $NDVI_P$ surface, while the other six sites were located in the $NDVI_M$ category. There was no change in the sites in the $NDVI_D$ surfaces.

The $NDVI_P$ surfaces did not meet the EE criteria for products from both satellites with low percentage of retrievals within EE (< 67%) (Table 4.7). Moreover, it was determined that the product tended to overestimate in the region with high RMB values (~ 1.5). The results suggested that $NDVI_M$ may be used with appropriate EE values. The Bucharest station could not provide the EE value with a small difference similar to the 3 km product for Aqua satellite. It was found that the data tended to underestimate with a high EE (34%) than the other site in the same surface classes.

Figure 4.23 shows the scatter plots of the validation for the DT-10km product over the NDVI surfaces. Low correlation coefficients were observed in the $NDVI_P$ surface. The number of collocations of the Terra satellite was greater than the Aqua satellite over all surfaces. $NDVI_P$ surface tended to overestimate AOD. The RMB value was found to be close to 1 over the $NDVI_D$ surfaces. However, the percentage of the retrievals within EE was found to be smaller than the $NDVI_M$. This difference was not differed in the results obtained from the Terra satellite, while it was higher in the results obtained from the Aqua satellite. In addition, high correlation coefficients were found in the $NDVI_M$ surfaces.

Figure 4.24 shows scatter plots of seasonal validation for the DT-10km product over the NDVI surfaces. The highest number of data was obtained in the summer season and the lowest number of data was obtained in the winter season for all NDVI surfaces. Except for the $NDVI_P$ surfaces, there were no significant differences in the validation results between all surfaces. When seasonal validation results were evaluated with the RMSE and RMB parameters, the accuracy of data on the seasonal basis were approximately similar. However, the Aqua satellite over the $NDVI_D$ surfaces tended to underestimate because of the winter season (RMB=0.451). The low correlation coefficient and high RMB values were obtained in autumn compared to other seasons over the $NDVI_P$ surfaces.

When two different spatial resolution products (DT-10km and DT-3km) obtained by the DT algorithm were compared, it was determined that both products did not perform well over the $NDVI_P$ surfaces. However, these products performed well over the $NDVI_M$ surfaces. When the region was evaluated as a whole, the DT algorithms were convenient for the $NDVI_D$ surface.

Table 4.7 Validation results for MODIS DT-10km AOD retrievals over the different vegetated surfaces

NDVI	**AERONET Station**	**Satellite**	**n**	**RMSE**	**RMB**	**Mean AOD**		**=EE**	**<EE**	**>EE**
						MODIS	**AERONET**			
Partially vegetated surface ($NDVI_P$)	TUBITAK_UZAY_Ankara	Aqua	80	0.100	1.46	0.24	0.16	47.50	2.50	50.00
		Terra	109	0.129	1.54	0.29	0.19	36.70	0.92	62.39
Moderately vegetated surface ($NDVI_M$)	ATHENS-NOA	Aqua	200	0.069	1.25	0.22	0.18	76.50	0.50	23.00
		Terra	280	0.077	1.24	0.23	0.18	73.57	0.36	26.07
	CUT-TEPAK	Aqua	824	0.081	1.28	0.23	0.18	71.24	0.73	28.03
		Terra	885	0.081	1.39	0.22	0.16	64.63	0.34	35.03
	Eforie	Aqua	522	0.060	0.96	0.15	0.16	81.42	11.30	7.28
		Terra	553	0.058	1.06	0.17	0.16	84.45	5.79	9.76
	FORTH_CRETE	Aqua	1198	0.059	1.23	0.20	0.16	78.63	0.67	20.70
		Terra	1156	0.074	1.36	0.21	0.16	66.44	0.17	33.39
	IMS-METU-ERDEMLI	Aqua	1493	0.057	0.99	0.20	0.21	90.82	4.76	4.42
		Terra	1390	0.070	1.05	0.22	0.21	83.53	5.61	10.86
	Sevastopol	Aqua	805	0.043	0.94	0.15	0.15	91.18	5.71	3.11
		Terra	750	0.044	1.06	0.17	0.16	91.87	1.73	6.40
	Thessaloniki	Aqua	997	0.078	1.04	0.20	0.19	77.83	7.62	14.54
		Terra	1114	0.076	1.13	0.21	0.19	78.10	4.40	17.50
Densely vegetated surface ($NDVI_D$)	Xanthi	Aqua	250	0.072	0.83	0.19	0.23	76.40	20.80	2.80
		Terra	276	0.048	0.96	0.20	0.20	92.03	2.54	5.43
	Bucharest_Inoe	Aqua	423	0.092	0.79	0.16	0.21	59.10	34.04	6.86
		Terra	536	0.082	0.94	0.19	0.20	70.90	18.10	11.01

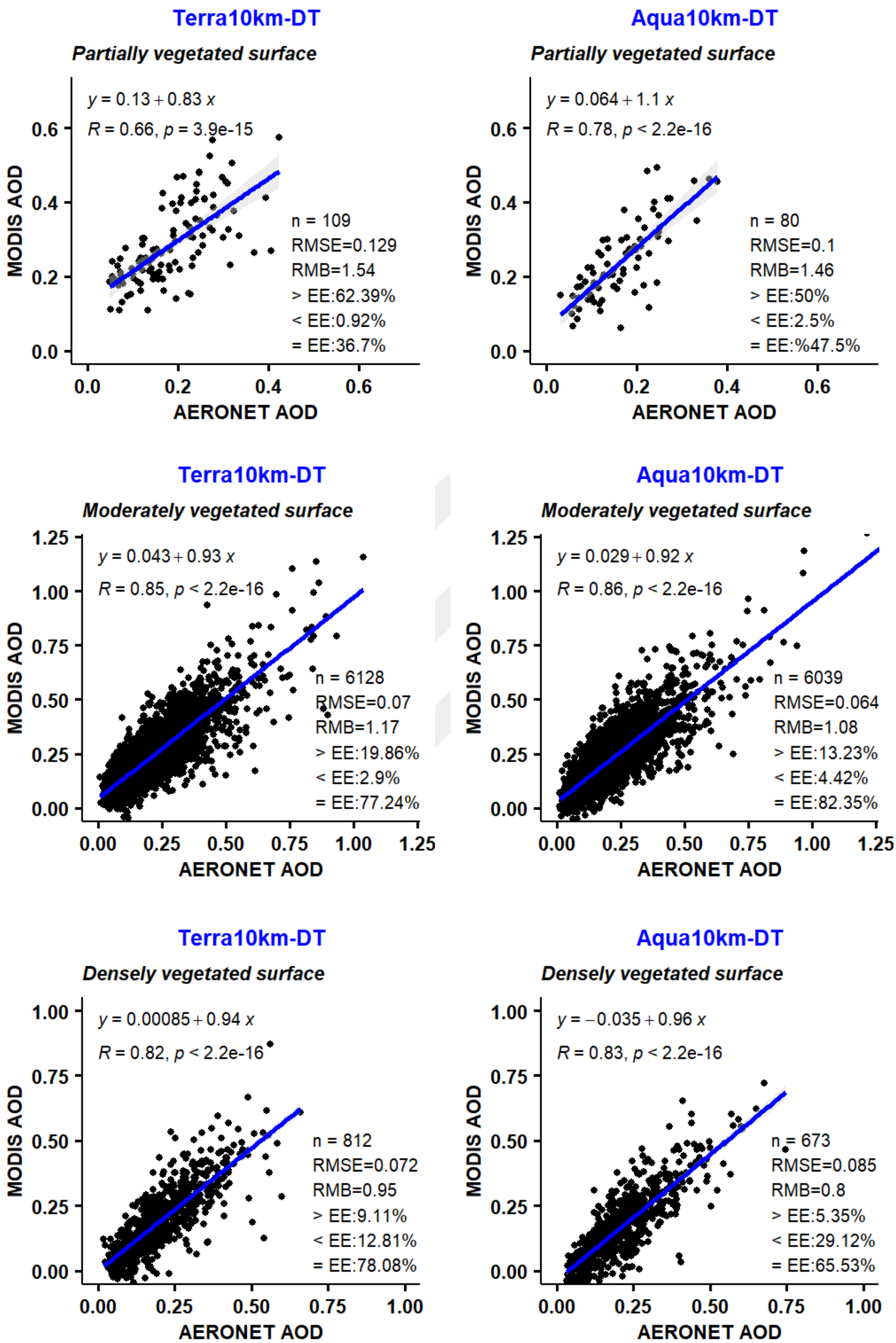

Figure 4.23 Validation of the MODIS DT-10km AOD retrievals against AERONET AOD in terms of NDVI categories

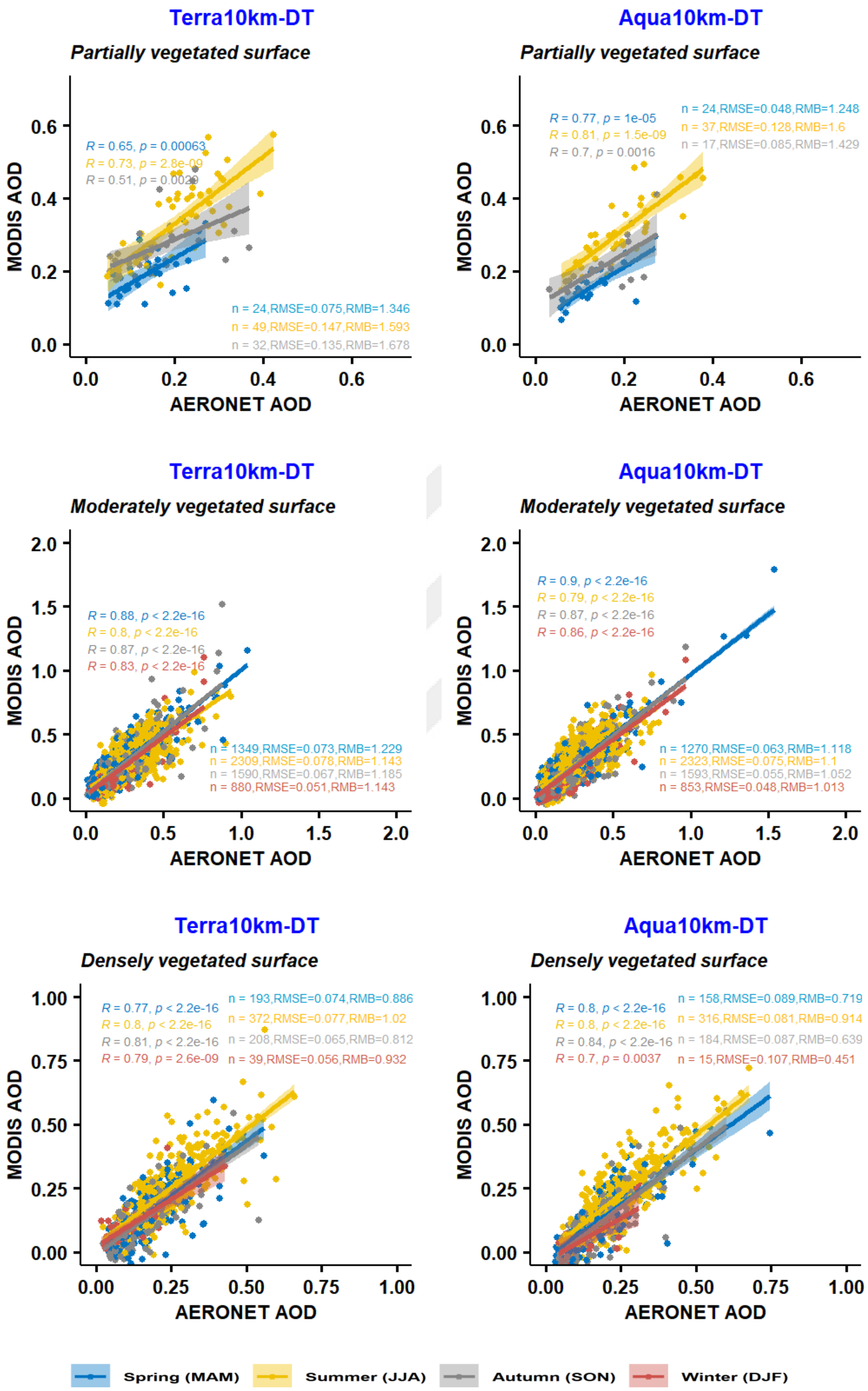

Figure 4.24 Seasonal validation of the MODIS DT-10km retrievals against AERONET in terms of NDVI categories

The validation results for the DB-10km product at ten sites categorized according to NDVI classification were given in Table 4.8. Compared with the two DT algorithm products, the $NDVI_P$ surfaces provided expected error target with the DB-10km products (> 67%). High RMB and RMSE value were not observed in the DB-10km products, especially compared to the DT-3km products. Tian et al. (2018) reported that DB products performed better over an urban site with the low NDVI value. Although the RMB value was very close to 1, the value in the Terra satellite was lower than the Aqua (0.85). The high percentage of EE showed that the Terra satellite tended to underestimate AOD than the Aqua satellite. Stations over $NDVI_M$ surfaces generally could not provide the expected target with their existing EE rates performance. Moreover, it was observed that sites with urbanization in Sevastopol and Thessaloniki provide the expected target with the DB algorithm. It was observed that the DB algorithm could be used in these sites. In the Bucharest station, it was observed that more data remained within the EE compared to DT algorithms over the $NDVI_D$ surface. According to the global validation results, the DB algorithm performed with higher accuracy for small regions than in areas with $NDVI_M$ and $NDVI_D$ (Wei et al., 2019). Wei et al. (2019) reported that half of the stations in Europe showed high accuracy results with the DB algorithm. It is known that the DB algorithm tends to show higher accuracy in regions with complex topography and aerosol composition. In this study, the DB algorithm tended to underestimate AOD compared to the AERONET AOD. This situation is much clearer at some sites (Athens-NOA, IMS-METU-ERDEMLI, Xanthi, etc.). The DB-10km AOD retrievals tended mainly to underestimate when compared to the DT-10km.

Figure 4.25 shows scatter plots of the validation for the DB-10km product over the NDVI surfaces. The correlations were lower in the $NDVI_P$ surfaces and higher in the $NDVI_M$ surfaces just as the DT products. The numbers of Aqua collocations were lower than the numbers of Terra, except $NDVI_P$ surface. The RMB values were below 1 in all surfaces. The DB algorithm tended to underestimate AOD in $NDVI_M$ and $NDVI_D$ surfaces. The RMSE values were observed to be similar and small in all surfaces.

Figure 4.26 shows scatter plots of seasonal validation for the DT-10km product over the NDVI surfaces. The low correlations were observed in the $NDVI_P$ surfaces in the autumn season. The autumn season tended to underestimate. The correlations in the $NDVI_M$ and $NDVI_D$ surfaces were small in summer compared to other seasons. In addition, the small RMB values were obtained in the winter season (~0.5). There was no significant difference between the Terra and Aqua satellites in both NDVI surfaces. The results showed that the DB algorithm is more convenient over the $NDVI_P$ surfaces in the urban site.

Table 4.8 Validation results for MODIS DB-10km AOD retrievals over the different vegetated surfaces

NDVI	AERONET Station	Satellite	n	RMSE	RMB	Mean AOD		=EE	<EE	>EE
						MODIS	AERONET			
Partially vegetated surface ($NDVI_P$)	TUBITAK_UZAY_Ankara	Aqua	88	0.075	0.95	0.14	0.15	68.18	13.64	18.18
		Terra	80	0.082	0.85	0.15	0.18	67.50	22.50	10.00
Moderately vegetated surface ($NDVI_M$)	ATHENS-NOA	Aqua	262	0.088	0.62	0.10	0.15	60.31	38.93	0.76
		Terra	309	0.103	0.55	0.09	0.17	45.63	53.72	0.65
	CUT-TEPAK	Aqua	150	0.081	0.74	0.13	0.18	70.00	28.00	2.00
		Terra	172	0.081	0.65	0.10	0.15	64.53	34.30	1.16
	Eforie	Aqua	330	0.068	1.08	0.16	0.15	63.64	14.24	22.12
		Terra	400	0.076	1.10	0.17	0.15	61.25	15.25	23.50
	FORTH_CRETE	Aqua	567	0.084	1.12	0.19	0.17	69.49	7.23	23.28
		Terra	687	0.088	1.11	0.18	0.16	69.00	9.46	21.54
	IMS-METU-ERDEMLI	Aqua	304	0.104	0.48	0.07	0.15	37.17	62.83	-
		Terra	386	0.114	0.47	0.08	0.16	37.82	62.18	-
	Sevastopol	Aqua	253	0.040	0.96	0.13	0.13	89.72	5.93	4.35
		Terra	271	0.049	0.87	0.13	0.15	80.07	14.02	5.90
	Thessaloniki	Aqua	1032	0.069	0.87	0.15	0.18	72.38	20.06	7.56
		Terra	1042	0.072	0.83	0.15	0.19	70.83	24.47	4.70
Densely vegetated surface ($NDVI_D$)	Xanthi	Aqua	234	0.106	0.63	0.14	0.22	52.14	47.86	-
		Terra	253	0.098	0.61	0.12	0.20	42.69	56.92	0.40
	Bucharest_Inoe	Aqua	478	0.073	0.97	0.19	0.20	69.87	16.32	13.81
		Terra	592	0.081	0.95	0.19	0.20	68.24	17.74	14.02

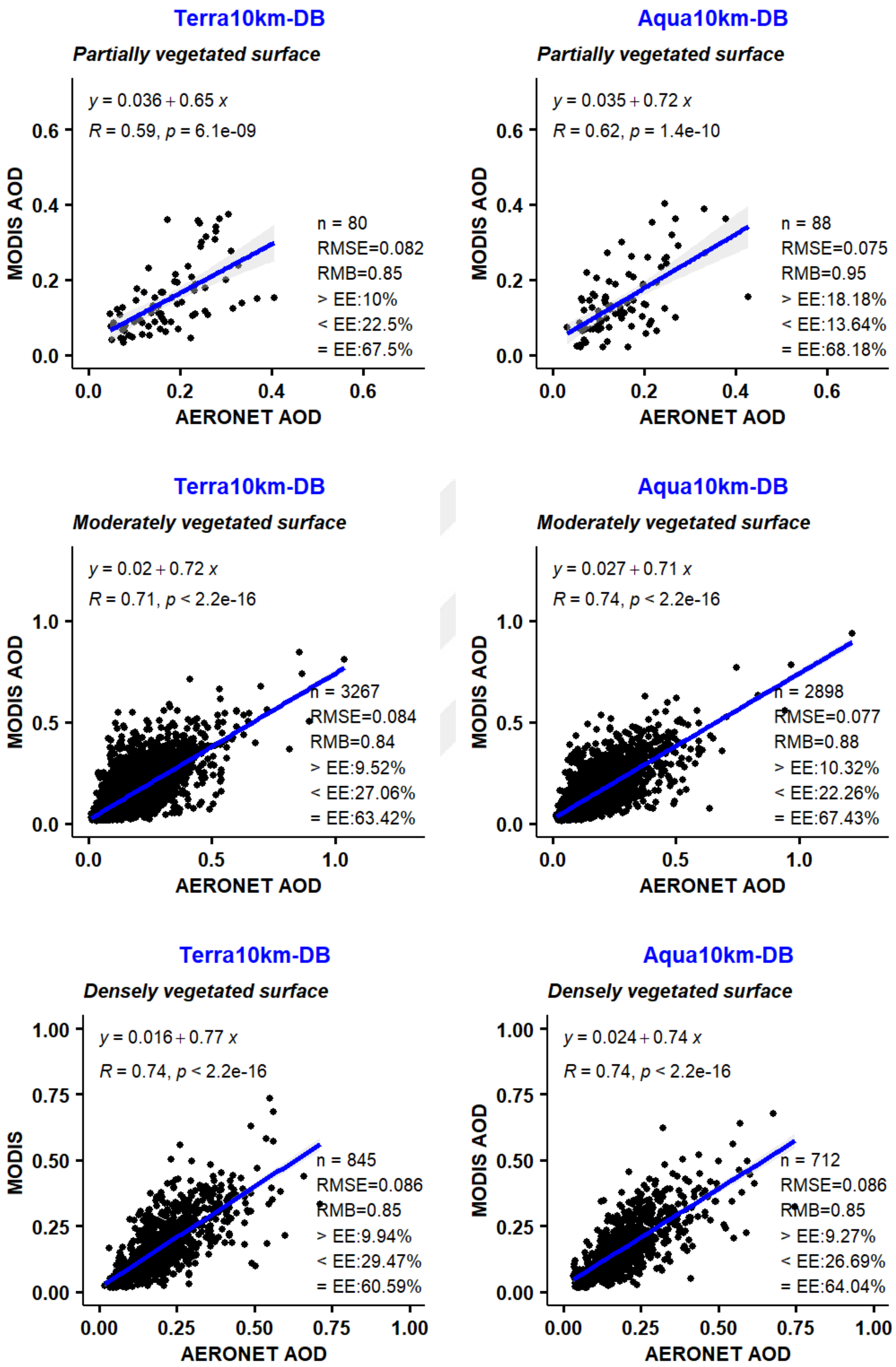

Figure 4.25 Validation of the MODIS DB-10km AOD retrievals against AERONET AOD in terms of NDVI categories

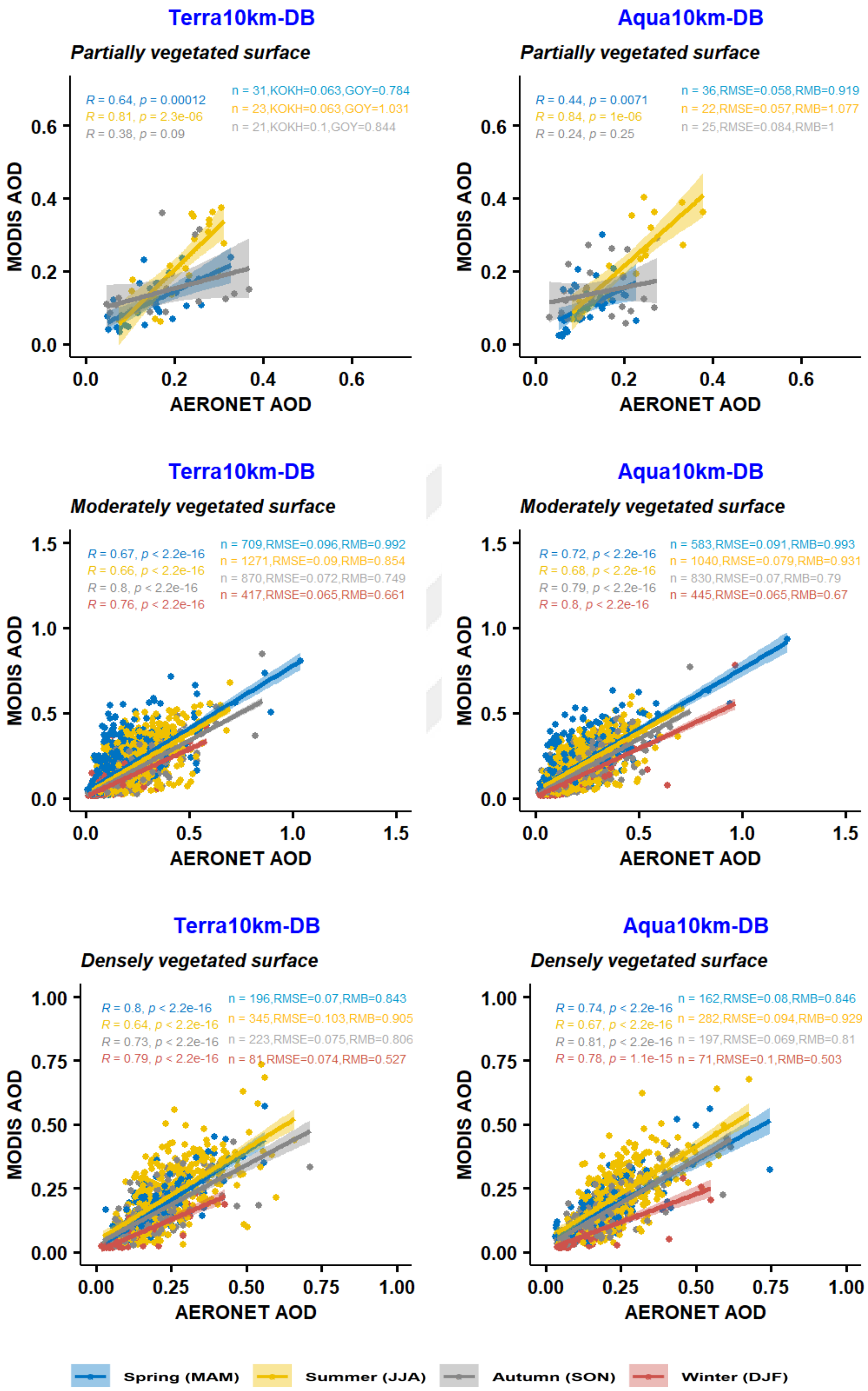

Figure 4.26 Seasonal validation of the MODIS DT-10km retrievals against AERONET in terms of NDVI categories

4.3 Spatial and Temporal Variations of MODIS AOD Datasets

The spatial and temporal variation of all validated MODIS AOD products were studied. Spatial distributions of multiannual average MODIS AOD values for both Aqua and Terra satellites are shown as maps in Figure 4.27. The highest AOD values were obtained from DT-3km datasets. Moreover, the DT 10 km dataset was generally lower than the DT 3 km data for most of the regions. There was also a difference between the DT and DB algorithms with the 10 km resolution. The DB retrievals were lower than DT retrievals all over Turkey. All algorithms and products had similar results around Tuz Lake and its surrounding. The AOD values in this region were quite above the country mean. Large AOD values are due to several factors as low NDVI values in this region and the high salt content of the lake. It is known that retrievals were affected by surface reflectance.

Higher AOD values were obtained from the Terra satellite. Differences between the Terra and Aqua satellites were reported by Wei et al. (2019). High AOD values were predominantly observed in the Marmara, Aegean, and Central Anatolia regions. However, generally smaller aerosol loadings were widely distributed throughout the rest of the areas. High AOD values were observed in big cities such as Istanbul, Izmir, Ankara, Bursa, Kocaeli, etc. This indicated that increasing anthropogenic activities caused more aerosol loadings over these regions. Additionally, as mentioned in Chapter 4.2 the DT algorithm tended to overestimate AOD due to the surface reflectance and low NDVI value over the urban area. The DT product showed many missing values in most arid areas concentrated at the southeastern part of Turkey due to the limitations of the DT algorithm. However, it was observed that the DB algorithm performed better over these areas like Syria. It was observed that data was generated with the DB algorithm in areas where DT algorithm left blank and could not produce data. Moreover, it was observed that the DB algorithm produced high AOD values at some points near the sea, or on small islands.

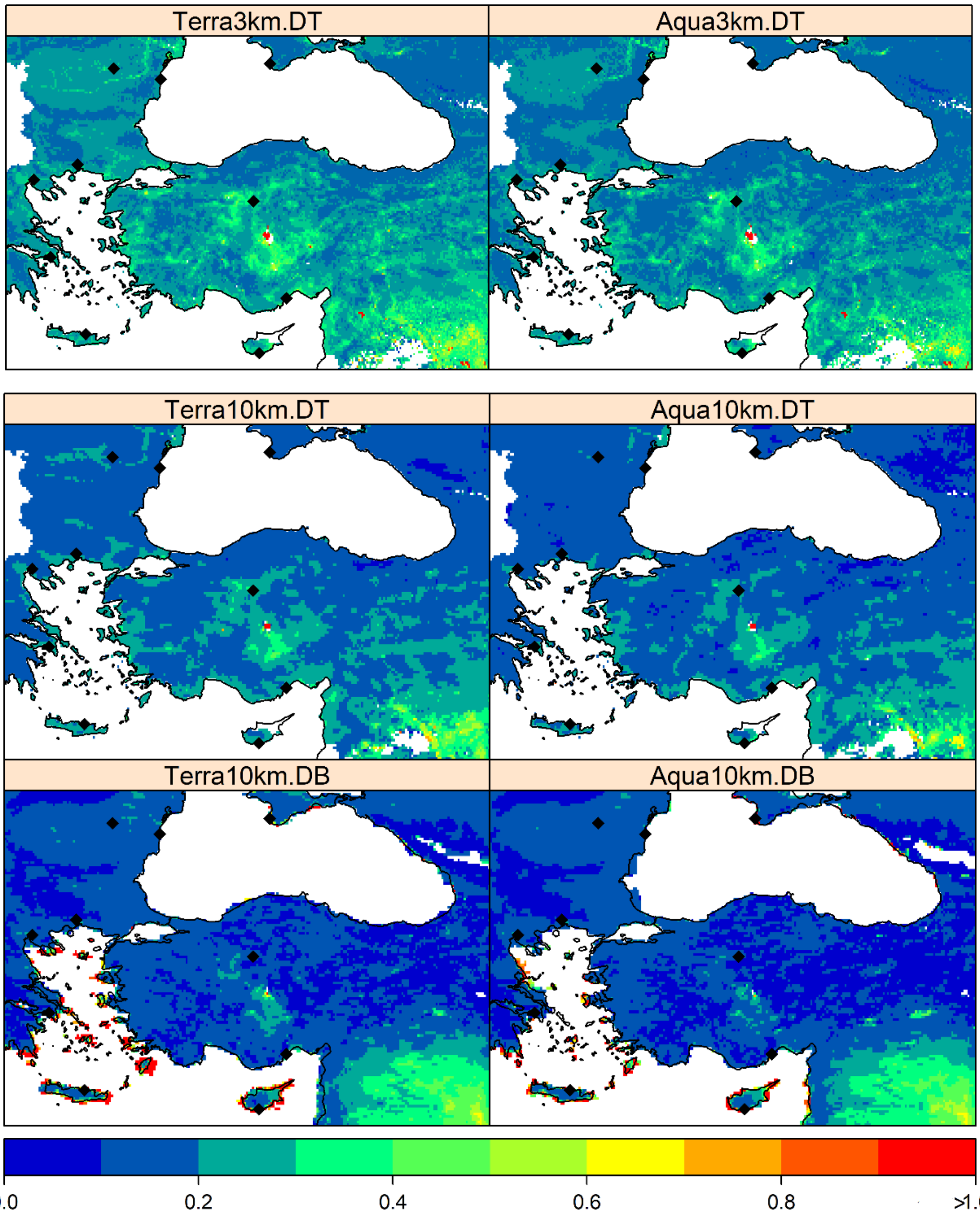

Figure 4.27 Spatial distribution of the multiannual mean Terra and Aqua-MODIS AOD retrievals for DT 3 km, DT and DB 10 km over the study area

Spatial distributions of the multi annual seasonal mean MODIS DT 3 km AOD for both Terra and Aqua satellites are shown in Figures 4.28 and 4.29. Low AOD values (0-0.2) were observed throughout the region in autumn and winter from the Terra satellite. High AOD values (0-0.5) were observed in summer and spring. It was observed that the highest AOD values for each season occurred in the Tuz Lake and its surroundings, where the NDVI values were very low (<0.1). The highest values (ranged between 0.5-0.6 interval) were observed on the Tuz Lake and especially in the south of the lake in the spring and summer seasons. It was observed that there were data gaps in some regions on the distribution maps of the winter season. These were the regions in the eastern part of Turkey with very low NDVI and high topography. The DT algorithm did not have the potential to produce data in arid regions and deserts. For this reason, data could not be produced in a large area of Syria which is neighbouring to southeastern part of Turkey. High AOD values were observed in the spring and summer seasons especially in Central Anatolia, Marmara and Aegean regions. Highest seasonal mean AODs over the urban site were observed during summer due to low precipitation, presence of aerosols in the atmosphere formed because of the photochemical reactions, anthropogenic emissions from industrial facilities and emissions due to forest fires or biomass burning activities at rural areas (Fotiadi et al., 2006; Ozdemir et al., 2020).

Spatial distribution of the multi annual monthly mean MODIS DT 3 km AOD obtained both from the Aqua and Terra satellites are shown in Figures 4.30 and 4.31. There was no AOD data in the winter season, especially in the Eastern and Southeastern Anatolia in January and February. It is evaluated that the high level of cloud cover and snow are challenging for the satellite aerosol retrieval during these months. It was observed that data can only be produced in December over the region. During the spring season, the lower AOD values were observed in March when compared to April and May. Figures 4.30 and 4.31 indicated that high AOD value was observed in May. There was no significant difference between the summer months but, the highest AOD values were observed in August. The high AOD values were obtained in September and October. The Terra satellite dataset was generally higher than the Aqua satellite in monthly averages.

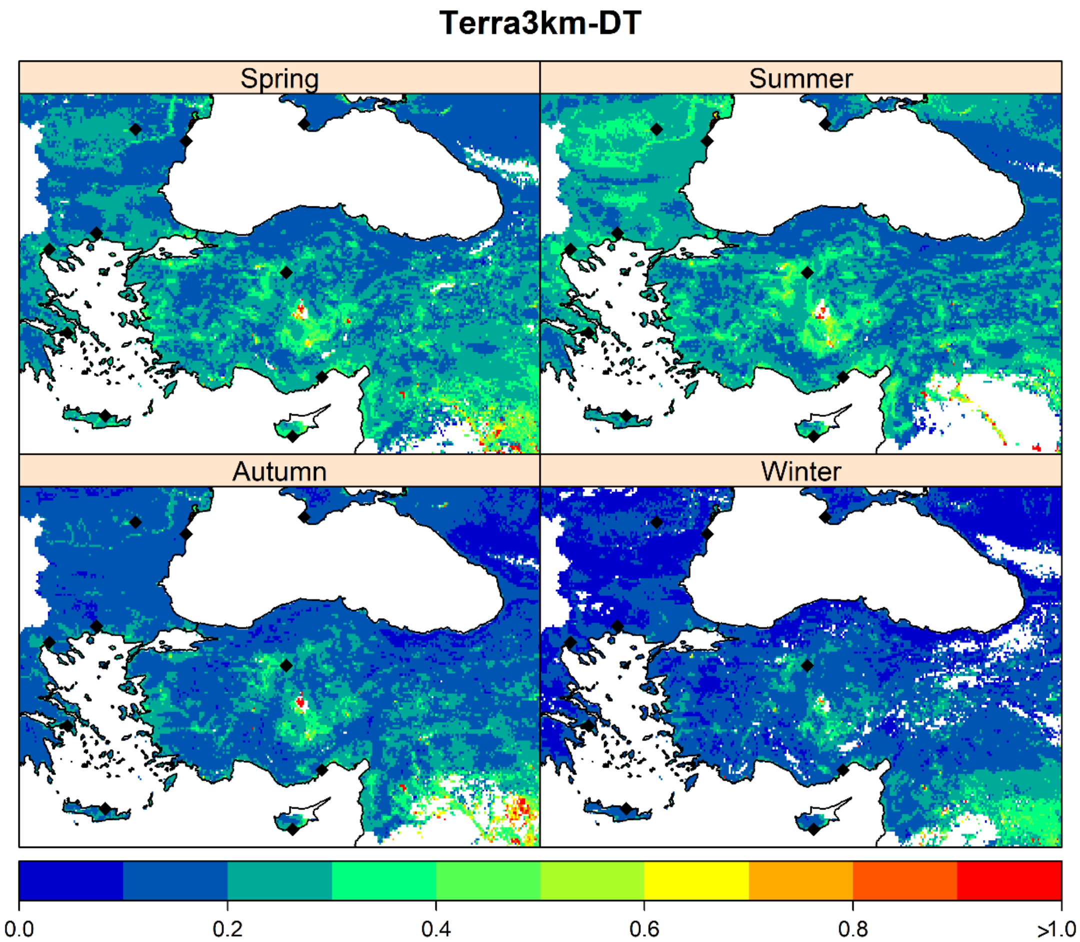

Figure 4.28 Spatial distribution of the seasonal mean Terra MODIS DT 3 km AOD products

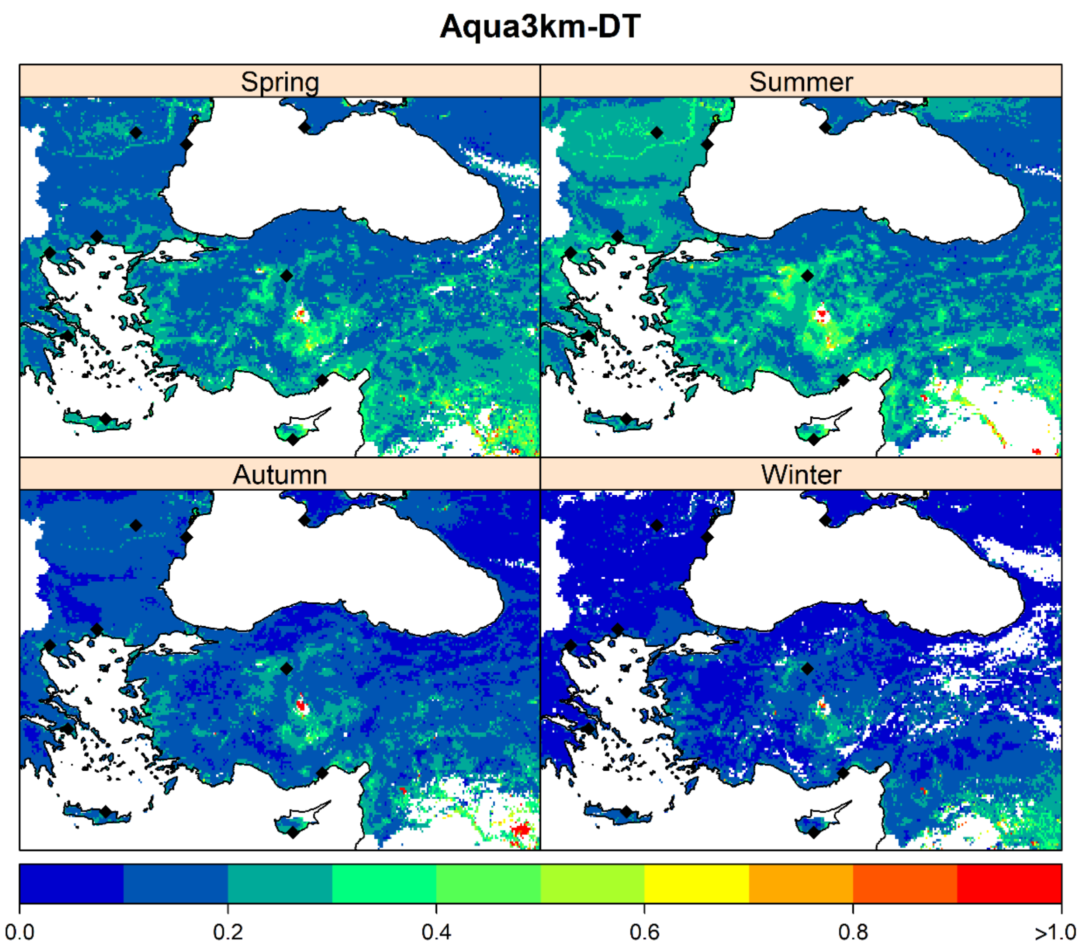

Figure 4.29 Spatial distribution of the seasonal mean Aqua MODIS DT 3 km AOD products

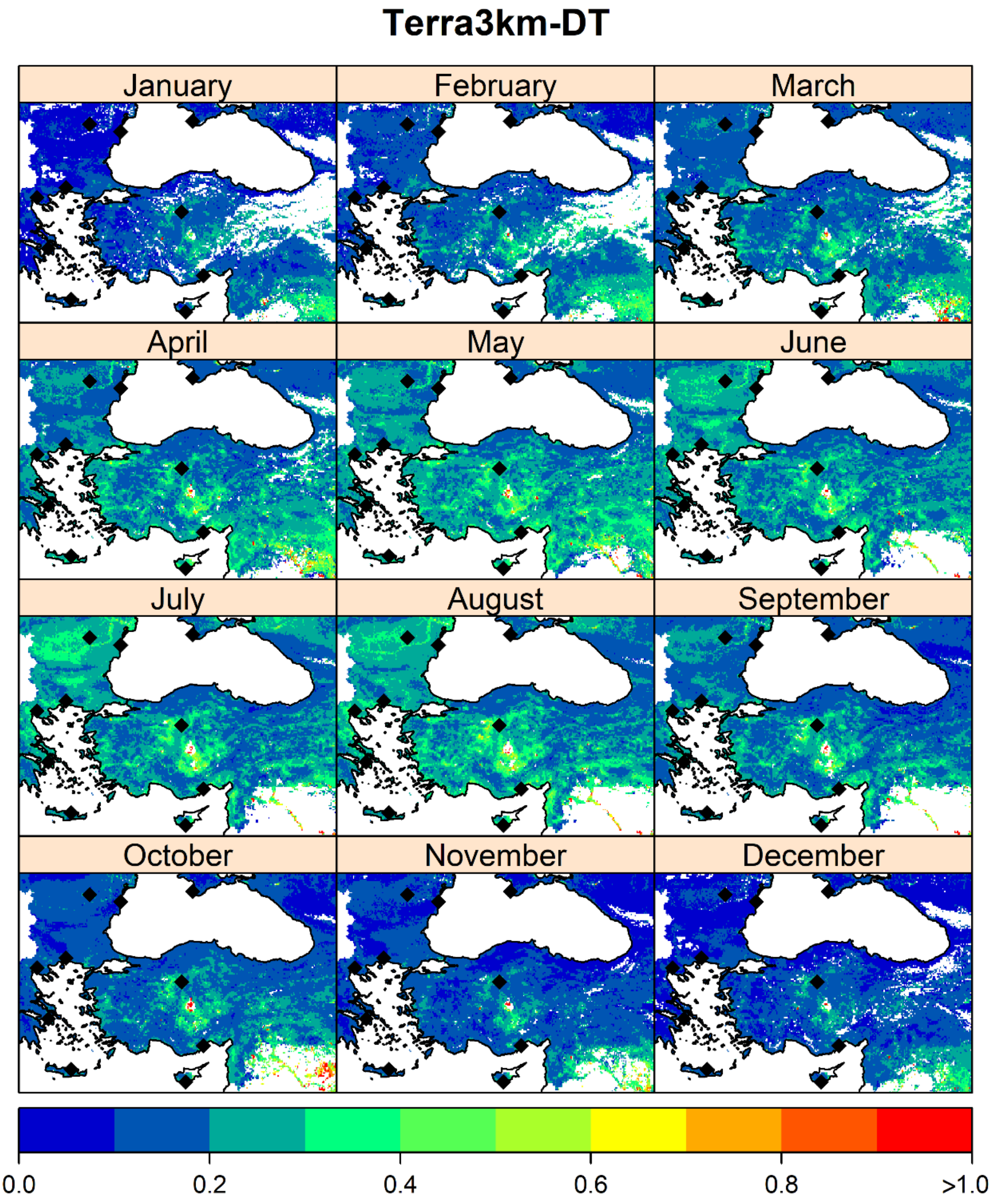

Figure 4.30 Spatial distribution of monthly mean Terra MODIS DT 3 km AOD products

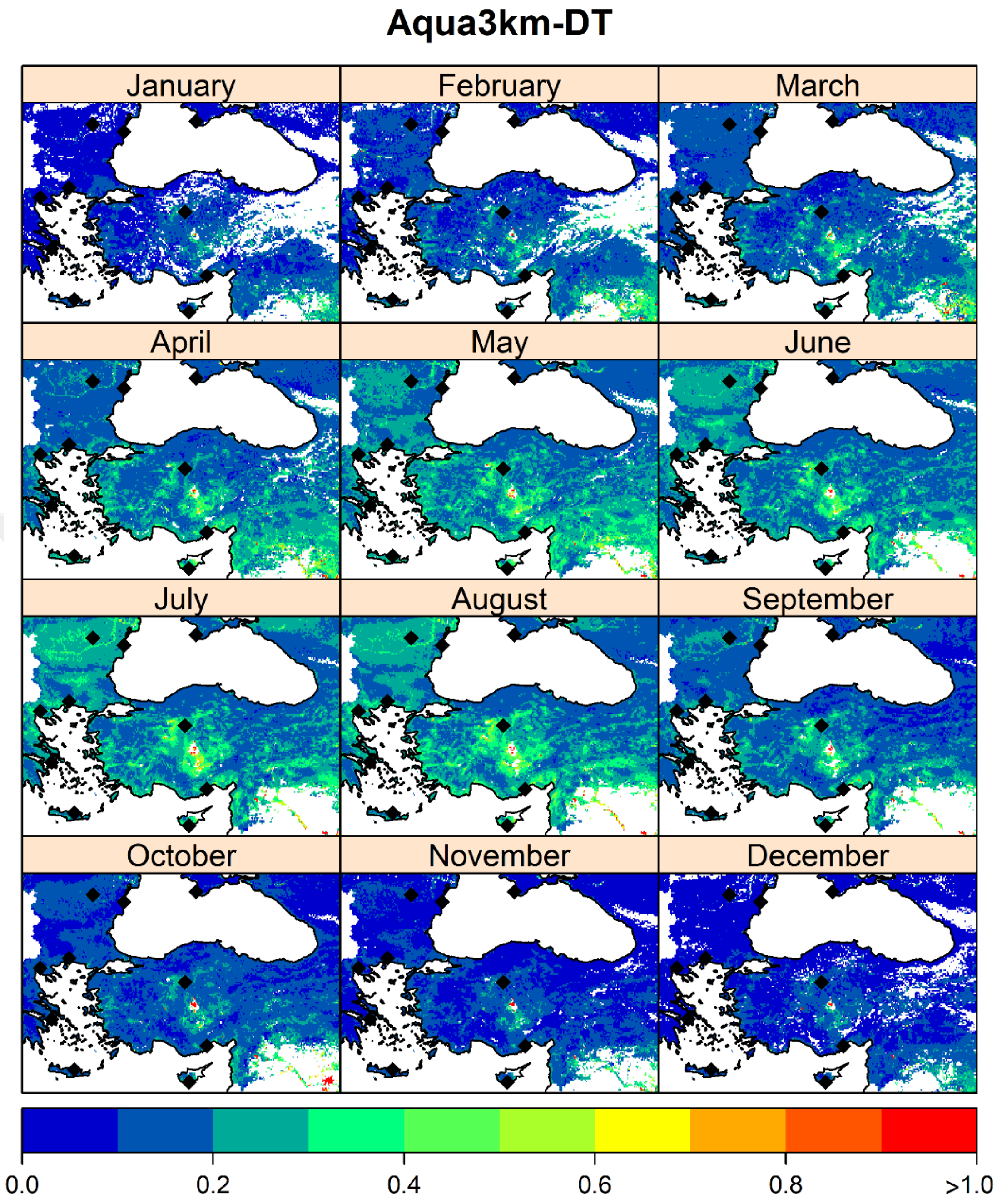

Figure 4.31 Spatial distribution of monthly mean Aqua MODIS DT 3 km AOD products

Spatial distributions of the multi annual seasonal mean MODIS DT 10 km AOD for both the Terra and Aqua satellites are shown in Figures 4.32 and 4.33, respectively. Seasonal distribution of DT-10km product were similar to DT-3km product. High AOD values were also observed over the same regions. However, the AOD values obtained were lower than the DT-3km product. Low AOD values were still observed in autumn and winter. During these seasons, the AOD value exceeding 0.3 in the region was quite low. AOD values were generally varied between 0.1 to 0.2 in both seasons. Much smaller (0-0.1) AOD values were observed in Thrace Region and Eastern European countries in winter. These values were more common in the map obtained from the Aqua satellite. The differences between Terra and Aqua satellites were more obvious in spring and summer, similar to the 3 km product. When monthly spatial distributions analyzed, both satellites (especially Aqua satellite) demonstrated many data gaps in north and east part of Turkey especially in January (Figures 4.34 and 4.35). Aqua satellite still continues to perform data gaps in December. The high AOD values were observed mostly in May throughout the region as in the 3 km product. The highest AOD values were observed also in August throughout the year due to high humidity and NDVI value as in the 3 km product. Lower mean AOD values were obtained in October and November in whole Turkey. Especially in the northern and western parts of Turkey, AOD values were ranging from 0 to 0.1 for the Aqua satellite.

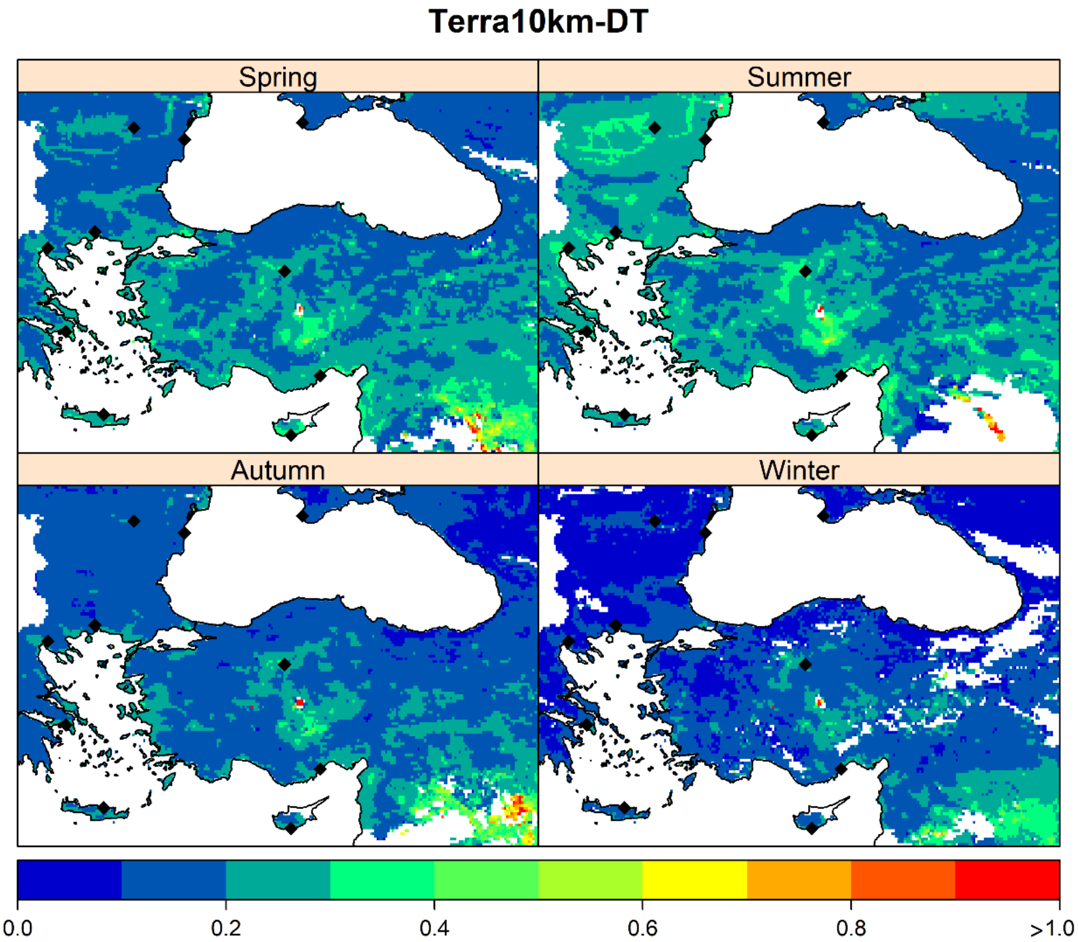

Figure 4.32 Spatial distribution of the seasonal mean Terra MODIS DT 10 km AOD products

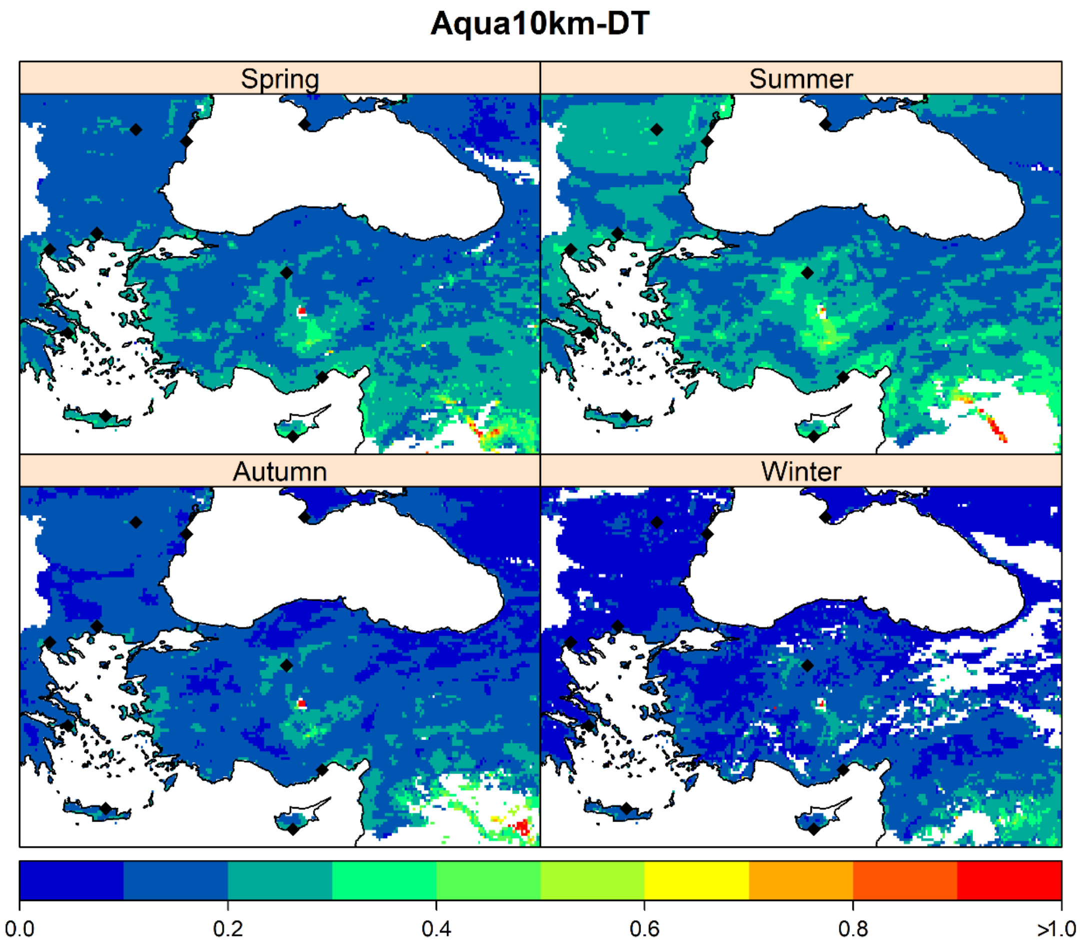

Figure 4.33 Spatial distribution of the seasonal mean Aqua MODIS DT 10 km AOD products

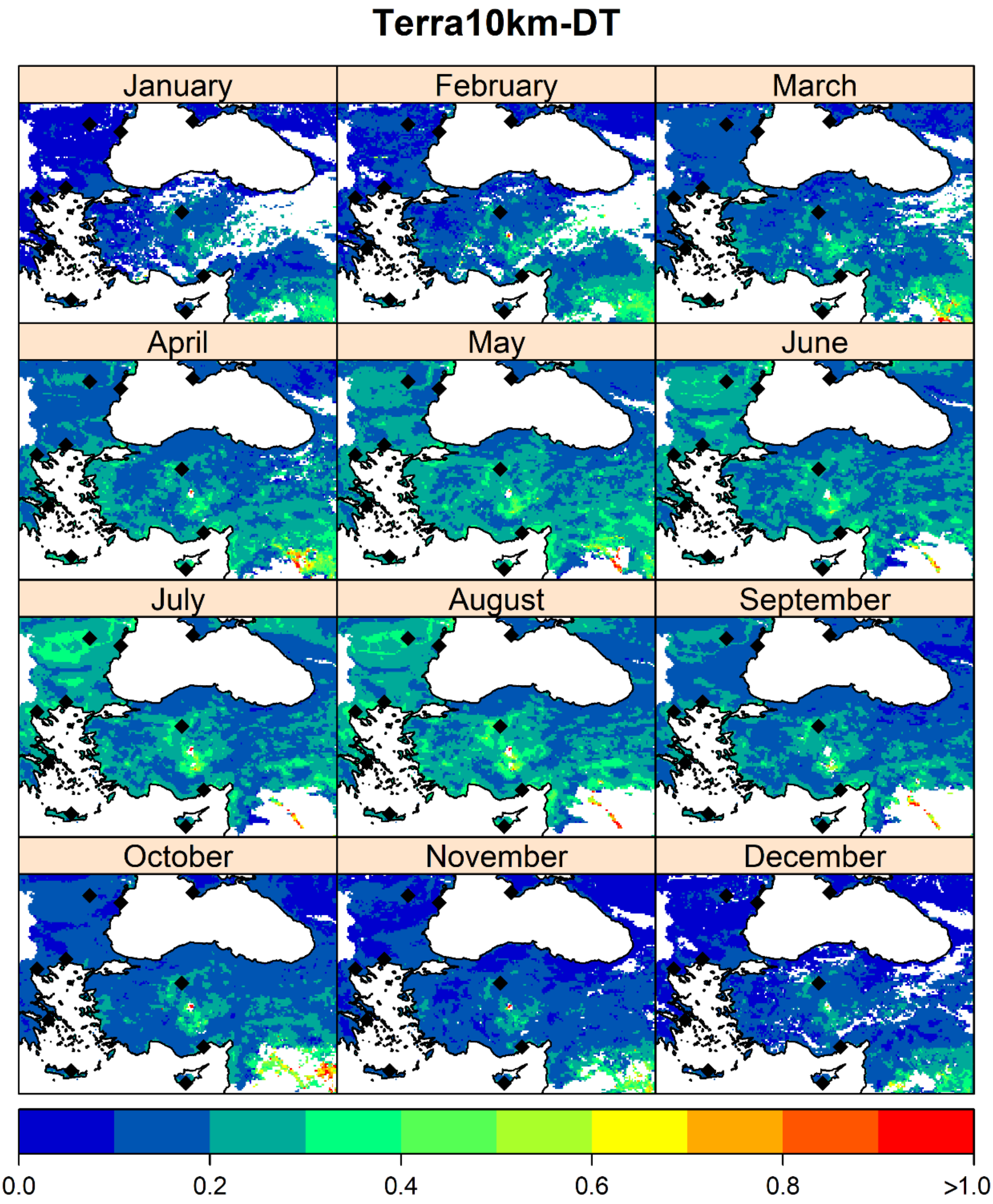

Figure 4.34 Spatial distribution of monthly mean Terra MODIS DT 10 km AOD products

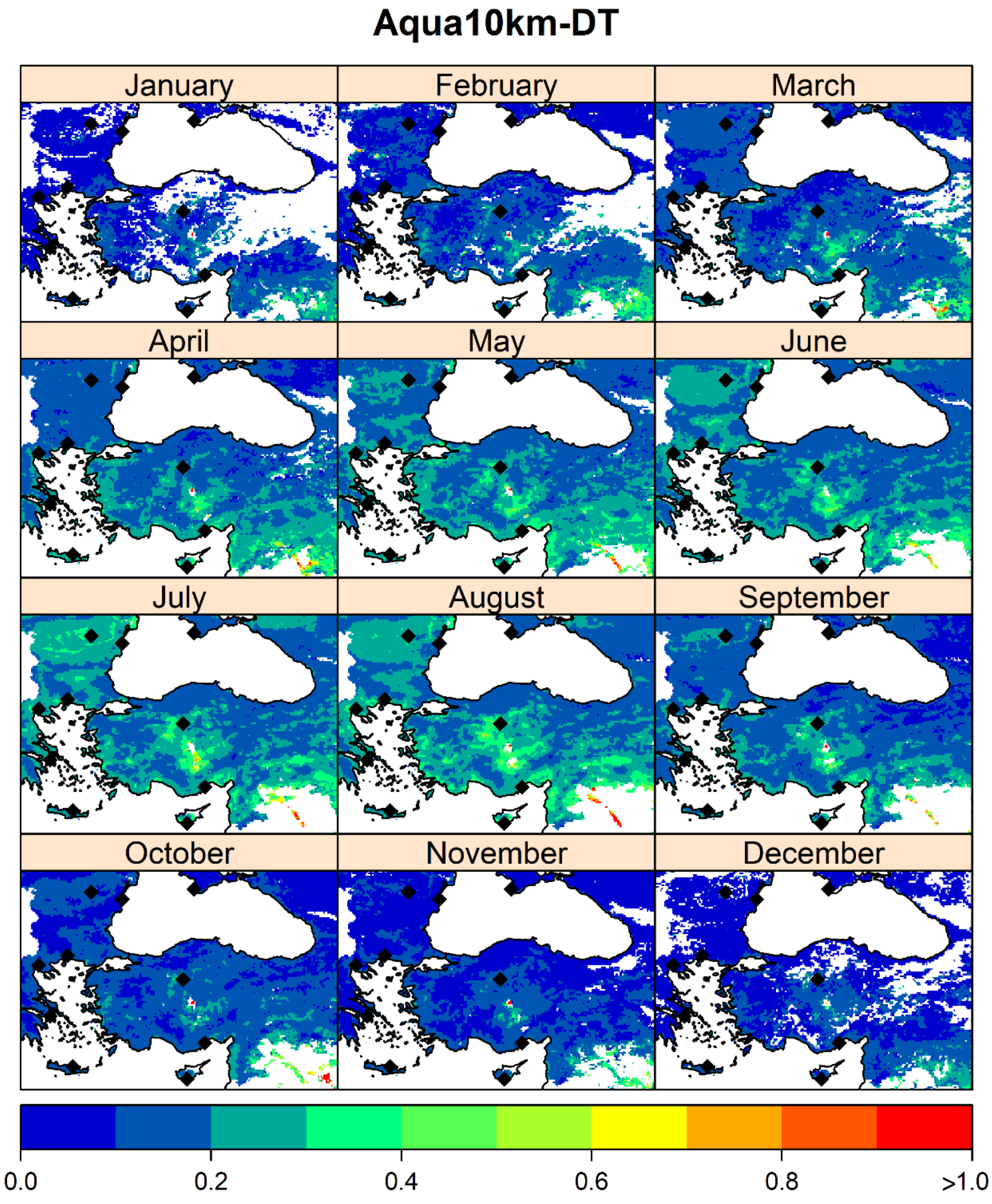

Figure 4.35 Spatial distribution of monthly mean Aqua MODIS DT 10 km AOD products

The multi annual seasonal spatial distributions of mean MODIS DB 10 km AOD for both the Terra and Aqua satellites are shown in Figures 4.36 and 4.37, respectively. The results showed that DB values were quite low (ranging from 0 to 0.1) compared to DT algorithm data. Although the autumn season had AOD values as small as the winter season (ranging from 0.1 to 0.2), higher AOD values were observed in the western and northern regions compared to winter season. Higher AOD values (0.4-0.6) were observed in Tuz Lake and its surroundings compared to other regions. These values were generally obtained from spring and summer seasons. Unlike the DT algorithm, small AOD values were dominant in the region in summer. Lower AOD values were observed than in spring, especially part of Central Anatolia and Eastern Anatolia regions. It is known that the DB algorithm tends to underestimate during periods with high NDVI values. The results indicated that DB algorithm cannot demonstrate acceptable accuracy performance for estimation over moderately vegetated surface ($NDVI_M$). In spring and summer seasons, higher AOD values were observed in urban areas including south of Istanbul and Aegean coasts compared to other regions. Multi annual mean AOD values obtained from Aqua satellite were lower than Terra satellite similar to DT algorithm. Spatial distributions of the multiannual monthly mean MODIS DB 10 km AOD for both the Aqua and Terra satellites are shown in Figures 4.38 and 4.39 as maps. When compared, it was observed that it had higher AOD data in February than the other winter months namely December and January. Both satellites showed many missing values in east part of Turkey in January, February, and December similar to DT algorithm. The high values observed around Tuz Lake, especially between April and September. June had lower AOD values compared to other summer months. This situation was similar for both satellites. It was observed that the lowest AOD values obtained in November in autumn season.

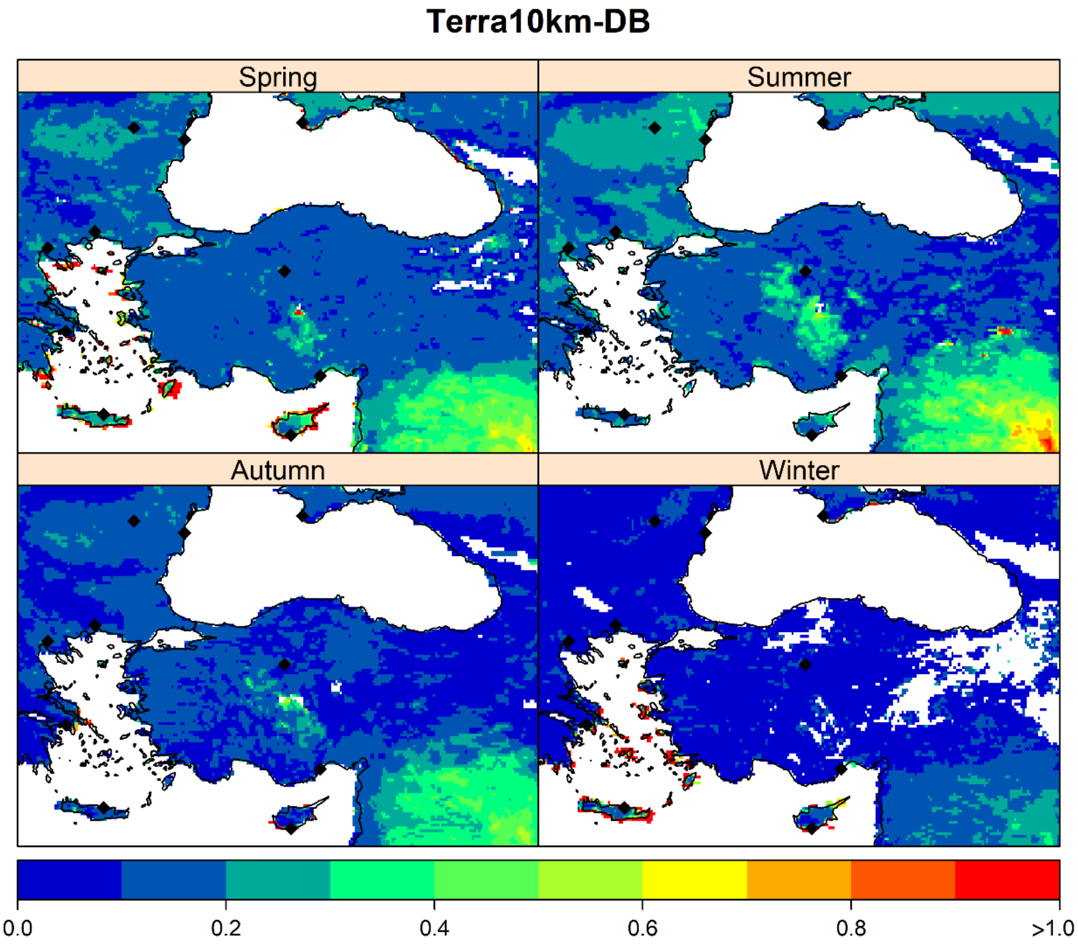

Figure 4.36 Spatial distribution of the seasonal mean Terra MODIS DB 10 km AOD products

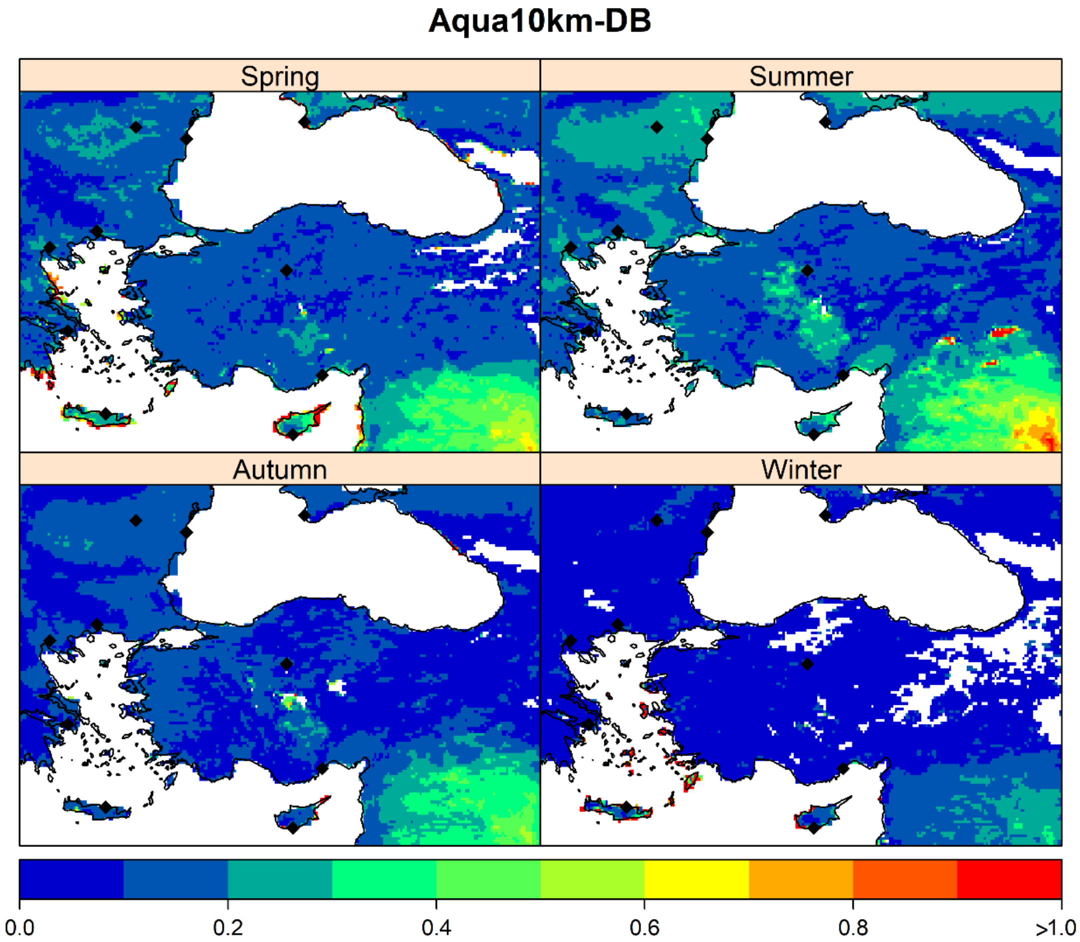

Figure 4.37 Spatial distribution of the seasonal mean Aqua MODIS DB 10 km AOD products

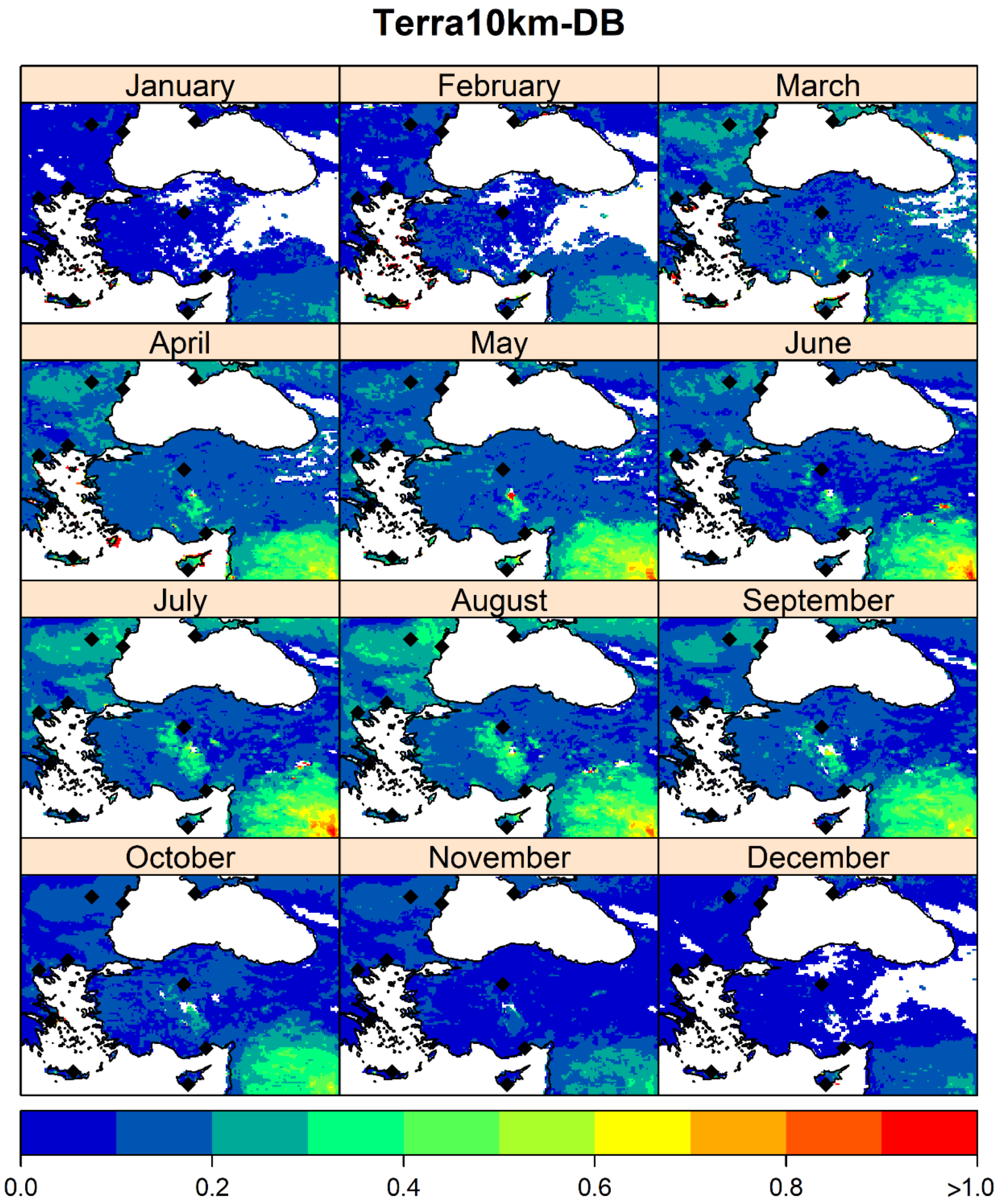

Figure 4.38 Spatial distribution of monthly mean Terra MODIS DB 10 km AOD products

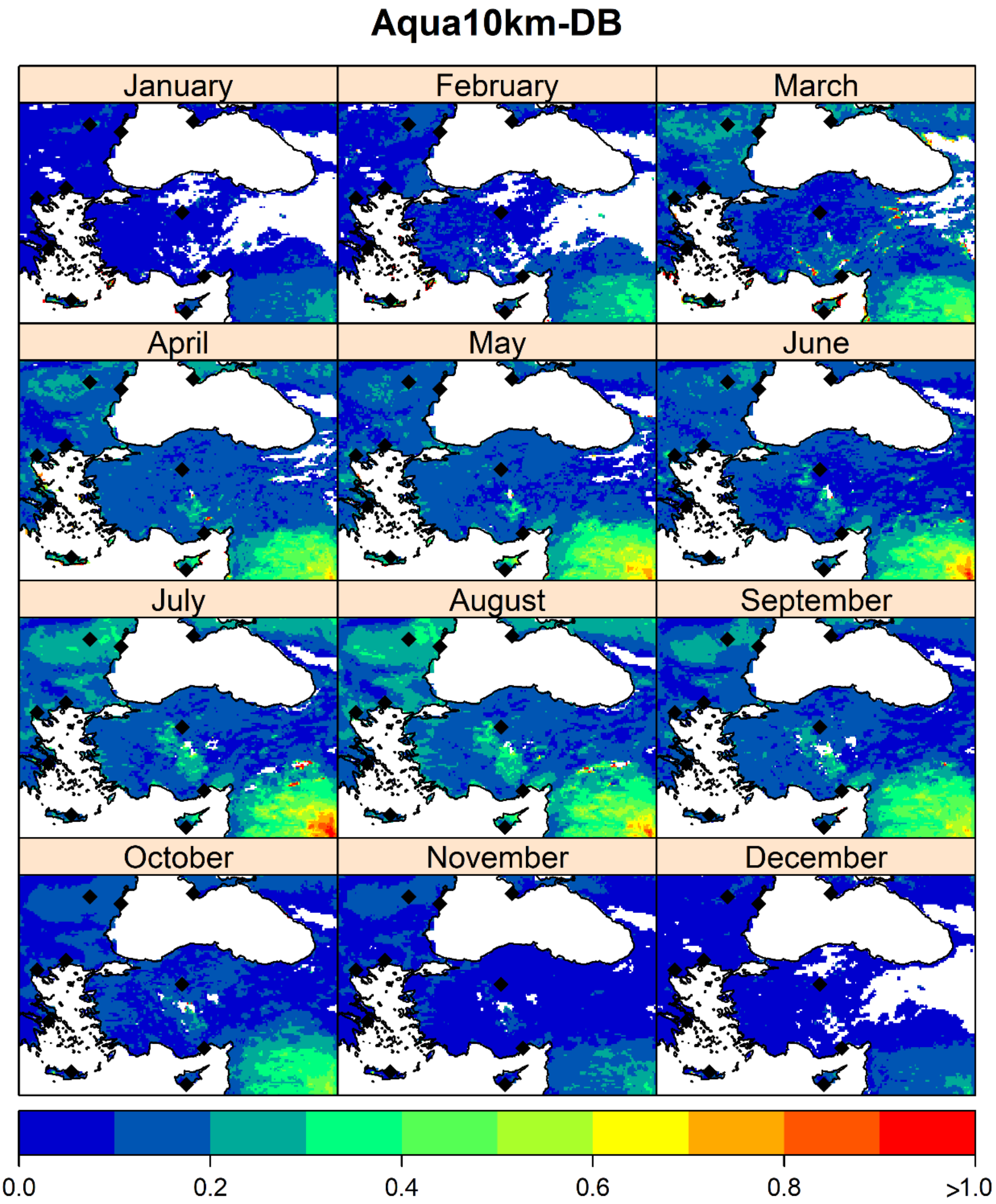

Figure 4.39 Spatial distribution of monthly mean Aqua MODIS DB 10 km AOD products

CHAPTER FIVE
CONCLUSION AND RECOMMENDATIONS

5.1 Conclusion and Recommendations

This study comprehensively validated and analyzed the performance of the latest Terra and Aqua MODIS Collection 6.1 (C6.1) Level 2 aerosol products in characterizing the spatial and temporal variations over Turkey. Dark Target (DT) and Deep Blue (DB) daily aerosol optical depth (AOD) products during 2002–2019 were collected and compared against newest AERONET Version 3 AOD measurements at 10 sites. In order to determine the effects of the surface characteristics on aerosol properties, performances of the aerosol products related to diverse surface types were discussed with analyzing normalized difference vegetation index (NDVI). The sites were classified into partially vegetated surface ($NDVI_P$), moderately vegetated surface ($NDVI_M$) and densely vegetated surface (($NDVI_D$). The spatiotemporal characteristics were also investigated to provide a clearer and better understanding of MODIS aerosol products over regional scale.

The results showed that adequate number of AOD data were obtained from Terra and Aqua satellites for Turkey. For the three aerosol datasets, neither one can consistently outperformed among the others due to the diversity of surface vegetation over Turkey. Results also illustrated that although the C6.1 DT AOD retrievals was compliant with AERONET AOD measurements at the regional scale, noticeable differences exist at site scales. Regional validation results showed that the DT algorithm is more suitable for moderately and densely vegetated and low aerosol-loading areas in Turkey. However, the DB algorithm performed better with higher fractions of the retrievals within the EE and lower estimation uncertainties than the DT algorithm in partially vegetated urban areas. Similar to DT 10 km, the error of DT 3 km aerosol products is mainly due to an underestimation of surface reflectance, especially over partially vegetated areas. Therefore, DT products could be a good option to represent the aerosol variation over densely vegetated surfaces such as Black Sea, Mediterranean, Aegean and Marmara regions. DB products could be good option for partially vegetated surfaces such as south-eastern and eastern Anatolia, and inner Anatolia.

Furthermore, three aerosol datasets from two satellites can accurately capture the aerosol trends over the region, and similar performances were found with small differences between the Terra and Aqua satellite-derived aerosol products. However, Terra products relatively overestimated AOD values and were less accurate than the Aqua products. More rapid degradation of MODIS-Terra instrument can cause differences between Terra and Aqua satellites. This study recommends that the Aqua satellite products should be selected for related aerosol studies (i.e., model simulations and validations, long-term aerosol changes, aerosol-cloud radiation interactions) over Turkey. It was also found that there were different seasonal variations for the AOD products over the study area. The higher AOD values were observed in spring and summer, while lower values were observed in autumn and winter in the region.

This study achieved more representative and comprehensive validation results of C6.1 DT and DB AOD and may help further to improve the DT and DB retrieval algorithms over the region. These results will provide better understanding of the key features and differences among different aerosol datasets, and which one is more suitable for use in different applications over diverse vegetated surfaces of Turkey. Observed poor performance of DT-3 km over urban areas with relatively low aerosol loadings, confirms the deficiency of DT's surface reflectance assumptions when applied at 3-km resolution. An alternative solution may be to develop the DB algorithm at the finer 3-km resolution, as it is specifically targeted for retrieval over bright surfaces. This study will also contribute to development of statistical models to predict ground level particle matter concentrations over Turkey.

REFERENCES

Agacayak, T. (2014). *Investigation of impacts of aerosols on Eastern Mediterranean region climate*. Phd Thesis, Istanbul Technical University, İstanbul.

Agacayak, T., Kindap, T., Unal, A., Pozzoli, L., Mallet, M., & Solmon, F. (2015). A case study for Saharan dust transport over Turkey via RegCM4.1 model. *Atmospheric Research*, *153*, 392–403.

Ahmad, M., Alam, K., Tariq, S., Anwar, S., Nasir, J., & Mansha, M. (2019). Estimating fine particulate concentration using a combined approach of linear regression and artificial neural network. *Atmospheric Environmen*t, *219*, 117050.

Aldabash, M., Balcik, F. B., & Glantz, P. (2020). Validation of MODIS C6.1 and MERRA-2 AOD using AERONET observations: A comparative study over Turkey. *Atmosphere*, *11*(9), 905.

Almazroui, M. (2019). A comparison study between AOD data from MODIS deep blue collections 51 and 06 and from AERONET over Saudi Arabia. *Atmospheric Research*, *225*(December 2018), 88–95.

Anderson, J. C., Wang, J., Zeng, J., Leptoukh, G., Petrenko, M., Ichoku, C., & Hu, C. (2013). Long-term statistical assessment of Aqua-MODIS aerosol optical depth over coastal regions: bias characteristics and uncertainty sources. *Tellus B: Chemical and Physical Meteorology*, *65*(1), 20805.

Applied Remote Sensing and Training Program (ARSET) (2018). *New and Upcoming Satellite Capabilities for Air Quality Monitoring. Data Analysis Tools for High Resolution Air Quality Satellite Datasets*. Retrieved February 1, 2021, https://appliedsciences.nasa.gov/sites/default/files/2020-11/HighResAQ_Part3b.pdf.

Banerjee, T., Kumar, M., Mall, R. K., & Singh, R. S. (2017). Airing ‘clean air’ in Clean India Mission. *Environmental Science and Pollution Research*, *24*(7), 6399-6413.

Barnaba, F., & Gobbi, G. P. (2004). Aerosol seasonal variability over the Mediterranean region and relative impact of maritime, continental and Saharan dust particles over the basin from MODIS data in the year 2001. *Atmospheric Chemistry and Physics*, *4*(9–10), 2367–2391.

Bellouin, N. (2015). AEROSOLS | Role in Climate Change. *Reference Module in Earth Systems and Environmental Sciences*, 76-85.

Benas, N., Beloconi, A., & Chrysoulakis, N. (2013). Estimation of urban PM10 concentration, based on MODIS and MERIS/AATSR synergistic observations. *Atmospheric Environment*, *79*, 448–454.

Bibi, H., Alam, K., Chishtie, F., Bibi, S., Shahid, I., & Blaschke, T. (2015). Intercomparison of MODIS, MISR, OMI, and CALIPSO aerosol optical depth retrievals for four locations on the Indo-Gangetic plains and validation against AERONET data. *Atmospheric Environment*, *111*, 113–126.

Bilal, M., Nazeer, M., Nichol, J., Qiu, Z., Wang, L., Bleiweiss, M. P., Shen, X., Campbell, J. R., & Lolli, S. (2019). Evaluation of terra-MODIS C6 and C6.1 aerosol products against Beijing, XiangHe, and Xinglong AERONET sites in China during 2004-2014. *Remote Sensing*, *11*(5), 486.

Bilal, M., Nazeer, M., Qiu, Z., Ding, X., & Wei, J. (2018). Global validation of MODIS C6 and C6.1 merged aerosol products over diverse vegetated surfaces. *Remote Sensing*, *10*(3), 475.

Bilal, M., Nichol, J. E., & Wang, L. (2017). New customized methods for improvement of the MODIS C6 Dark Target and Deep Blue merged aerosol product. *Remote Sensing of Environment*, *197*, 115–124.

Bright, J. M., & Gueymard, C. A. (2019). Climate-specific and global validation of MODIS Aqua and Terra aerosol optical depth at 452 AERONET stations. *Solar Energy*, *183*, 594–605.

Butt, M. J., Assiri, M. E., & Ali, M. A. (2017). Assessment of AOD variability over Saudi Arabia using MODIS Deep Blue products. *Environmental Pollution*, *231*, 143–153.

Chan, K. L., & Chan, K. L. (2017). Aerosol optical depths and their contributing sources in Taiwan. *Atmospheric Environment*, *148*, 364–375.

Che, H., Yang, L., Liu, C., Xia, X., Wang, Y., Wang, H., Wang, H., Wang, H., Lu, X., & Zhang, X. (2019). Long-term validation of MODIS C6 and C6.1 Dark Target aerosol products over China using CARSNET and AERONET. *Chemosphere*, *236,* 124268.

Chen, Z. Y., Zhang, T. H., Zhang, R., Zhu, Z. M., Ou, C. Q., & Guo, Y. (2018). Estimating PM2.5 concentrations based on non-linear exposure-lag-response associations with aerosol optical depth and meteorological measures. *Atmospheric Environment*, *173,* 30–37.

Chouza, F., Reitebuch, O., Benedetti, A., & Weinzierl, B. (2016). Saharan dust long-range transport across the Atlantic studied by an airborne Doppler wind lidar and the MACC model. *Atmospheric Chemistry and Physics*, *16*(18), 11581–11600.

De Meij, A., & Lelieveld, J. (2011). Evaluating aerosol optical properties observed by ground-based and satellite remote sensing over the Mediterranean and the Middle East in 2006. *Atmospheric Research*, *99*(3–4), 415–433.

Douglas, A.D. (2015). *A geographical comparison of the relationship between aerosol optical depth and fine particulate matter in Indiana*. M.Sc. Thesis, Indiana University, Bloomington.

Dündar, C., Oğuz, K., Öz, N., & Güllü G., (2015). Aerosol Optik Derinliği verilerinin Türkiye için alansal ve zamansal değişimlerinin incelenmesi. *VII. Atmosfer Bilimleri Sempozyumu*, 841-852.

Filonchyk, M., Hurynovich, V., & Yan, H. (2020). Trends in aerosol optical properties over Eastern Europe based on MODIS-Aqua. *Geoscience Frontiers*, *11*(6), 2169–2181.

Floutsi, A. A., Korras-Carraca, M. B., Matsoukas, C., Hatzianastassiou, N., & Biskos, G. (2016). Climatology and trends of aerosol optical depth over the Mediterranean basin during the last 12 years (2002-2014) based on Collection 006 MODIS-Aqua data. *Science of the Total Environment*, *551–552*, 292–303.

Fotiadi, A., Hatzianastassiou, N., Drakakis, E., Matsoukas, C., Pavlakis, K. G., Hatzidimitriou, D., Gerasopoulos, E., Mihalopoulos, N., & Vardavas, I. (2006). Aerosol physical and optical properties in the Eastern Mediterranean Basin, Crete, from Aerosol Robotic Network data. *Atmospheric Chemistry and Physics*, *6*(12), 5399–5413.

Friedl, M. A., Sulla-Menashe, D., Tan, B., Schneider, A., Ramankutty, N., Sibley, A., & Huang, X. (2010). MODIS Collection 5 global land cover: Algorithm refinements and characterization of new datasets. *Remote Sensing of Environment*, *114*(1), 168–182.

Georgoulias, A. K., Alexandri, G., Kourtidis, K. A., Lelieveld, J., Zanis, P., Pöschl, U., Levy, R., Amiridis, V., Marinou, E., & Tsikerdekis, A. (2016). Spatiotemporal variability and contribution of different aerosol types to the aerosol optical depth over the Eastern Mediterranean. *Atmospheric Chemistry and Physics*, *16*(21), 13853–13884.

Ghotbi, S., Sotoudeheian, S., & Arhami, M. (2016). Estimating urban ground-level PM10 using MODIS 3km AOD product and meteorological parameters from WRF model. *Atmospheric Environment*, *141*, 333–346.

Giles, D. M., Sinyuk, A., Sorokin, M. S., Schafer, J. S., Smirnov, A., Slutsker, I., Eck, T. F., Holben, B. N., Lewis, J. R., Campbell, J. R., Welton, E. J., Korkin, S. V., & Lyapustin, A. (2018). Advancements in the Aerosol Robotic Network (AERONET) Version 3 database – automated near real-time quality control algorithm with improved cloud-screening for sun photometer Aerosol Optical Depth (AOD) measurements. *Atmospheric Measurement Techniques Discussions*, 1–78.

Glantz, P., Freud, E., Johansson, C., Noone, K. J., & Tesche, M. (2019). Trends in MODIS and AERONET derived aerosol optical thickness over Northern Europe. *Tellus, Series B: Chemical and Physical Meteorology*, *71*(1), 1–21.

Guo, Y., Feng, N., Christopher, S. A., Kang, P., Zhan, F. B., & Hong, S. (2014). Satellite remote sensing of fine particulate matter (PM2.5) air quality over Beijing using MODIS. *International Journal of Remote Sensing*, *35*(17), 6522–6544.

Gupta, P., Levy, R.C., Mattoo, S., Remer, L.A., Munchak, L.A., & (2016). A surface reflectance scheme for retrieving aerosol optical depth over urban surfaces in MODIS Dark Target retrieval algorithm. *Atmospheric Measurement Techniques*, *9*, 3293–3308.

Gupta, P., Remer, L. A., Levy, R. C., & Mattoo, S. (2018). Validation of MODIS 3km land aerosol optical depth from NASA’s EOS Terra and Aqua missions. *Atmospheric Measurement Techniques*, *11*(5), 3145–3159.

He, Q., Zhang, M., Huang, B., & Tong, X. (2017). MODIS 3 km and 10 km aerosol optical depth for China: Evaluation and comparison. *Atmospheric Environment*, *153*, 150–162.

Horne, J. R., & Dabdub, D. (2017). Impact of global climate change on ozone, particulate matter, and secondary organic aerosol concentrations in California: A model perturbation analysis. *Atmospheric Environment*, *153*, 1–17.

Hsu N.C. (2017). *Changes to MODIS deep blue aerosol products between collection 6 and collection 6.1*. Retrieved February 1, 2021, from https://modis-atmosphere.gsfc.nasa.gov/sites/default/files/ModAtmo/modis_deep_blue_c61_changes2.pdf.

Hsu, N. C., Jeong, M. J., Bettenhausen, C., Sayer, A. M., Hansell, R., Seftor, C. S., Huang, J., & Tsay, S. C. (2013). Enhanced Deep Blue aerosol retrieval algorithm: The second generation. *Journal of Geophysical Research Atmospheres*, *118*(16), 9296–9315.

Hu, X., Waller, L. A., Lyapustin, A., Wang, Y., & Liu, Y. (2014). 10-year spatial and temporal trends of PM2.5 concentrations in the southeastern US estimated using high-resolution satellite data. *Atmospheric Chemistry and Physics*, *14*(12), 6301–6314.

Huang, Y., Zhu, B., Zhou, X., Chen, D., Zhu, Z., Zhang, T., Xia, X., Ji, Y., Gong, Y., & Wang, L. (2019). Evaluation and comparison of MODIS Collection 6.1 and Collection 6 Dark Target Aerosol Optical Depth over mainland China under various conditions including spatiotemporal distribution, haze effects, and underlying surface. *Earth and Space Science*, *6*(12), 2575–2592.

Ichoku, C., Allen Chu, D., Mattoo, S., Kaufman, Y. J., Remer, L. A., Tanré, D., Slutsker, I., & Holben, B. N. (2002). A spatio-temporal approach for global validation and analysis of MODIS aerosol products. *Geophysical Research Letters*, *29*(12), MOD1-1-MOD1-4.

Jiang, T., Chen, B., Nie, Z., Ren, Z., Xu, B., & Tang, S. (2021). Estimation of hourly full-coverage PM2.5 concentrations at 1-km resolution in China using a two-stage random forest model. *Atmospheric Research*, *248*, 105146.

Jin, Q., Crippa, P., & Pryor, S. C. (2020). Spatial characteristics and temporal evolution of the relationship between PM2.5 and aerosol optical depth over the eastern USA during 2003–2017. *Atmospheric Environment*, *239*, 117718.

Jing, Y., Zhang, P., Chen, L., & Xu, N. (2017). Integrated analysis of dust transport and budget in a severe asian dust event. *Aerosol and Air Quality Research*, *17*(10), 2390–2400.

Kabataş, B. (2016). *Quantification of Saharan dust influences on Eastern Mediterranean air quality via atmospheric modelling*. Istanbul Technical University: Eurasia Institute of Earth Sciences.

Kabatas, B., Unal, A., Pierce, R. B., Kindap, T., & Pozzoli, L. (2014). The contribution of Saharan dust in PM10 concentration levels in Anatolian Peninsula of Turkey. *Science of the Total Environment*, *488–489*(1), 413–421.

Kamarul Zaman, N. A. F., Kanniah, K. D., & Kaskaoutis, D. G. (2017). Estimating particulate matter using satellite based aerosol optical depth and meteorological variables in Malaysia. *Atmospheric Research*, *193*, 142–162.

Kharol, S. K., Badarinath, K. V. S., Sharma, A. R., Kaskaoutis, D. G., & Kambezidis, H. D. (2011). Multiyear analysis of Terra/Aqua MODIS aerosol optical depth and ground observations over tropical urban region of Hyderabad, India. *Atmospheric Environment*, *45*(8), 1532–1542.

Kloog, I., Sorek-Hamer, M., Lyapustin, A., Coull, B., Wang, Y., Just, A. C., Schwartz, J., & Broday, D. M. (2015). Estimating daily PM2.5 and PM10 across the complex geo-climate region of Israel using MAIAC satellite-based AOD data. *Atmospheric Environment*, *122*, 409–416.

Kong, L., Xin, J., Zhang, W., & Wang, Y. (2016). The empirical correlations between PM2.5, PM10 and AOD in the Beijing metropolitan region and the PM2.5, PM10 distributions retrieved by MODIS. *Environmental Pollution*, *216*, 350–360.

Kubilay, N., Cokacar, T., & Oguz, T. (2003). Optical properties of mineral dust outbreaks over the northeastern Mediterranean. *Journal of Geophysical Research: Atmospheres*, *108*(21), 4666.

Kubilay, N., Nickovic, S., Moulin, C., & Dulac, F. (2000). An illustration of the transport and deposition of mineral dust onto the eastern Mediterranean. *Atmospheric Environment*, *34*(8), 1293–1303.

Kubilay, N., Oguz, T., Koçak, M., & Torres, O. (2005). Ground-based assessment of Total Ozone Mapping Spectrometer (TOMS) data for dust transport over the northeastern Mediterranean. *Global Biogeochemical Cycles*, *19*(1), 1–9.

Kubilay, N., & Koçak, M. (2009). Doğu Akdeniz bölgesindeki aerosollerin iklimsel önemi. TUBITAK, Project Number: 105Y368-GSRT, Mersin.

Lee, H. J., Chatfield, R. B., & Strawa, A. W. (2016). Enhancing the applicability of satellite remote sensing for PM2.5 estimation using MODIS Deep Blue AOD and land use regression in California, United States. *Environmental Science and Technology*, *50*(12), 6546–6555.

Lee, H. J., Kang, C. M., Coull, B. A., Bell, M. L., & Koutrakis, P. (2014). Assessment of primary and secondary ambient particle trends using satellite aerosol optical depth and ground speciation data in the New England region, United States. *Environmental Research*, *133*, 103–110.

Lee, Y. C., Lam, Y. F., Kuhlmann, G., Wenig, M. O., Chan, K. L., Hartl, A., & Ning, Z. (2013). An integrated approach to identify the biomass burning sources contributing to black carbon episodes in Hong Kong. *Atmospheric Environment*, *80*, 478–487.

Levy, R. C., Mattoo, S., Munchak, L. A., Remer, L. A., Sayer, A. M., Patadia, F., & Hsu, N. C. (2013). The Collection 6 MODIS aerosol products over land and ocean. *Atmospheric Measurement Techniques, 6*(11), 2989–3034.

Li, B., Yuan, H., Feng, N., & Tao, S. (2009). Comparing MODIS and AERONET aerosol optical depth over China. *International Journal of Remote Sensing*, *30*(24), 6519–6529.

Li, T. Y., Tan, H. B., Wang, C. L., Chen, J. Y., Yang, L. L., Hong, Y. Y., & Wang, J. C. (2020). The method and the correspongding effect of ground fine partical concentration retrieved by satellite remote sensing AOD. *Zhongguo Huanjing Kexue/China Environmental Science*, *40*(1), 13–23.

Logothetis, S. A., Salamalikis, V., & Kazantzidis, A. (2020). Aerosol classification in Europe, Middle East, North Africa and Arabian Peninsula based on AERONET Version 3. *Atmospheric Research, 239,* 104893.

Loría-Salazar, S. M., Holmes, H. A., Patrick Arnott, W., Barnard, J. C., & Moosmüller, H. (2016). Evaluation of MODIS columnar aerosol retrievals using AERONET in semi-arid Nevada and California, U.S.A., during the summer of 2012. *Atmospheric Environment*, *144*, 345–360.

Mallet, M., Dubovik, O., Nabat, P., Dulac, F., Kahn, R., Sciare, J., Paronis, D., & Léon, J. F. (2013). Absorption properties of Mediterranean aerosols obtained from multiyear ground-based remote sensing observations. *Atmospheric Chemistry and Physics*, *13*(18), 9195–9210.

Mattoo, S. (2017). *Aerosol dark target (10km & 3km) collection 6.1 changes*. Retrieved February 1, 2021, from https://modis-atmosphere.gsfc.nasa.gov/sites/default/files/ModAtmo/C061_Aerosol_Dark_Target_ v2.pdf.

Mhawish, A., Banerjee, T., Broday, D. M., Misra, A., & Tripathi, S. N. (2017). Evaluation of MODIS Collection 6 aerosol retrieval algorithms over Indo-Gangetic Plain: Implications of aerosols types and mass loading. *Remote Sensing of Environment*, *201*, 297–313.

Nabat, P., Somot, S., Mallet, M., Chiapello, I., Morcrette, J. J., Solmon, F., Szopa, S., Dulac, F., Collins, W., Ghan, S., Horowitz, L. W., Lamarque, J. F., Lee, Y., Naik, V., Nagashima, T., Shindell, D., Skeie, R. & (2013). A 4-D climatology (1979-2009) of the monthly tropospheric aerosol optical depth distribution over the Mediterranean region from a comparative evaluation and blending of remote sensing and model products. *Atmospheric Measurement Techniques*, *6*(5), 1287–1314.

National Aeronautics and Space Administration (NASA) (2021a). *Atmospheric aerosols: What are they, and why are they so important?*. Retrieved February 1, 2021, from https://www.nasa.gov/centers/langley/news/factsheets/Aerosols.html.

National Aeronautics and Space Administration (NASA) (2021b). *MODIS standard collection 6.1 update*. Retrieved February 1, 2021, from https://atmosphere-imager.gsfc.nasa.gov/documentation/collection-61.

National Aeronautics and Space Administration (NASA) (2020a). Retrieved December 1, 2020, from https://aeronet.gsfc.nasa.gov/.

National Aeronautics and Space Administration (NASA) (2020b). *MODIS design*. Retrieved December 1, 2020, from https://modis.gsfc.nasa.gov/about/design.php.

National Aeronautics and Space Administration (NASA) (2020c). Retrieved December 1, 2020, from https://ladsweb.modaps.eosdis.nasa.gov/missions-and-measurements/science-domain/l3-atmosphere/.

National Aeronautics and Space Administration (NASA) (2020d). Retrieved December 1, 2020, from https://weather.msfc.nasa.gov/sport/modis/#:~:text=MODIS%20(Moderate%20Resolution%20Imaging%20Spectroradiometer,coverage%20every%201%20%2D2%20days.

Nichol, J. E., & Bilal, M. (2016). Validation of MODIS 3 km resolution aerosol optical depth retrievals over Asia. *Remote Sensing*, *8*(4), 3–12.

Ningombam, S. S., Larson, E. J. L., Dumka, U. C., Estellés, V., Campanelli, M., & Steve, C. (2019). Long-term (1995–2018) aerosol optical depth derived using ground based AERONET and SKYNET measurements from aerosol aged-background sites. *Atmospheric Pollution Research*, *10*(2), 608–620.

National Oceanic and Atmospheric Administration (NOAA) (2021). Retrieved March 1, 2021, from https://www.esrl.noaa.gov/gmd/grad/surfrad/aod/index.html.

Ozdemir, E., Tuna Tuygun, G., & Elbir, T. (2020). Application of aerosol classification methods based on AERONET version 3 product over eastern Mediterranean and Black Sea. *Atmospheric Pollution Research*, *11*(12), 2226–2243.

Park, S., Shin, M., Im, J., Song, C. K., Choi, M., Kim, J., Lee, S., Park, R., Kim, J., Lee, D. W., & Kim, S. K. (2019). Estimation of ground-level particulate matter concentrations through the synergistic use of satellite observations and process-based models over South Korea. *Atmospheric Chemistry and Physics*, *19*(2), 1097–1113.

Rea, G., Turquety, S., Menut, L., Briant, R., Mailler, S., & Siour, G. (2015). Source contributions to 2012 summertime aerosols in the Euro-Mediterranean region. *Atmospheric Chemistry and Physics*, *15*(14), 8013–8036.

Remer, L. A., Mattoo, S., Levy, R. C., & Munchak, L. A. (2013). MODIS 3 km aerosol product: Algorithm and global perspective. *Atmospheric Measurement Techniques*, *6*(7), 1829–1844.

Rupakheti, D., Kang, S., Bilal, M., Gong, J., Xia, X., & Cong, Z. (2019). Aerosol optical depth climatology over Central Asian countries based on Aqua-MODIS Collection 6.1 data: Aerosol variations and sources. *Atmospheric Environment*, *207*, 205–214.

Sayer, A. M., Munchak, L. A., Hsu, N. C., Levy, R. C., Bettenhausen, C., & Jeong, M. J. (2014). Modis collection 6 aerosol products: Comparison between aqua's e-deep blue, dark target, and "merged" data sets, and usage recommendations. *Journal of Geophysical Research*, *119*(22), 13,965-13,989.

Seo, S., Kim, J., Lee, H., Jeong, U., Kim, W., Holben, B. N., Kim, S. W., Song, C. H., & Lim, J. H. (2015). Estimation of PM10 concentrations over Seoul using multiple empirical models with AERONET and MODIS data collected during the DRAGON-Asia campaign. *Atmospheric Chemistry and Physics*, *15*(1), 319–334.

Sever, L., Alpert, P., Lyapustin, A., Wang, Y., & Chudnovsky, A. (2017). An example of aerosol pattern variability over bright surface using high resolution MODIS MAIAC: The eastern and western areas of the Dead Sea and environs. *Atmospheric Environment*, *165*, 359–369.

Shaheen, A., Wu, R., & Aldabash, M. (2020). Long-term AOD trend assessment over the Eastern Mediterranean region: A comparative study including a new merged aerosol product. *Atmospheric Environment*, *238*, 117736.

Shen, L., Hao, F., Gao, M., Wang, H., Zhu, B., Gao, J., Cheng, Y., & Xie, F. (2020). Real-time geochemistry of urban aerosol during a heavy dust episode by single-particle aerosol mass spectrometer: Spatio-temporal variability, mixing state and spectral distribution. *Particuology*, *53*, 197–207.

Shtein, A., Karnieli, A., Katra, I., Raz, R., Levy, I., Lyapustin, A., Dorman, M., Broday, D. M., & Kloog, I. (2018). Estimating daily and intra-daily PM10 and PM2.5 in Israel using a spatio-temporal hybrid modeling approach. *Atmospheric Environment*, *191*, 142–152.

Stafoggia, M., Bellander, T., Bucci, S., Davoli, M., de Hoogh, K., de' Donato, F., Gariazzo, C., Lyapustin, A., Michelozzi, P., Renzi, M., Scortichini, M., Shtein, A., Viegi, G., Kloog, I., & Schwartz, J. (2019). Estimation of daily PM10 and PM2.5 concentrations in Italy, 2013–2015, using a spatiotemporal land-use random-forest model. *Environment International*, *124*, 170–179.

Su, Y., Xie, Y., Tao, Z., Hu, Q., Yu, T., & Gu, X. (2021). Validation and inter-comparison of MODIS and VIIRS aerosol optical depth products against data from multiple observation networks over East China. *Atmospheric Environment*, *247,* 118205.

Taheri Shahraiyni, H., Karimi, K., Habibi Nokhandan, M., & Hafezi Moghadas, N. (2015). Monitoring of dust storm and estimation of aerosol concentration in the Middle East using remotely sensed images. *Arabian Journal of Geosciences*, *8*(4), 2095–2110.

Tao, M., Chen, L., Wang, Z., Tao, J., Che, H., Wang, X., & Wang, Y. (2015). Comparison and evaluation of the MODIS Collection 6 aerosol data in China. *Journal of Geophysical Research*, *120*(14), 6992–7005.

Tian, X., Liu, Q., Li, X., & Wei, J. (2018). Validation and comparison of MODIS C6.1 and C6 aerosol products over Beijing, China. *Remote Sensing*, *10*(12), 1–18.

Tsai, F., Tu, J. Y., Hsu, S. C., & Chen, W. N. (2014). Case study of the Asian dust and pollutant event in spring 2006: Source, transport, and contribution to Taiwan. *Science of the Total Environment*, *478*, 163–174.

Tuna Tuygun, G., Ozdemir, E., & Elbir, T. (2020). Evaluation of MODIS C6 and C6.1 Dark Target AOD products over Turkey based on NDVI and aerosol type. *Atmospheric Pollution Research*, *11*(12), 2335–2349.

Tutsak, E., & Koçak, M. (2019). Long-term measurements of aerosol optical and physical properties over the Eastern Mediterranean: Hygroscopic nature and source regions. *Atmospheric Environment*, *207*, 1–15.

Tutsak, E., & Koçak, M. (2020). Optical and microphysical properties of the columnar aerosol burden over the Eastern Mediterranean: Discrimination of Aerosol types. *Atmospheric Environment*, *229*, 117463.

Van Donkelaar, A., Martin, R. V., Brauer, M., & Boys, B. L. (2015). Use of satellite observations for long-term exposure assessment of global concentrations of fine particulate matter. *Environmental Health Perspectives*, *123*(2), 135–143.

Wang, C., Liu, Q., Ying, N., Wang, X., & Ma, J. (2013). Air quality evaluation on an urban scale based on MODIS satellite images. *Atmospheric Research*, *132–133*, 22–34.

Wang, Y., Wang, J., Levy, R. C., Xu, X., & Reid, J. S. (2017). MODIS retrieval of aerosol optical depth over turbid coastalwater. *Remote Sensing*, *9*(6), 595.

Wang, Y., Yuan, Q., Li, T., Shen, H., Zheng, L., & Zhang, L. (2019). Evaluation and comparison of MODIS Collection 6.1 aerosol optical depth against AERONET over regions in China with multifarious underlying surfaces. *Atmospheric Environment*, *200*, 280–301.

Wei, J., Li, Z., Peng, Y., & Sun, L. (2019). MODIS Collection 6.1 aerosol optical depth products over land and ocean: validation and comparison. *Atmospheric Environment*, *201*(2018), 428–440.

Wei, J., Li, Z., Sun, L., Peng, Y., Liu, L., He, L., Qin, W., et al. (2020). MODIS Collection 6.1 3 km resolution aerosol optical depth product: global evaluation and uncertainty analysis. *Atmospheric Environment*, *240*, 117768.

Wei, J., Peng, Y., Guo, J., & Sun, L. (2019a). Performance of MODIS Collection 6.1 Level 3 aerosol products in spatial-temporal variations over land. *Atmospheric Environment*, *206*, 30–44.

Xu, H., Guang, J., Xue, Y., de Leeuw, G., Che, Y. H., Guo, J., He, X. W., et al. (2015). A consistent aerosol optical depth (AOD) dataset over mainland China by integration of several AOD products. *Atmospheric Environment*, *114*, 48–56.

Xu, X., Xie, L., Yang, X., Wu, H., Cai, L., & Qi, P. (2020). Aerosol optical properties at seven AERONET sites over Middle East and Eastern Mediterranean Sea. *Atmospheric Environment*, *243*, 117884.

Yang, Q., Yuan, Q., Yue, L., Li, T., Shen, H., & Zhang, L. (2019). The relationships between PM2.5 and aerosol optical depth (AOD) in mainland China: About and behind the spatio-temporal variations. *Environmental Pollution*, *248*, 526–535.

You, W., Zang, Z., Pan, X., Zhang, L., & Chen, D. (2015). Estimating PM2.5 in Xi'an, China using aerosol optical depth: A comparison between the MODIS and MISR retrieval models. *Science of the Total Environment, 505*, 1156–1165.

You, W., Zang, Z., Zhang, L., Zhang, M., Pan, X., & Li, Y. (2016). A nonlinear model for estimating ground-level PM10 concentration in Xi'an using MODIS aerosol optical depth retrieval. *Atmospheric Research*, *168*, 169–179.

Zeydan, Ö.& Yildirim, Y. (2012). Uzaktan algılama ile atmosferik partikül madde konsantrasyonlarının belirlenmesi. *IV. Uzaktan Algılama ve Coğrafi Bilgi Sistemleri Sempozyumu Bildiri Özetleri Kitabı*, 1-7.

Zeydan, Ö., & Wang, Y. (2019). Using MODIS derived aerosol optical depth to estimate ground-level PM2.5 concentrations over Turkey. *Atmospheric Pollution Research*, *10*(5), 1565–1576.

Zhang, M., Liu, J., Li, W., Bilal, M., Zhao, F., Zhang, C., Yuan, B., & Khedher, K. (2019). Evaluation of the aqua-MODIS C6 and C6.1 aerosol optical depth products in the Yellow River Basin, China. *Atmosphere*, *10*(8), 426.

Zhang, Y., Hu, R., & Zheng, X. (2018). Large-scale coherent structures of suspended dust concentration in the neutral atmospheric surface layer: A large-eddy simulation study. *Physics of Fluids, 30*(4), 046601.

Zhang, T. H., & Liao, H. (2016). Aerosol absorption optical depth of fine-mode mineral dust in eastern China. *Atmospheric and Oceanic Science Letters*, *9*(1), 7–14.

Zhang, Y., & Li, Z. (2015). Remote sensing of atmospheric fine particulate matter (PM2.5) mass concentration near the ground from satellite observation. *Remote Sensing of Environment*, *160*, 252–262.

Zhang, Z., Wenig, M., Zhou, W., Diehl, T., Chan, K. L., & Wang, L. (2014). The contribution of different aerosol sources to the aerosol optical depth in Hong Kong. *Atmospheric Environment*, *83*, 145–154.

Zhao, S., Zhang, H., Feng, S., & Fu, Q. (2015). Simulating direct effects of dust aerosol on arid and semi-arid regions using an aerosol-climate coupled system. *International Journal of Climatology*, *35*(8), 1858–1866.